UNIVERSITY OF CALIFORNIA SAN DIEGO

SAN DIEGO STATE UNIVERSITY

Spatiotemporal Dynamics of Functional Brain Networks in Autism Spectrum Disorder

A dissertation submitted in partial satisfaction of the
requirements for the degree Doctor of Philosophy

in

Clinical Psychology

by

Lisa Elena Mash

Committee in charge:

University of California San Diego

Frank Haist
Thomas Liu
Jeanne Townsend

San Diego State University

Ralph-Axel Müller, Chair
Jonathan Helm

2021

The Dissertation of Lisa Elena Mash is approved, and it is acceptable in quality and form for publication on microfilm and electronically:

Chair

University of California San Diego

San Diego State University

2021

TABLE OF CONTENTS

LIST OF TABLES

LIST OF FIGURES

ACKNOWLEDGEMENTS

I am extremely grateful to the many people who have generously guided and supported me throughout my time in graduate school. I would first like to acknowledge Dr. Ralph-Axel Müller, my dissertation chair, for his invaluable scientific insight over the years it took to produce this work. Many thanks to Dr. Jeanne Townsend for both her professional and personal guidance. I also would like to thank my dissertation committee, my coauthors, Dr. Inna Fishman, and Dr. Ruth Carper for their collaboration, mentorship and support over the years. To my partner, Chris, my family, my JDP/BDIL families, and my friends who have cheered me on year after year- thank you for your unwavering support, and for always believing in me and my dreams.

Please note that Chapter 1, in part, is a reprint of the material as it appears in Developmental Neurobiology, 78, 456-473. Mash, L. E., Reiter, M. A., Linke, A. C., Townsend, J., & Müller, R.-A. Wiley, 2017. Chapter 2, in full, is a reprint of the material as it appears in Human Brain Mapping, 40, 2377-2389. Mash, L. E., Linke, A. C., Olson, L. A., Fishman, I., Liu, T. T., & Müller, R.-A. Wiley, 2019. Chapter 3, in full, is currently under review for publication. Mash, L. E., Linke, A. C., Gao, Y., Wilkinson, M., Olson, M. A., Jao Keehn, R. J., & Müller, R.-A. Chapter 4, in full, is a reprint of the material as it appears in Brain Connectivity, 10, 18-28. Mash, L. E., Keehn, B., Linke, A. C., Liu, T. T., Helm, J. L., Haist, F., Townsend, J., & Müller, R.-A. Mary Ann Liebert, 2020. The dissertation author was the primary investigator and author of each of these papers.

VITA

2021	**Doctor of Philosophy** in Clinical Psychology San Diego State University/ University of California San Diego Joint Doctoral Program in Clinical Psychology Major Area of Study: Neuropsychology Emphasis: Child and Adolescent Psychopathology Dissertation Chair: Ralph-Axel Müller, Ph.D. Dissertation Title: *Spatiotemporal Dynamics of Functional Brain Networks in Autism Spectrum Disorder*
2020-2021	**Pre-doctoral Internship** Emory University School of Medicine Major Area of Study: Adult/Pediatric Neuropsychology
2017	**Master of Science** in Clinical Psychology San Diego State University Thesis Chair: Jeanne Townsend, Ph.D. Thesis Title: *A Gaming Approach to the Assessment of Attention Networks in Autism Spectrum Disorder*
2013	**Bachelor of Science** in Integrative Neuroscience, Summa Cum Laude Binghamton University – State University of New York

PEER-REVIEWED PUBLICATIONS

Olson, L. A., Chen, B., Ibarra, I., Wang, T., **Mash, L. E.,** Linke, A. C., Kinnear, M. K., & Fishman, I. (2021). Externalizing behaviors are associated with increased parenting stress in caregivers of young children with autism. *Journal of Autism and Developmental Disorders.* https://doi.org/10.1007/s10803-021-04995-w

Linke, A.C., **Mash, L. E.,** Fong, C. H., Kinnear, M. K., Kohli, J. S., Wilkinson, M., Tung, R., Jao Keehn, R. J., Carper, R., Fishman, I., & Müller, R.-A. (2020). Dynamic time warping outperforms Pearson correlation in detecting atypical functional connectivity in autism spectrum disorders. *NeuroImage, 223*, 117383. https://doi.org/10.1016/j.neuroimage.2020.117383

Olson, L. A., **Mash, L. E.,** Linke, A. C., Fong, C. H., Müller, R.-A., & Fishman, I. (2020). Sex-related patterns of intrinsic functional connectivity in children and adolescents with autism spectrum disorders. *Autism, 24(8),* 2190-2201. https://doi.org/10.1177/1362361320938194

Quinde-Zlibut, J. M., Okitondo, C. D., Williams, Z. J., Weitlauf, A., **Mash, L. E.,** Heflin, B. H., Woodward, N. D., Cascio, C. J. (2020). Elevated thresholds for light touch in children with autism reflect more conservative perceptual decision-making rather than a sensory deficit. *Frontiers in Human Neuroscience, 14,* 122. https://doi.org/10.3389/fnhum.2020.00122

Mash, L. E., Keehn, B., Linke, A. C., Liu, T. T., Helm, J. L., Haist, F., Townsend, J., & Müller, R.-A. (2020). Atypical relationships between spontaneous EEG and fMRI activity in autism. *Brain Connectivity*, *10,* 18-28. https://doi.org/10.1089/brain.2019.0693

Failla, M. D., Bryant, L. K., Heflin, B. H., **Mash, L. E.,** Schauder, K. B., Davis, S., Gerdes, M. B., Weitlauf, A., Rogers, B. P., & Cascio, C. J. (2020). Neural correlates of cardiac interoceptive focus across development: Implications for social symptoms in autism spectrum disorder. *Autism Research, 13,* 908-920. https://doi.org/10.1002/aur.2289

Mash, L. E., Klein, R. M., & Townsend, J. (2020). A gaming approach to the assessment of attention networks in autism spectrum disorder and typical development. *Journal of Autism and Developmental Disorders. 50,* 2607-2615. https://doi.org/10.1007/s10803-018-3635-5

Mash, L. E., Linke, A. C., Olson, L. A., Fishman, I., Liu, T. T., & Müller, R.-A. (2019). Transient states of network connectivity are atypical in autism: A dynamic functional connectivity study. *Human Brain Mapping, 40,* 2377-2389. https://doi.org/10.1002/hbm.24529

Reiter, M. A., **Mash, L. E.,** Linke, A. C., Fong, C. H., Fishman, I., & Müller, R.-A. (2019). Distinct patterns of atypical functional connectivity in lower-functioning autism. *Biological Psychiatry: Cognitive Neuroscience and Neuroimaging, 4*, 251-259. https://doi.org/10.1016/j.bpsc.2018.08.009

Mash, L. E., Reiter, M. A., Linke, A. C., Townsend, J., & Müller, R.-A. (2018). Multimodal approaches to functional connectivity in autism spectrum disorders: An integrative perspective. *Developmental Neurobiology, 78,* 456-473. https://doi.org/10.1002/dneu.22570

Naviaux, R. K., Curtis, B. C., Li, K., [+13 authors] … **Mash, L. E.,** Chukoskie, L., Lincoln, A., & Townsend, J. (2017). Low-dose suramin in autism spectrum disorder: a small, phase I/II, randomized clinical trial. *Annals of Clinical and Translational Neurology, 4*, 491-505. https://doi.org/10.1002/acn3.424

Mash, L. E., Schauder, K. B., Channing, C., Park, S., & Cascio, C. J. (2017). Associations between interoceptive cognition and age in autism spectrum disorder and typical development. *Journal of Cognitive Education and Psychology, 16,* 23-37. https://doi.org/10.1891/1945-8959.16.1.23

Foss-Feig, J. H., McGugin, R. W., Gauthier, I., **Mash, L. E.,** Ventola, P., & Cascio, C. J. (2016) A functional neuroimaging study of fusiform response to restricted interests in children and adolescents with autism spectrum disorder. *Journal of Neurodevelopmental Disorders, 8*, 15. https://doi.org/10.1186/s11689-016-9149-6

Molet, M., Kosinski, T., Craddock, P., Miguez, G., **Mash, L. E.,** & Miller, R. R. (2016). Attenuating social affective learning effects with Memory Suppression manipulations. *Acta Psychologica, 164,* 136-143. https://doi.org/10.1016/j.actpsy.2016.01.001

Schauder, K. B., **Mash, L. E.,** Bryant, L. K. & Cascio, C. J. (2015). Interoceptive ability and body awareness in autism spectrum disorder. *Journal of Experimental Child Psychology, 131*, 193-200. https://doi.org/10.1016/j.jecp.2014.11.002

Miguez, G., **Mash, L. E**. Polack, C. W., & Miller, R. R. (2014). Failure to observe renewal following retrieval-induced forgetting. *Behavioural Processes. 103,* 43-51. https://doi.org/10.1016/j.beproc.2013.11.008

ABSTRACT OF THE DISSERTATION

Spatiotemporal Dynamics of Functional Brain Networks in Autism Spectrum Disorder

by

Lisa Elena Mash

Doctor of Philosophy in Clinical Psychology

University of California San Diego, 2021
San Diego State University, 2021

Professor Ralph-Axel Müller, Chair

Autism spectrum disorder (ASD) is a behaviorally diagnosed neurodevelopmental condition that is associated with atypical functional connectivity (FC). However, no consistent biomarkers have been identified. Most studies to date have focused on static FC, and relatively little is known about time-varying properties of FC. This three-paper dissertation aimed to better characterize brain networks in ASD by evaluating: 1) transient connectivity states, 2) BOLD lag

structure, and 3) associations between hemodynamic and electrophysiological measures of brain function. Study 1 (Mash et al., 2019) used sliding window analysis to examine FC variability and describe transient connectivity states in children and adolescents (ages 6-18) with ASD (n = 62) and their typically developing (TD) peers (n = 57). Across all regions, the ASD group showed FC overconnectivity and hypervariability, on average. Distinct patterns of FC group differences were found in two transient states, but not in static FC analyses. Study 2 (Mash et al., under review) explored resting-state and task-related BOLD lag structure in adolescents and young adults (ages 12-21) with ASD (n = 28) and typical development (n = 22). Lag patterns did not significantly differ between groups, with common 'early' and 'late' regions emerging in both groups. However, lag structure was associated with both task condition and vascular supply, suggesting a combination of neural and vascular contributions to BOLD latency. Study 3 (Mash et al., 2020) characterized relationships between separately acquired resting-state fMRI and EEG activity in a sample of children and adolescents (ages 6-18) with ASD and typical development (EEG-only: n = 36 per group; fMRI-only: n = 66 ASD, 57 TD; EEG-fMRI: n = 17 per group). Reduced EEG alpha power, increased BOLD activity in right temporal regions, and widespread thalamocortical BOLD overconnectivity were observed in the ASD group. Multilevel modeling (with brain regions nested within individuals) revealed mostly positive relationships between EEG alpha power and regional BOLD activity in typical development, which were not observed in ASD. Overall, findings suggest that in comparison to conventional static FC studies, dynamic and multimodal analyses reveal more complex FC and activity patterns that may distinguish ASD from typical development.

Chapter 1:

Integrated Introduction

The content within this section, titled "Chapter 1: Integrated Introduction," reflects material from a paper that has been published in the journal *Developmental Neurobiology.* The full citation is as follows:

Mash, L. E., Reiter, M. A., Linke, A. C., Townsend, J., & Müller, R.-A. (2018). Multimodal approaches to functional connectivity in autism spectrum disorders: An integrative perspective. *Developmental Neurobiology, 78,* 456-473. https://doi.org/10.1002/dneu.22570

Integrated Introduction

Autism spectrum disorders (ASDs) are neurodevelopmental disorders characterized by deficits in social communication and restricted or repetitive behaviors (American Psychiatric Association, 2013). These symptoms typically emerge within the first few years of life and persist throughout the lifespan. ASDs are a major research priority, as the Centers for Disease Control and Prevention estimate that 1 in 54 school-aged children in the United States are affected (Maenner, Shaw, Baio et al., 2020). The neuroimaging literature broadly indicates that ASDs are characterized by altered connectivity within and between brain networks (Di Martino, Yan, Li et al., 2014). Brain 'connectivity' can refer to structural (i.e., physical properties of neuronal connections), functional (i.e., a statistical relationship between activity in two or more regions), or effective (i.e., causal association between regions) relationships. Both structural and functional connectivity have been studied extensively in ASDs; however, this dissertation will focus on *functional connectivity* (FC).

Functional imaging data have extraordinary potential to characterize distributed brain activity across both space and time. However, reproducible biomarkers of ASDs have yet to be identified. This is likely, in part, due to the considerable heterogeneity across individuals on the autism spectrum. Phenotypic expression and outcome vary widely (Olsson, Westerlund, Lundstrom et al., 2015) and etiologically distinct variants of ASDs are likely (Geschwind & State, 2015). However, another major source of variability is methodological. Functional MRI (fMRI) and electroencephalography (EEG) are two commonly reported measures of FC in this population. These data have distinct neural bases and are best suited to different analyses; analyses in a single imaging modality are generally limited with respect to either spatial (e.g., electroencephalography [EEG]) or temporal (e.g., functional magnetic resonance imaging

[fMRI]) resolution. This has complicated efforts to compare and integrate findings across unimodal studies.

These discrepancies can be addressed in several ways: 1) Novel unimodal analyses may overcome the limitations of a given method, to some degree. For example, most functional connectivity MRI (fcMRI) research describes static relationships between brain regions over several minutes of scanning. However, dynamic fcMRI methods aim to explore changes in these relationships over time, despite the relatively low temporal resolution of MRI. Analyses have also been proposed to examine BOLD 'lag structure,' thought to reflect propagation between regions comprising functional networks (Mitra, Snyder, Blazey et al., 2015; Mitra, Snyder, Hacker et al., 2014). 2) Data acquired in multiple modalities can be jointly analyzed to improve our understanding of the relationship between electrophysiological and fMRI measures, aiding in comparison and integration across previous unimodal work. The vast majority of functional imaging research in ASDs to date is unimodal, although interest has recently shifted toward increasingly dynamic, multimodal approaches (Mash, Reiter, Linke et al., 2018).

As mentioned above, EEG and fMRI detect distinct physiological signals and have largely complementary strengths and limitations. EEG directly measures summated post-synaptic potentials (PSPs), arising mostly from pyramidal neurons, using sensors placed at the scalp (Niedermeyer, Schomer, & Lopes da Silva, 2011). This approach provides high temporal resolution and captures neural oscillations across a broad frequency range (Buzsaki, 2006). Within given frequency bands, connectivity is typically measured in terms of power (the magnitude of voltage calculated from amplitude, often following time-frequency decomposition of waveforms), or coherence (phase-coupling across distant electrodes; for a review of coherence approaches see Bowyer, 2016). However, the spatial resolution of EEG is limited, particularly

for deep brain structures. Additionally, the measured signal at the scalp represents the summation of signal from many sources, and skull and tissue conductivity may cause EEG signals to blur across sensors (van den Broek, Reinders, Donderwinkel et al., 1998). Magnetoencephalography (MEG) is another commonly reported electrophysiological recording method with some key differences from EEG, but these will not be discussed in detail, as MEG is outside scope of this dissertation (Hillebrand & Barnes, 2002; Supek & Aine, 2014; Winter, Nunez, Ding et al., 2007)

In fMRI, the blood oxygenation level-dependent (BOLD) signal is a hemodynamic proxy for neural activity. Compared to EEG, fMRI can accurately localize signals from both cerebral cortex and deep brain structures (i.e., high spatial-resolution, full brain coverage). Therefore, fMRI is useful for identifying both regional brain activity and correlations among functionally related areas over a scan period (i.e., functional connectivity; Biswal, Yetkin, Haughton et al., 1995; Fox & Raichle, 2007). Temporal resolution, however, is limited by low sampling rates (typically ~ 2 seconds) and the shape of the hemodynamic response, which peaks about 5 seconds after corresponding neuronal activity changes. Therefore, BOLD correlations are commonly measured in frequency bands below .1 Hz (Cordes, Haughton, Arfanakis et al., 2000), although functional networks may also be detected at slightly higher frequencies (Gohel & Biswal, 2015).

Functional Connectivity in ASDs

Despite the large and fast-growing fcMRI literature exploring ASDs, functional network organization in this disorder remains poorly understood. Early FC findings appeared to support general underconnectivity within distributed cortical networks during a variety of tasks (Just, Cherkassky, Keller et al., 2007; Just, Cherkassky, Keller et al., 2004; Kana, Keller, Cherkassky et al., 2006; Kleinhans, Richards, Sterling et al., 2008; Koshino, Kana, Keller et al., 2008;

Mostofsky, Powell, Simmonds et al., 2009). However, other studies have found more complex patterns of mixed over- and under-connectivity associated with memory tasks (Koshino, Carpenter, Minshew et al., 2005; Noonan, Haist, & Müller, 2009). Task-free (i.e., resting-state) fMRI studies testing intrinsic FC reveal functional network architecture at rest (Biswal et al., 1995; Van Dijk, Hedden, Venkataraman et al., 2010). This approach, in contrast with task-based methods, has frequently produced mixed patterns of under- and over-connectivity in ASDs (e.g., Fishman et al., 2014; Supekar et al., 2013; for reviews, refer to Hull et al., 2016 and Rane et al., 2015). Methodological differences likely account for some of the discrepancies observed between studies using task-based and resting-state designs (Jones, Bandettini, Kenworthy et al., 2010; Müller, Shih, Keehn et al., 2011; Nair, Keown, Datko et al., 2014).

In light of mixed findings, underconnectivity between distant regions and increased local connectivity was proposed (Belmonte, Allen, Beckel-Mitchener et al., 2004). However, neither long-range underconnectivity nor short-range overconnectivity is consistently supported by the existing literature (for review, see Vissers, Cohen, & Geurts, 2012). Indeed, not a single fcMRI study examining local connectivity, using graph theory (Itahashi, Yamada, Watanabe et al., 2015; Keown, Shih, Nair et al., 2013) or regional homogeneity methods (Dajani & Uddin, 2016; Jiang, Hou, Yang et al., 2015; Maximo, Keown, Nair et al., 2013; Nair, Jao Keehn, Berkebile et al., 2017), has found broadly consistent local overconnectivity in ASDs. Rather, findings have been mixed and region-specific, even in studies analyzing fMRI data without regional homogeneity standardization (Maximo et al., 2013; Nair et al., 2017), which could theoretically obscure global group differences in local connectivity.

Similar to fcMRI, EEG and MEG findings in ASDs have been inconsistent, with both increased and decreased coherence observed across various task and analysis designs. This is

further complicated by differences between frequency bands and brain regions (Kitzbichler, Khan, Ganesan et al., 2015; Ye, Leung, Schafer et al., 2014) . A recent review concluded that reduced coherence between distant electrodes, often interpreted as underconnectivity, is generally supported, but is found most consistently in low frequencies, with mixed findings in higher frequencies (O'Reilly, Lewis, & Elsabbagh, 2017). Unlike coherence, power appears to be increased in ASDs at low and high frequencies, but decreased in middle frequencies, such as alpha and beta (Wang, Barstein, Ethridge et al., 2013). Although power and coherence are each affected by synchronized neural activity, these are ultimately different measures of 'connectivity', and it is therefore difficult to interpret their distinct frequency-related patterns. Even more importantly, there is no clear translation between these constructs and those measured in fMRI (i.e., BOLD correlations). Therefore, EEG and MEG findings may not be readily suited to addressing fcMRI under- and overconnectivity hypotheses.

Many recent studies have shifted away from an overconnectivity/underconnectivity framework toward a broader network organization perspective. A growing literature suggests that neural networks in ASDs may be inefficiently organized due to poor functional differentiation and integration. Specifically, several fMRI studies have revealed reduced connectivity within networks, but increased connectivity between networks (Fishman et al., 2014; Rudie, Shehzad, Hernandez et al., 2012; Shih, Keehn, Oram et al., 2011). This theory has found additional support in studies using graph theory metrics to characterize network properties of both fMRI (Chen, Nomi, Uddin et al., 2017; Keown, Datko, Chen et al., 2017; Rudie, Brown, Beck-Pancer et al., 2012) and EEG/MEG data (Peters, Taquet, Vega et al., 2013; Pollonini, Patidar, Situ et al., 2010; Tsiaras, Simos, Rezaie et al., 2011), suggesting possible consensus across recording methods at the network level. However, opposite findings have also been

reported in fMRI, suggesting *increased* modularity in ASDs (Barttfeld, Wicker, Cukier et al., 2011; Yerys, Herrington, Satterthwaite et al., 2017). Additionally, group differences in network efficiency appear to vary across MEG frequency bands (Kitzbichler et al., 2015). The precise characterization of network organization in ASDs remains an area of active, ongoing study.

Although several promising themes have emerged across the fMRI and EEG literatures, no single hypothesis accommodates all reported findings. This highlights the importance of adopting novel unimodal and multimodal analysis strategies to better understand connectivity in ASDs (Mash et al., 2018). Because fMRI and EEG are generated by different sources and suited to different analyses, these literatures have remained largely separate in ASD research. This has limited our ability to draw conclusions across modalities. For an integrated interpretation of fcMRI and EEG findings, the neurophysiological bases of different signals must first be reconciled.

Neural Bases of fMRI and EEG

The direct relationship between EEG signals and extracellular, postsynaptic activity (measured as local field potentials; LFPs) is well-established. The BOLD signal, however, is a secondary hemodynamic measure that relies on neurovascular coupling, which is not perfectly understood (Hillman, 2014). Simultaneous fMRI and intracortical recordings have been used to investigate the neurovascular bases of BOLD changes. Overall, intracortical recordings suggest that, like the EEG signal, fluctuations in BOLD are more closely related to synaptic activity (LFPs, specifically in the gamma band) than action potentials. This has been demonstrated in anesthetized animals (Logothetis, Pauls, Augath et al., 2001) and awake animals (Hutchison, Hashemi, Gati et al., 2015; Magri, Schridde, Murayama et al., 2012; Shmuel & Leopold, 2008), as well as in humans during task performance (Conner, Ellmore, Pieters et al., 2011 ; Gaglianese,

Vansteensel, Harvey et al., 2017; Nir, Fisch, Mukamel et al., 2007) and at rest (He, Snyder, Zempel et al., 2008; Nir et al., 2007; Nir, Mukamel, Dinstein et al., 2008).

Compared to intracortical recordings, simultaneous EEG and fMRI acquisition is less invasive and therefore far more widely used in human research. EEG-fMRI studies have sought to further clarify the relationship between electrical signals measured at the scalp, localized BOLD activity, and BOLD correlations across networks (for reviews, see Mulert, 2013; Murta, Leite, Carmichael et al., 2015). EEG alpha rhythms (~8-12 Hz) are dominant at rest and have been most widely studied in relation to spontaneous BOLD signal changes. Increases in alpha power are associated with simultaneously reduced BOLD activity in frontal, occipital, and parietal areas (Bridwell, Wu, Eichele et al., 2013; Goldman, Stern, Engel et al., 2002; Laufs, Kleinschmidt, Beyerle et al., 2003; Olbrich, Mulert, Karch et al., 2009); a similar relationship has been reported for beta power increases (Murta, Chaudhary, Tierney et al., 2017; Scheeringa, Fries, Petersson et al., 2011). However, a consistently *positive* relationship has been found between alpha power and thalamic BOLD (Bridwell et al., 2013; de Munck, Goncalves, Huijboom et al., 2007; Goldman et al., 2002).

Although most early studies focused on the alpha frequency band, different EEG frequencies, each associated with distinct functional states (Buzsaki, 2006), may relate differently to the BOLD signal. Unique relationships between BOLD networks derived from independent component analysis (ICA) and specific EEG frequency bands have been demonstrated (Mantini, Perrucci, Del Gratta et al., 2007; Neuner, Arrubla, Werner et al., 2014). In line with the intracortical literature, positive associations have consistently been found between EEG gamma power and local BOLD activity (Bridwell et al., 2013; Murta et al., 2017;

Scheeringa et al., 2011). Furthermore, Scheeringa and colleagues (2011) reported that fast (gamma) and slower (alpha and beta) oscillations predict unique variance in the BOLD signal.

Relatively less is understood about links between EEG power and BOLD correlations (i.e., FC). One relatively consistent finding is an inverse relationship between alpha power and coupling (positive or negative) between networks; in other words, increased alpha power is associated with less positive BOLD correlations in correlated networks, and less negative BOLD correlations in anticorrelated networks (Allen, Damaraju, Eichele et al., 2017; Scheeringa, Petersson, Kleinschmidt et al., 2012). However, one study found increased modularity (anticorrelation) between default mode and dorsal attention networks associated with increased alpha power (Chang, Liu, Chen et al., 2013). Another group reported that relationships between BOLD connectivity and alpha/beta power appear to be state-dependent (Tagliazucchi, von Wegner, Morzelewski et al., 2012). This study also identified many BOLD connections that were positively associated with gamma (which, however, may be confounded by muscle activity; Muthukumaraswamy, 2013). Overall, the relationship between BOLD correlations and electrophysiological power is poorly understood, and appears to depend on regions of interest, cognitive state, and frequency band studied.

Dynamic Functional Connectivity Approaches

Most fcMRI studies to date have used a traditional, 'static' approach to estimating BOLD connectivity by using all data points of a scan to generate a single estimate of FC. However, communication between brain networks is highly flexible, and a static approach may therefore mischaracterize FC by ignoring important temporal information (Calhoun, Miller, Pearlson et al., 2014; Ciric, Nomi, Uddin et al., 2017). Dynamic properties of brain activity have long been a focus of electroencephalography (EEG) and magnetoencephalography (MEG), whereas dynamic

fcMRI approaches have only recently been developed (for reviews: Hutchison, Womelsdorf, Allen et al., 2013; Preti, Bolton, & Van De Ville, 2017). Interest in dynamic fcMRI methods has grown considerably in recent years, with recent studies demonstrating reproducible spatiotemporal network connectivity patterns using various methods, such as sliding window functional connectivity (Allen, Damaraju, Plis et al., 2014; Nomi, Farrant, Damaraju et al., 2016) and exploration of quasi-periodic patterns of anticorrelated activity in opposing functional networks (Abbas, Bassil, & Keilholz, 2019; Abbas, Belloy, Kashyap et al., 2019).

Direct comparisons of fMRI connectivity measures (e.g., BOLD correlations) with EEG connectivity measures (e.g., power, coherence) are challenging at best, and possibly inappropriate. However, the study of transient brain states through dynamic fcMRI may provide a novel solution to this problem. Sliding window analysis is a popular and relatively straightforward dynamic connectivity approach (Allen et al., 2014; Hutchison et al., 2013). This method generates a series of temporally contiguous connectivity matrices. These can then be clustered into representations of transient, repeating connectivity patterns (i.e., brain states), which are thought to correspond to cognitive states (Vidaurre, Smith, & Woolrich, 2017). Crucially, electrophysiological and hemodynamic measures of neural activity may be integrated more readily when assessed at the level of states and their dynamic changes over time, compared to static measures of over- and underconnectivity (Allen et al., 2017).

However, there is currently little consensus about best practices concerning window length and overlap, which have been shown to affect findings (Hindriks, Adhikari, Murayama et al., 2016; Shakil, Lee, & Keilholz, 2016). Furthermore, the temporal resolution of single-modality dynamic fcMRI remains limited by the slowness of the BOLD response. While some have questioned the meaning of BOLD dynamics altogether (Laumann, Snyder, Mitra et al.,

2016; Nalci, Rao, & Liu, 2019), others have found the approach to be generally reliable (Abrol, Damaraju, Miller et al., 2017; Smith, Zhao, Keilholz et al., 2018). Despite these limitations, the study of transient connectivity states may be one of the most promising avenues towards integrating electrophysiological and hemodynamic measures of brain function.

Whereas sliding window analysis captures time-varying changes of BOLD correlations at 'zero-lag', resting state lag analysis (RSLA) examines whether these relationships are better modeled using offset timeseries (Mitra et al., 2014). In other words, cross-covariance is calculated between each pair of timeseries at different lags, and covariance at each lag is plotted. Parabolic interpolation is then used to estimate the 'optimal' lag of the given timeseries. Using this method, putative sources and sinks of neural activity have been identified in typically developing adults (Mitra et al., 2015; Mitra et al., 2014; Raut, Mitra, Marek et al., 2019). Early work suggests that latencies observed using RSLA change as a function of task performance, time of day, and eye status, which has been interpreted as evidence for a neural basis for lag topographies (Mitra et al., 2014). However, it is also important to consider hemodynamic impacts on the timing of the BOLD signal; the same study reported that BOLD latencies were biased toward large venous sinuses. The degree to which other vascular properties (e.g., arterial transit time, arterial flow territories) affect BOLD lag structure remains unclear.

Evolving Methods in ASD Research

The fcMRI literature on ASDs remains largely inconclusive, with reported methods typically limited to static and unimodal analyses. While EEG and MEG work have provided some important insights about oscillatory activity at finer time scales, dynamic and multimodal approaches show great promise in uniting these bodies of work.

Interest in dynamic fcMRI in ASDs has recently grown, with a number of studies turning to transient brain states to better understand complex spatiotemporal patterns of brain connectivity. Some early studies have reported associations between static underconnectivity and increased variability in connection strength over time (Chen et al., 2017; Falahpour, Thompson, Abbott et al., 2016), reduced switching between transient brain states (de Lacy, Doherty, King et al., 2017; Fu, Tu, Di et al., 2018; Watanabe & Rees, 2017), and transient overconnectivity between default mode and non-default mode networks (de Lacy et al., 2017; Mash, Linke, Olson et al., 2019). Dynamic methods have also been used to identify diagnostic subtypes (Easson, Fatima, & McIntosh, 2018), and to predict ASD diagnostic status (Wee, Yap, & Shen, 2016; Zhu, Zhu, Zhang et al., 2016). However, this line of research is at an early stage, with many studies reporting different analytic approaches and dynamic measures. Therefore, there is much work to be done to clarify the nature of time-varying FC in ASDs.

In a similar vein, there is some evidence that the temporal lag structure of the BOLD signal may be atypical in ASDs. Using resting state lag analysis, Mitra, Snyder, Constantino et al. (2017) reported that compared to typically developing (TD) individuals, ASD participants showed atypically 'early' activity in frontopolar cortex and putamen, and atypically 'late' activity in occipital cortex, with respect to the rest of the brain; there were no group differences in zero-lag BOLD correlations. Another study reported predominant overconnectivity in ASDs compared to typical development *only* when using lagged BOLD correlations, regardless of lag direction, but not zero-lag correlations (King, Prigge, King et al., 2018). This was interpreted as evidence of atypically prolonged synchrony over time. However, group differences in hemodynamic variables cannot be entirely ruled out as an explanation for atypical BOLD lag. Differences in neurotransmitter synthesis (e.g., GABA) and metabolic activity, which have been

implicated in ASDs, may directly impact neurovascular coupling (Reynell & Harris, 2013). Furthermore, a recent study found that the shape of the hemodynamic response function (HRF) in the precuneus significantly differed in individuals with ASDs, and that some group differences in functional connectivity were only observed after deconvolving BOLD time series with the HRF (Yan, Rangaprakash, & Deshpande, 2018). Overall, the relative neural and hemodynamic contributions to group differences in BOLD lag are unclear. However, the few previous studies in this area suggest that this is an important aspect of dynamic FC to consider in ASDs.

Finally, multimodal FC research in ASDs remains extremely limited to date (Mash et al., 2018). To our knowledge, only two simultaneous EEG-fMRI studies have been published in this population; both included relatively small samples ($n < 15$ per group) and focused primarily on cortical responses to audiovisual stimulation (Hames, Murphy, Rajmohan et al., 2016; Jochaut, Lehongre, Saitovitch et al., 2015). However, there have been no studies jointly analyzing resting-state EEG and fMRI, either simultaneously or separately acquired. As described earlier, there is a relatively well-documented relationship between EEG alpha power, thalamocortical BOLD activity, and BOLD network synchronization in typical adults. Abnormalities in alpha power (Wang et al., 2013), network integration and segregation (Fishman et al., 2014; Rudie, Shehzad, et al., 2012; Shih et al., 2011) and thalamocortical connectivity (Nair, Carper, Abbott et al., 2015; Nair, Treiber, Shukla et al., 2013; Woodward, Giraldo-Chica, Rogers et al., 2017) are among best replicated findings in the ASD literature. Therefore, multimodal studies addressing the relationship between alpha power and BOLD activity in individuals with ASDs are warranted.

General aims

The main goals of this three-paper dissertation are as follows: 1) to better characterize dynamic FC fluctuations and transient brain states using sliding window analysis and k-means clustering, 2) to examine resting-state and task-related BOLD lag structure and its relation to the hemodynamic variables, and 3) to explore interindividual relationships between separately acquired resting-state EEG and fMRI measures in ASDs and typical development.

Dissertation Author Note

Chapter 1, in part, is a reprint of the material as it appears in Developmental Neurobiology, 78, 456-473. Mash, L. E., Reiter, M. A., Linke, A. C., Townsend, J., & Müller, R.-A. Wiley, 2017.

Chapter 2:

Study 1

The content within this section, titled "Chapter 2: Study 1," reflects material from a paper that has been published in the journal *Human Brain Mapping.* The full citation is as follows:

Mash, L. E., Linke, A. C., Olson, L. A., Fishman, I., Liu, T. T., & Müller, R.-A. (2019). Transient states of network connectivity are atypical in autism: A dynamic functional connectivity study. *Human Brain Mapping, 40,* 2377-2389. https://doi.org/10.1002/hbm.24529

Abstract

There is ample evidence of atypical functional connectivity (FC) in autism spectrum disorders (ASDs). However, transient relationships between neural networks cannot be captured by conventional static FC analyses. Dynamic FC approaches have been used to identify repeating, transient connectivity patterns ("states"), revealing spatiotemporal network properties not observable in static FC. Recent studies have found atypical dynamic FC in ASDs, but questions remain about the nature of group differences in transient connectivity, and the degree to which states persist or change over time. This study aimed to 1) describe and relate static and dynamic FC in typical development and ASDs, 2) describe group differences in transient states and compare them with static FC patterns, and 3) examine temporal stability and flexibility between identified states. Resting-state functional magnetic resonance imaging (fMRI) data were collected from 62 ASD and 57 typically developing (TD) children and adolescents. Whole-brain, data-driven regions of interest were derived from group independent component analysis. Sliding window analysis and k-means clustering were used to explore dynamic FC and identify transient states. Across all regions, static overconnnectivity and increased variability over time in ASDs predominated. Furthermore, significant patterns of group differences emerged in two transient states that were not observed in the static FC matrix, with group differences in one state primarily involving sensory and motor networks, and in the other involving higher order cognition networks. Default mode network segregation was significantly reduced in ASDs in both states. Results highlight that dynamic approaches may reveal more nuanced transient patterns of atypical FC in ASDs.

Introduction

Autism spectrum disorders (ASDs) are characterized by atypical social communication and restricted and repetitive behaviors or interests (American Psychiatric Association, 2013) and have high prevalence, recently estimated at 1 in 45 school-aged children in the United States (Zablotsky, Black, Maenner, Schieve, & Blumberg, 2015). Improved understanding of the biological bases of these disorders is therefore a high research priority. Of particular focus in the past decade have been studies of brain network connectivity in ASDs, given increasing awareness that symptomatology cannot be explained exclusively by localized brain anomalies (Müller, 2007; Rippon, Brock, Brown, & Boucher, 2007).

Functional connectivity MRI (fcMRI) refers to a type of analysis that detects spontaneous, temporally coherent blood oxygen level-dependent (BOLD) activity in functionally related regions (Biswal, Yetkin, Haughton, & Hyde, 1995; Fox & Raichle, 2007). The term "fcMRI" distinguishes this from functional connectivity analyses in other modalities (e.g., EEG or MEG). Correlated BOLD activity among distant brain regions in the resting state (i.e., in absence of a task) is considered to reflect a history of shared activation (Cordes et al., 2000), which can be interpreted as membership in a common functional network. Therefore, fcMRI is useful for examining intrinsic functional connectivity (iFC) within and between distinct brain networks. However, the fcMRI literature on ASDs has generated many inconsistencies with respect to over- and underconnectivity, without converging on a single explanatory model. Early research examined BOLD correlations during specific cognitive tasks, rather than at rest. These studies appeared to support general underconnectivity in ASDs during some tasks (Just, Cherkassky, Keller, Kana, & Minshew, 2007; Just, Cherkassky, Keller, & Minshew, 2004; Kana, Keller, Cherkassky, Minshew, & Just, 2006; Kleinhans et al., 2008; Koshino et al., 2008;

Mostofsky et al., 2009). However, task-free iFC studies exploring spontaneous BOLD correlations have often found more complex patterns of over- and under-connectivity between various regions (Fishman, Keown, Lincoln, Pineda, & Müller, 2014; Supekar et al., 2013; for reviews, see Hull, Jacokes, Torgerson, Irimia, & Van Horn, 2016; Rane et al., 2015). Methodological differences between task-based and resting-state designs likely play an important role in these discrepancies, as do various preprocessing and analysis decisions (for review, Müller et al., 2011). A dichotomy of long-range underconnectivity and short-range overconnectivity has been proposed to accommodate diverse findings (Belmonte et al., 2004), but supportive evidence is weak, with mixed findings of over- and under-connectivity in studies testing local (Dajani & Uddin, 2016; Itahashi et al., 2015; Keown et al., 2013; Maximo, Keown, Nair, & Müller, 2013; Nair et al., 2017) and long-distance connectivity in ASDs (e.g., Abbott et al., 2016; Doyle-Thomas et al., 2015). Of note, the terms "overconnectivity" and "underconnectivity" refer to relative group differences between BOLD correlations. For example, "overconnectivity" can refer to either increased correlation or decreased anticorrelation of time series in two brain regions.

As described above, the fcMRI literature in ASDs to date has included both task-based and resting-state designs. However, both types of studies have almost exclusively used traditional, 'static' approaches to estimating BOLD connectivity. Static analyses use all data points of a scan to generate a single estimate of iFC, and may therefore overlook crucial time-varying properties of iFC. However, neural communication between networks is highly flexible, and important temporal information is therefore lost in static fcMRI analysis (Ciric, Nomi, Uddin, & Satpute, 2017). Dynamic properties of brain activity have long been a focus of electroencephalography (EEG) and magnetoencephalography (MEG), whereas dynamic

functional connectivity (dFC) MRI approaches have only recently been developed (for reviews: Hutchison et al., 2013; Preti, Bolton, & Van De Ville, 2017). The most common 'sliding window' method involves calculating FC across overlapping time windows to generate a series of temporally contiguous connectivity matrices. In one widely used data-driven method, developed by Allen et al. (2014), functional networks are derived through independent component analysis (ICA), sliding window connectivity between networks is calculated, and windows are subsequently clustered into distinct 'states'. Although strictly speaking mathematical abstractions, these dynamic FC states are thought to represent distinct, underlying cognitive states experienced by individuals during a scan (Vidaurre, Smith, & Woolrich, 2017). However, dynamic FC methods are relatively new, and gold standards have yet to be agreed upon with respect to sliding window parameters such as window length and overlap. Indeed, some have raised doubts about the reliability of sliding window methods, and the degree to which resulting states represent true functional connectivity configurations (Laumann et al., 2016; Nalci, Rao, & Liu, 2019; Shakil et al., 2016). For example, in heterogeneous samples differences in dynamic FC measures may arise from non-neuronal sources of variability (Lehmann, White, Henson et al., 2017).

Nevertheless, the existence of discrete cognitive and neural states is supported by evidence from the EEG and simultaneous EEG/fMRI literature. Spontaneous, mutually exclusive 'microstates' have long been a focus of EEG studies (for review, Khanna, Pascual-Leone, Michel, & Farzan, 2015), and simultaneous EEG/fMRI research suggests that EEG microstates are highly correlated with specific BOLD networks (Britz, Van De Ville, & Michel, 2010; Musso, Brinkmeyer, Mobascher, Warbrick, & Winterer, 2010; Yuan, Zotev, Phillips, Drevets, & Bodurka, 2012). Although the duration of EEG microstates is very short (~100 ms), their

relationship with low-temporal resolution static fcMRI networks may be explained by evidence of scale-free temporal dynamics of EEG microstates; in other words, EEG microstates exhibit consistent temporal patterns even at time scales of multiple seconds (Van de Ville, Britz, & Michel, 2010). Complementing the links between EEG microstates and static BOLD networks, dynamic fcMRI states have shown associations with distinct patterns of EEG power across frequency bands (Allen, Damaraju, Eichele, Wu, & Calhoun, 2017).

Despite their recent emergence and lack of a definitive gold standard, dynamic approaches may help to resolve inconsistencies in the static fcMRI literature described earlier. Atypical functional connectivity in ASDs is likely considerably more complex than static approaches suggest. For example, group differences in connectivity may vary between transient brain states, resulting in changes over time that cannot be detected in static analyses. dFC approaches have been applied recently to other psychiatric populations, such as schizophrenia and bipolar disorder (Damaraju et al., 2014; Du et al., 2017; Rashid, Damaraju, Pearlson, & Calhoun, 2014). While evidence for dFC abnormalities in ASDs remains very limited, initial studies show promise. For example, unique regional patterns of group differences have been demonstrated in transient states, which differ from those observed in static connectivity analyses (Chen et al., 2017; de Lacy et al., 2017). Furthermore, dynamic connectivity measures have been found to improve diagnostic prediction of ASDs (Wee, Yap, & Shen, 2016; Zhu et al., 2016), and have also been explored as a potential subtype classifier (Easson et al., 2018). However, findings with respect to transient state duration and flexibility have been more difficult to interpret. Two studies reported that static underconnectivity in ASDs was associated with atypically increased variability over time (Chen, Nomi, Uddin, Duan, & Chen, 2017; Falahpour et al., 2016). In one of these, mediation analysis indicated that static underconnectivity between

two nodes of the default mode network (DMN) was directly affected by increased temporal variability of that same connection (Falahpour et al., 2016). This suggests that common underconnectivity findings do not necessarily indicate 'weaker' connections, but may instead reflect greater variability in functional connectivity over time. Using different approaches to study temporal dynamics of functional connectivity, other studies have reported less frequent switching between transient states in ASDs, suggesting overly *stable* dynamic properties (de Lacy, Doherty, King, Rachakonda, & Calhoun, 2017; Fu et al., 2018; Watanabe & Rees, 2017). Similarly, Rashid, Blanken, Muetzel et al. (2018) found that in a large sample of typically developing (TD) children, autistic traits were associated with longer dwell times in a 'globally disconnected' state. This is further supported by a recent EEG study of brain network dynamics, which reported longer duration of quasi-stable resting state networks in children with ASDs (Malaia, Bates, Seitzman et al., 2016). However, state-switching and dwell-time are higher-order measures of 'stability', which do not necessarily map directly to variability of individual region-to-region correlations, as measured by Falahpour et al. For example, it is possible that higher-order measures of stability, such as reduced state-switching, may underlie perseverative, inflexible behavior associated with ASDs, whereas increased variability between regions may be related to specific functional impairments in language and social domains. Therefore, these findings are not mutually exclusive, but do raise important questions that warrant additional research. In particular, on measures of ASD symptomatology (e.g., ADOS-2, ADI-R, SRS-2), restricted and repetitive behavior subscales may be higher for individuals who dwell longer in each state and switch less frequently between them, whereas social communication scores may relate predominantly to time-varying fluctuations between regions involved in language or salience.

The current paper applied a data-driven, ICA-based method to an in-house dataset of children and adolescents with and without ASDs. The aims of this investigation were to explore the following questions: 1) Are static iFC and iFC variability inversely related across a broad range of regions and networks (i.e., can iFC variability lead to erroneous conclusions about static underconnectivity in ASD)?, 2) Are group differences in transient brain states distinct from group differences in static iFC (i.e., can multiple transient state configurations account for inconsistent static iFC findings)?, and 3) Do individuals with ASDs show increased or reduced state-switching compared to TD participants (i.e., do ASD participants show differences in neural stability and flexibility)?

Methods

Participants

The study included 119 individuals (62 ASD, 57 TD) ages 6-18 years. All ASD diagnoses were confirmed using the Autism Diagnostic Interview–Revised (ADI-R, Lord, Rutter, & Le Couteur, 1994) and the Autism Diagnostic Observation Schedule, Second Edition (ADOS-2, Gotham, Risi, Pickles, & Lord, 2007). The Wechsler Abbreviated Scales of Intelligence-Second Edition (WASI-II, Wechsler, 2011) and Social Responsiveness Scale, Second Edition (SRS-2, Constantino & Gruber, 2012) parent report form were administered to individuals in both groups. The SRS-2 was missing for two TD participants. Groups were matched on age, handedness, sex, nonverbal IQ, and head motion (Table 1a). All TD participants were unmedicated. Twenty-eight ASD participants were reportedly taking medication, 29 were unmedicated, and medication status was not documented for the remaining five. Select analyses were conducted using the full sample, and repeated with only unmedicated ASD participants. Comorbid psychiatric diagnoses were documented in twenty ASD

participants. Details regarding medication usage and comorbid diagnoses are reported in Supplemental Table 1.

Data acquisition

Imaging data were acquired on a GE 3T MR750 scanner with an 8-channel head coil at the Center for Functional MRI (University of California, San Diego). High-resolution structural images were acquired with a standard FSPGR T1-weighted sequence (TR: 8.108ms, TE: 3.172 ms, flip angle: 8°; FOV 256 mm; 1mm^3 resolution; 172 slices). Functional T2*-weighted images were acquired using a single-shot gradient-recalled, echo-planar imaging pulse sequence (TR: 2000ms; TE: 30 ms; flip angle: 90°; 3.4mm^3 resolution; FOV: 220mm; matrix: 64 x 64; 42 axial slices). One 6:10 minute resting-state scan was obtained consisting of 185 whole-brain volumes. The first five volumes were discarded to account for T1-equilibration effects. Subjects were instructed to fixate on a cross projected onto the middle of a screen, viewed through a mirror in the bore, and to "Let your mind wander, relax, but please stay as still as you can. Do not fall asleep." Compliance with instructions to remain still and awake was monitored via video recording.

fMRI data processing

Functional images were processed using Analysis of Functional NeuroImages software (AFNI v17.2.07; Cox, 1996) and FSL (v5.0; Smith et al., 2004). Images were slice-time corrected and each functional volume was registered to the middle time point of the scan to adjust for motion via rigid-body realignment as implemented in AFNI. Field map correction was applied to minimize distortions due to magnetic field inhomogeneity. The functional images were registered to the anatomical scan via FSL's FLIRT (Jenkinson & Smith, 2001). Anatomical and functional images were resampled to 3mm isotropic voxels and standardized to the atlas

space of the Montreal Neurological Institute (MNI) template using FSL's nonlinear registration tool (FNIRT). AFNI's 3dBlurToFWHM was used to smooth functional images to a Gaussian full width at half-maximum (FWHM) of 6 mm. Functional MRI time series were bandpass filtered ($.008 < f < .08$ Hz) using a second-order Butterworth filter, which was also applied to the 10 nuisance regressors (see below).

Given the known impact of motion on BOLD correlations (Power et al., 2014), additional measures were taken to correct for motion. The mean signal from ventricles and white matter masks (obtained from FSL segmentation of T1-weighted structural image and eroded by 1 voxel) as well as six motion parameters (obtained from rigid-body realignment) and their first temporal derivatives were regressed from the signal. Residuals from nuisance regression were used for all subsequent functional connectivity analyses. Root mean squared displacement (RMSD), an estimate of head motion across all time points, was calculated for each participant as the square root of the sum of squares of the six motion parameters described above. Framewise displacement (FD) was calculated as a volume-by-volume measure of motion. Time points with > 0.5 mm FD as well the two subsequent time points were censored. Time series fragments with < 10 consecutive time points remaining after censoring were also excluded. Of note, dynamic FC analyses typically avoid time point censoring in order to maintain a continuous time series. However, in this analysis a very small amount of censoring was deemed necessary to avoid 1) artefact introduced by noisy time points and 2) reducing our sample size by using only participants with complete time series < 0.5 mm FD. On average, both groups underwent minimal censoring (mean: 1.4% timepoints in each group). No censoring was needed in 38 ASD participants (61%) and 36 TD participants (63%), and the maximum number of censored time points for any individual was 21 (12%) in the ASD group, and 20 (9%) in the TD group. The two

groups did not significantly differ with respect to number of timepoints censored ($t(117) = .18$, $p = .85$). Supplemental analyses demonstrate that RMSD was not related to group differences in connectivity patterns (cf. Supplemental Fig. 4). All structural and functional data were visually inspected at every preprocessing stage by at least two blinded reviewers to ensure acceptable data quality.

Overview of Analyses

Our analytical approach is briefly summarized here to aid readers in navigating the following sections, which describe each step in detail. First, data-driven regions of interest (ROIs) were identified and classified by functional network. We then examined static iFC between each ROI and each network. The variability of these functional connections was then assessed using sliding windows. Static iFC and iFC variability were then compared across all ROI pairs and networks. Finally, k-means clustering was used to identify transient iFC states and compare them across groups at the ROI- and network-levels.

Regions of Interest (ROIs)

A data-driven approach was used to define functionally related areas (ROIs) to be used in subsequent analysis. Preprocessed functional data from both groups (combined) were subjected to group independent component analysis (ICA) using FSL's Multivariate Exploratory Linear Optimized Decomposition into Independent Components (MELODIC). A multi-session temporal concatenation approach was used to generate 75 group components. High-order group ICA was selected, as in previous papers using this method (Allen et al., 2014; de Lacy et al., 2017), to isolate regionally specific subsets of large functional networks. Independent components were assessed using a semi-automatic selection process. The main criteria considered were percentage overlap with gray matter and weighted spatial correlation with the ten primary low-order ICA

networks derived by Smith et al. (2009) from the BrainMap database (Laird, Lancaster, & Fox, 2005; fmrib.ox.ac.uk/datasets/brainmap+rsns). A conservative 99% threshold was used to calculate gray matter overlap using AFNI's 3dABoverlap, because non-artefactual (especially subcortical) components were expected to expand into non-gray matter compartments due to smoothness and spatial normalization. Components with ≥ 65% gray matter overlap and correlation of $r \geq .10$ with at least one BrainMap component were considered acceptable. The spatial correlation threshold was liberal because our high-order ICA resulted in smaller and more numerous components compared to the BrainMap components. Based on visual inspection and consensus among multiple raters (n = 4), several additional components that clearly matched known functional networks were also included (e.g., subcortical components, which had no corresponding BrainMap component).

A final set of 47 components (shown in detail in Supplemental Fig. 1) was selected for the subsequent analyses. These components were conceptualized as falling into one of eight broad functional networks: default mode (DMN), executive (Exec), frontoparietal (FP), auditory (Aud), visual (Vis), sensorimotor (SM), cerebellar (CB), and subcortical (SC). These are standard and commonly reported resting state networks (see Smith, Fox, Miller et al., 2009). Classification of components into one of these networks was guided by BrainMap component correlations, as well as visual inspection and multi-rater consensus (as described above).

In line with the methods reported in previous studies (Allen et al., 2014; de Lacy et al., 2017), individual participants' spatial maps were derived from each group component to account for inter-individual variability in network topography in the following analyses. This was accomplished using FSL's DualRegression, a method described by Filippini, MacIntosh, Hough et al. (2009), which is similar to the GICA1 backreconstruction method used by Allen et al.

(2014). Using AFNI's 3dclust, masks (i.e., 3-dimensional, binary subvolumes of selected voxels within the brain) were generated from each individualized spatial map by identifying positive voxels in the top 5% of absolute z-score values, belonging to a cluster of at least 100 voxels. These masks were used as subject-specific ROIs for all subsequent analyses, which were run using in-house MATLAB scripts.

Data-driven techniques (e.g., ICA) can be used to identify individualized ROIs. Compared to literature-derived ROIs, these better account for inter-individual variability and lead to more accurate calculations of functional connectivity (Sohn, Yoo, Lee et al., 2015). Pre-defined ROIs may be particularly problematic in pediatric and clinical populations. Therefore, we considered a data-driven approach indispensable in order to identify suitable ROIs for our cohort of children and adolescents with and without ASDs. The crucial criterion for ROI generation was therefore maximal functional homogeneity (i.e., high levels of signal covariance), which in some instances resulted in ROIs that were not spatially contiguous (cf. Supplemental Fig. 1). While this may differ from more typical use of spatially contiguous ROIs, our subsequent connectivity analyses (described below) followed standard ROI-ROI analysis methods.

Static Connectivity Analysis

ROI-Level

Static iFC was examined for all possible ROI-ROI unique pairs ([47x46]/2 = 1081 pairs). For each participant, the average timecourse over all available time points was extracted from each ROI mask using AFNI's 3dmaskave. Pearson correlations were calculated for the timecourses of all ROI pairs, and simple correlation values (r) were transformed to Fisher's z. This resulted in one static correlation matrix per participant. Groups were compared on all ROI

pairs (i.e., across the entire correlation matrix) using permutation testing to control for multiple comparisons (Chen, Witte, Heemsbergen et al., 2013). T-scores for all 1081 ROI pairs were compared to a null T_{max} distribution consisting of t-scores derived from random permutations of group assignment (ASD or TD; see Supplemental Materials for MATLAB code). This approach inherently controls for familywise Type 1 error, which was set to $\alpha = .05$. In addition, permutation methods make very few assumptions about underlying data, and are therefore more appropriate than parametric methods for comparing matrices of non-independent ROI-ROI correlations. A supplemental analysis was conducted using ANCOVA (MATLAB's mancovan function) to compare group differences with and without select covariates (age, RMSD, sex, and handedness). Medication and comorbidity were not included as covariates because they are not independent of group.

Network-Level

To characterize iFC within and between functional networks, ROI-ROI correlations were averaged within each network (e.g., all DMN-DMN ROIs) and between each network (e.g., all DMN-Vis ROIs), resulting in eight within-network cells and 28 between-network cells for each participant. Each of these averaged values was then compared between groups using the permutation procedure described above. Permutation tests were conducted separately for 8 within-network comparisons and 28 between-network comparisons at an $\alpha = .05$ significance level.

Dynamic Connectivity Analysis

Sliding windows were applied to each ROI timecourse. Following procedures in Allen et al. (2014), each window was 44s (22 TR) in length, with a 2s (1 TR) shift between windows. Windows were tapered by applying Gaussian weights to each timepoint, with heavier weighting

of middle time points (see Supplemental Materials). As in Falahpour et al., (2016) windows missing >20% of timepoints (>4 of 22) were excluded. For each participant, the first 123 usable windows (~4.8 minutes of data) were selected for further analysis (to avoid differences in number of windows between participants). For analyses requiring consecutive data (i.e., mean dwell time and state-switching), the first 123 consecutive usable windows were selected from a subset of participants meeting this criterion. Ten participants from the original sample (7 ASD, 3 TD) were excluded from these analyses, and remaining participants were group-matched as described above (Table 1b). The average timecourse within each window was then extracted from each ROI. As in the static iFC analysis, the timecourses of all ROI pairs were correlated, and *r* values were transformed to Fisher's z. This resulted in 123 temporally contiguous correlation matrices (one per window) per subject.

The standard deviation (Stdev-iFC) of each Fisher z-transformed ROI-ROI correlation was calculated across all dynamic windows. As in the static iFC analysis, stdev of each ROI pair was compared between groups using permutation tests, and a supplemental analysis was conducted to explore the effects of covariates on group differences. Network-level analyses were also conducted, as described above.

The relationship between static iFC (Fisher's z scores for all ROI pairs) and Stdev-iFC (variability of all Fisher's z scores across windows) describes the degree to which static overconnectivity or underconnectivity may reflect fluctuations in synchronization over time; this was explored in two ways. First, the correlation between group-averaged static iFC and stdev iFC was calculated across all ROI pairs within each group. Then, a stepwise general linear model (MATLAB stepwiseglm) was used to examine individual participants' static iFC-stdev correlations, with diagnosis, RMSD, age, sex, handedness, verbal IQ, nonverbal IQ, and SRS

total score as potential predictors. A linear starting model was specified, and all interactions were considered in the stepwise modeling process.

Transient State Analysis

Clustering analyses were performed separately for the ASD and TD groups to characterize transient connectivity states. This approach differs somewhat from earlier studies that clustered both groups together. However, states derived from k-means clustering on data from both groups may not reach optimal clustering solutions for either group. Our alternative choice of clustering separately by group accounts for the possibility that individuals with ASDs may experience qualitatively different states than TD individuals. All windowed correlation matrices for all subjects in each group underwent k-means clustering, with 100 replicates to avoid local minima. The elbow method (within cluster/between cluster variance ratio) and silhouette plots suggested that either three or four clusters best fit our data. We selected a four-cluster approach for our primary analysis, given that prior dFC studies using similar methods have identified as many as 5-7 clusters (Allen et al., 2014; Damaraju et al., 2014; de Lacy et al., 2017). A supplemental sensitivity analysis was also conducted using three and five clusters.

After generating clusters separately per group, each ASD cluster was matched to a TD cluster based on the maximum whole-matrix correlation (i.e., across all ROI pairs) between cluster centroids. If two ASD clusters were most similar to the same TD cluster, priority was given to the better matching pair. Groups were compared on all ROI pairs in each state, with and without covariates, as in the static iFC and stdev analyses. Network-level analyses of group differences (described above for the static connectivity matrix) were repeated for each of the four states by averaging of all windows belonging to a given state per participant. Number of participants experiencing each state and percentage of time spent in each state (regardless of

whether the state was experienced) were calculated, and groups were compared on these measures, using independent samples t-tests or chi-square tests of independence.

Additional analyses were then conducted in the subsample of participants with consecutive windows (55 ASD, 54 TD). Using the four states identified in the full sample, mean dwell time (MDT) per state and number of switches between states was calculated, as these analyses are most likely to be affected by nonconsecutive data. Group comparisons were carried out using independent samples t-tests.

Results

Static iFC

Static iFC matrices showed broadly similar patterns in both the ASD and TD groups, with no group differences reaching statistical significance (Fig 1A). The addition of covariates did not appreciably change the observed pattern of group differences (Supplemental Fig. 4). However, an additional permutation test (i.e., nonparametric one-sample t-test) determined that overconnectivity (ASD > TD) predominated across all ROI pairs ($t(1080) = 12.057$, $p < .001$, Hedges' $g = .37$). At the network level, Fisher's z correlation values averaged across same-network ROI pairings did not significantly differ between groups for any functional network (all $p > .43$). Similarly, no significant differences were found between functional networks (all $p > .14$).

Dynamic iFC

Stdev-iFC across all ROIs was calculated for the ASD and TD groups, with no group differences reaching statistical significance (Fig. 1B). As in the static analysis, group differences were robust to the addition of covariates. An additional permutation test (i.e., nonparametric one-sample t-test) across all ROI pairings revealed predominant hypervariability in the ASD group

(t(1080) = 9.72, p < .001, Hedges' g = .30). At the network level, stdev-iFC group differences did not reach significance either within networks (all p > .08) or between networks (all p > .33).

Static iFC-Dynamic iFC Relationship

The relationship between static iFC (Fisher's z scores for all ROI pairs) and Stdev-iFC (variability of all Fisher's z scores across windows) was studied in two different ways: 1) group-averaged correlations across all ROIs, and 2) a general linear model of individual participants' correlations across all ROIs. Group-averaged static iFC and stdev-iFC values showed significant negative correlations across all ROI pairings in both the ASD (r = -.344, $p < .001$) and TD (r = -.294, $p < .001$) groups (Supplemental Fig. 2). The stepwise general linear model determined that individual static iFC-stdev iFC correlations (one per participant; intercept β = -.04) were significantly less negative in ASD (coded TD = 0, ASD = 1; β = 0.09, $p = .04$), more negative in right-handed individuals (coded Left = 0, Right = 1; β = -0.05, $p = .04$), and negatively associated with NVIQ (β = -0.001, $p = .009$). SRS total score was also included in the model, but did not reach significance (β = -0.002, $p = .08$). Interaction effects and additional considered variables were not included in the final model, as they did not significantly improve model fit. The final model fit significantly better than the intercept-only model ($F(112) = 3.8$, $p = .006$).

Transient State Analyses

Four transient states were identified in both diagnostic groups (Fig. 2A). Overall, these states showed good concordance between the ASD and TD groups (corresponding state median correlation = 0.91; non-corresponding state median correlation = 0.72; Supplemental Table 2). Group differences across all ROI pairings did not change with addition of covariates (Supplemental Fig. 4), and permutation tests revealed significant group differences across multiple ROIs for States 1 and 2, but not for States 3 or 4 (Fig. 2A). Therefore, States 1 and 2

were also assessed at the network level. In State 1, significant underconnectivity was found within SM ROIs and between Vis-SM ROIs, while significant overconnectivity was found within Vis and between SM-DMN and Vis-DMN ROIs. In State 2, significant underconnectivity was found within Aud ROIs and between FP-Vis ROIs, while significant overconnectivity was found between DMN-Exec and DMN-FP ROIs (Fig. 2B, Table 2).

The percentage of time spent in each state did not differ between groups (all $p > .13$). However, a significantly larger proportion of ASD than TD participants experienced State 1 (i.e., had at least 1 window classified as State 1; ASD = 82%, TD = 53%; $\chi^2(1) = 11.99$, $p < .001$). State 2, on the other hand, was experienced by a larger proportion of TD participants (ASD = 81%, TD = 98%; $\chi^2(1) = 9.45$, $p = .002$). In the subsample of participants with consecutive windows of data, no group differences were found for mean dwell time in any state (all $p > .07$), nor for mean number of switches between states (ASD = 11.76, TD = 12.37, $p = .43$). Group comparisons for dynamic summary measures were also explored in an unmedicated subsample of ASD participants (n= 29). All comparisons with the TD group remained the same for this sample. There were also no significant differences between the medicated (n = 28) and unmedicated ASD samples with respect to any of these measures.

Supplemental analyses were conducted exploring group differences in three-state and five-state clustering solutions (Supplemental Fig.s 5a, 5b). For the three- and five-state solutions, the resulting states uniquely matched states from the primary analysis, with Pearson's correlations between corresponding states ranging from .96 to >.99 (Supplemental Table 3). Compared to the four-state analysis, a five-state analysis revealed almost identical patterns of group differences in States 1 and 2 at both the ROI- and network-levels. For the three-state analysis, State 1 was eliminated, but DMN-FP overconnectivity remained significant in State 2.

All higher-order results were consistent across analyses, with several exceptions: reduced state-switching in ASD was found only in the three-state analysis, and the ASD group had higher mean dwell times in State 1 only in the five-state analysis. Statistics are presented with Supplemental Fig. 5.

Discussion

Using a data-driven approach, this dynamic iFC study revealed group differences in transient states that were not observable in static iFC analyses. Across the whole-brain ROI matrix, broad patterns of static iFC overconnectivity and stdev-iFC hypervariability in the ASD group predominated. Although no findings at the ROI level survived correction, a significant inverse relationship between static iFC and stdev-iFC was discovered across all ROIs. Additionally, significant group differences were found for two transient states, at both the ROI and network levels.

Static iFC shows predominant overconnectivity in ASD

While no static group differences at the ROI or network levels survived multiple comparison correction, an overall trend toward overconnectivity (ASD > TD) was found across all ROI pairs. This was largely driven by network-level trends toward overconnectivity between DMN and frontoparietal, visual, and subcortical ROIs, which did not reach statistical significance (Fig. 1B). Overall, most ROI pairings linking DMN and subcortical networks with other networks showed relative (although not statistically significant) overconnectivity in the ASD group. Our exploratory design included numerous ROIs, and a necessarily conservative approach to significance testing. However, the direction of these findings is consistent with previous studies reporting poor functional segregation between DMN and other networks (Abbott et al., 2016; Rudie, Shehzad, et al., 2012; Yerys et al., 2015), as well as overconnectivity

between subcortical and cortical regions (Cerliani et al., 2015; Delmonte, Gallagher, O'Hanlon, McGrath, & Balsters, 2013; Di Martino et al., 2011).

iFC variability across time is mostly increased in ASD

Hypervariability (ASD > TD) across time windows predominated across all ROI pairings, despite an absence of significant group differences at the ROI or Network levels. A recent study using a different dynamic approach also showed overall FC hypervariability in ASDs (Chen et al., 2017). As in previous studies of typical development (Thompson & Fransson, 2015), static iFC was inversely related to iFC variability in both groups, suggesting that higher interregional correlations in static analyses tend to also be less variable over time. Previous research has also shown that static underconnectivity within the DMN in ASDs is associated with hypervariability over time (Falahpour et al., 2016). Our analysis corroborates this negative relationship between static iFC and stdev-iFC across numerous ROIs, and additionally suggests that this relationship is significantly weaker in ASD participants (controlling for handedness, non-verbal IQ, and symptom severity). This may explain seemingly contradictory findings of both overconnectivity *and* hypervariability in ASD compared to TD participants, which would be unexpected if the static-dynamic relationship was invariant across groups.

Two dynamic connectivity states differ between groups

Four connectivity states were identified, each with distinct connectivity patterns (Fig. 2; Supplemental Fig. 3). State 3 most closely resembled the static connectivity matrices, with both ASD and TD participants spending more time in this state than in any other (45% and 50% on average, respectively). In State 4, correlations were broadly elevated across the entire connectivity matrix, although network structure remained apparent. This hyperconnected state has been found in other studies using similar methods (de Lacy et al., 2017, Rashid et al., 2018),

and may be predominated by partially non-neuronal global signal fluctuations (Power et al., 2014.). However, global signal fluctuations have been shown to contain meaningful neural information (Schölvinck, Maier, Ye, Duyn, & Leopold, 2010) and may be particularly associated with vigilance (Wong, Olafsson, Tal, & Liu, 2012). Notably, the current study did not use global signal regression (GSR), a controversial method in which the time series of the averaged whole-brain signal is statistically removed from the data (Murphy, Birn, Handwerker, Jones, & Bandettini, 2009). This may explain the appearance of State 4 in the current dataset.

In States 1 and 2, distinct patterns of group differences were detected, with partly opposing functional network associations (Fig. 2). State 2 was characterized by high iFC within DMN, but anti-correlations between DMN and several other networks (Fig. 2A & Supplemental Fig. 3). State 2 may therefore represent differentiation of the DMN, with high levels of within-network integration and relatively strong segregation from other networks. All group differences involved frontoparietal, executive, and auditory regions, i.e., networks important for supramodal cognition and language. Some of these group differences reflected reduced segregation of the DMN, which was 'overconnected' with executive and frontoparietal networks (largely reflecting reduced anti-correlations). This was accompanied by underconnectivity (reduced integration) within the auditory network, and between frontoparietal and visual networks (Fig. 2B).

A simple functional interpretation of this pattern of findings is challenging, given the data-driven approaches selected in our study (i.e., ROIs defined through ICA; transient states identified using k-means clustering). However, the findings for State 2 can be grossly summarized as reflecting predominant segregation of DMN and integration between other networks – a pattern that was relatively distinct in the TD group, but significantly less pronounced in the ASD group. Notably, State 2 was experienced by significantly more TD than

ASD participants, suggesting that it is an almost ubiquitous state that is absent in an unexpectedly high number of children with ASDs (19% for ASD vs. 2% for TD).

State 1 showed partially opposite connectivity patterns compared to State 2 (Fig. 2 & Supplemental Fig. 3). While State 1 was seen in most ASD participants (82%), many TD participants (47%) did not experience this state. In both groups, the DMN was not as distinctly segregated in State 1 as in State 2, with coupling between DMN and executive and auditory networks. In the ASD group, anticorrelation between DMN and visual regions (seen in State 2 in both groups) was reversed and positive in State 1. Finally, for both groups, the sensorimotor network was segregated in State 1 (positive correlations within-network, anticorrelations with other networks). In TD participants experiencing State 1, positive within-network correlations and anticorrelations between sensorimotor and DMN networks were especially pronounced.

Group differences at the network-level were complementary for states 1 and 2 (i.e., largely non-overlapping). For State 1, they involved networks predominantly responsible for sensory and motor functions (Fig. 2B). Specifically, DMN was less segregated (i.e., overconnected) in ASD from visual, and sensorimotor networks. Reduced DMN segregation in ASD was also seen in State 2, but only affected executive and frontoparietal networks. In State 1, there was also significant overconnectivity within the visual network, underconnectivity within the sensorimotor network, and underconnectivity between sensorimotor and visual regions. Generally, group differences in State 2 involved more areas relevant for higher-order cognition and attention, as discussed above. The distinct patterns of group differences for the two states may relate to two distinct lines of ASD research documenting, on the one hand, executive and attentional abnormalities (Craig et al., 2016; Hill, 2004; Keehn, Müller, & Townsend, 2013) and atypical sensorimotor behaviors, on the other (Chukoskie, Townsend, & Westerfield, 2013;

Marco, Hinkley, Hill, & Nagarajan, 2011). They may also relate to previous findings in typical development of two hierarchical "meta-states", one associated with sensory and motor function, the other involving higher-order cognitive regions (Vidaurre et al., 2017). This latter study found the relative amount of time spent in each of these two states to be both heritable and associated with behavioral variables (e.g., cognitive abilities, personality traits), which is notable with regard to striking differences in the proportion of ASD and TD participants experiencing either state in our study.

In a supplemental analysis using a 3-cluster k-means solution, State 1 from the primary analysis was eliminated. Significant overconnectivity between DMN-FP regions was found for State 2, irrespective of whether a 3, 4, or five-state clustering solution was used. However, only the three-state solution suggested that individuals with ASDs switched less frequently between states, whereas no significant group difference was found for the four-state or five-state solution. One possible explanation for this is the elimination of State 1. Because this state was more often experienced by ASD participants, assigning State 1 windows to the next closest cluster should reduce the number of state switches to a greater degree in the ASD group than the TD group. In other words, the ASD participants may tend to rotate between a larger number of states than the TD group, but switch between those states equally often. This may explain why previous studies clustering all individuals together (i.e., forcing uniform states across groups) have reported reduced state-switching in ASD.

Across analyses, the most consistent finding was *overconnectivity* in ASD between DMN and other networks, which was evident in both States 1 and 2 at the network level, regardless of the number of k-means clusters used. This pattern did not significantly emerge in the static iFC analysis, but the direction of findings was broadly consistent. Although de Lacy et al. (2017)

primarily found underconnectivity in ASDs using a similar dynamic FC approach, overconnectivity was reported between anterior DMN and cingulo-opercular regions in both static and dynamic analyses. Importantly, this finding only appeared in one or two (depending on window size) of six brain states. Thus, as in our study, group differences suggested overconnectivity between DMN and non-DMN regions, and this finding appeared to be state-specific.

Our results are also consistent with previously reported fMRI evidence of reduced functional network segregation in ASDs, specifically involving the DMN (Rudie, Brown, et al., 2012; Yerys et al., 2015). However, our findings go beyond previous static fcMRI studies, suggesting that reduced DMN segregation (i.e., reduced anti-correlations or overconnectivity with non-DMN-networks) occurs in different patterns during different transient states (i.e, involving sensorimotor networks in one state but frontoparietal and executive networks in another). This also suggests that time-varying properties of functional connectivity in ASDs may help to explain inconsistencies in the existing literature. More specifically, our findings suggest that previously observed iFC patterns in ASDs, such as reduced network integration and segregation, may reflect some transient connectivity states, but not others (1 and 2 vs. 3 and 4 in the present study). In other words, whole brain functional connectivity may not be persistently atypical in ASD but may be characterized by atypical patterns affecting only some transient states.

Challenges and Perspectives

This study is among the first to apply dynamic fcMRI methods to examine transient connectivity states in ASDs. These findings have laid the groundwork for exciting future research in this disorder. In particular, group differences involving sensorimotor and higher-

order cognitive networks imply possible relationships with cardinal behavioral features of ASDs. Future studies may explore measures of repetitive behaviors, sensory abnormalities, and sociocommunicative impairment to determine whether these uniquely relate to specific brain states. Distinct neural correlates of different symptom profiles may elucidate the nature of heterogeneity of ASDs, which has proven particularly challenging. Dynamic fcMRI methods may inform future studies examining neural and behavioral subtypes, paving the way for precision diagnostic and treatment protocols.

Despite its promise, this novel approach remains in its early phases, and its limitations must be addressed. Although interest has been growing in sliding window fMRI analyses, there is little consensus on how to select parameters such as window length and overlap, which may substantially affect analysis outcomes (Shakil, Lee, & Keilholz, 2016). Furthermore, it has been shown that sliding window analyses may erroneously attribute non-neuronal noise (e.g., head motion, sleep state) to BOLD dynamics (Laumann et al., 2016). Therefore, controlling for these factors is of the utmost importance. It should further be noted that findings may relate to the use of resting state data in our study and may not correspond to dynamic connectivity differences associated with sensory stimulation or performance on various cognitive tasks (Gonzalez-Castillo & Bandettini, 2018). Finally, cluster centroids (states) were derived separately for each diagnostic group, an approach that diverged from the few other extant studies in this population. While this improves our ability to detect differences in overall state configuration, perfect state-matching between groups is not guaranteed.

Several challenges common in neuroimaging studies of children with ASDs should be noted. First, although the size of our ASD sample compared well to that in other single-site dynamic FC studies of clinical populations (Du, Fryer, Fu et al., 2017; Falahpour et al., 2016;

Rashid et al., 2018; Rashid, Damaraju, Pearlson et al., 2014), it was limited compared to multisite studies. However, use of single-site data circumvented issues associated with site and scanner differences. Additionally, use of psychotropic medications that may affect brain functioning is common in ASDs, as are comorbid psychiatric diagnoses. Our study recorded medication and comorbidity information for the majority of ASD participants and performed select analyses in an unmedicated subsample of the ASD group. Unfortunately, most fcMRI studies of ASDs do not report these important sample characteristics. Future studies with larger samples should consider focusing specifically on the effects of medication and comorbid diagnosis on dynamic FC metrics (Linke, Olson, Gao et al., 2017).

Furthermore, dynamic analyses of fMRI data remain limited by the slow hemodynamic BOLD response. While advanced analysis methods can reveal some information about dynamic phenomena, investigation of rapid, transient changes on faster timescales requires electrophysiological methods (EEG, MEG), which are in turn hampered by low spatial resolution and incomplete brain coverage. Integrative multimodal approaches will therefore be necessary for a more comprehensive understanding of time-varying properties of functional connectivity in ASDs (for review and discussion, see Mash, Reiter, Linke, Townsend, & Müller, 2018).

Conclusions

This study found overall predominance of static overconnectivity and hypervariability over time in ASDs across numerous brain regions. Results suggest that the nature of atypical functional connectivity in ASDs varies over time, with distinct patterns of group differences across transient states. Furthermore, state-specific group differences in connectivity aligned uniquely with sensorimotor and higher-order cognitive networks. Finally, reduced segregation of

the default mode network from other functional networks emerged as a common theme, present in multiple transient states but falling short of statistical significance in static analysis.

Acknowledgments

This work was funded by the National Institutes of Health R01 MH081023 (RAM), R21 MH102578 (RAM, TTL), K01 MH097972 (IF), R01 MH101173 (R.A.M). This work was also supported by the National Science Foundation Graduate Research Fellowship Program under Grant No. 1321850 (L.E.M). Any opinions, findings, and conclusions or recommendations expressed in this material are those of the authors and do not necessarily reflect the views of the National Science Foundation.

Dissertation Author Note

Chapter 2, in full, is a reprint of the material as it appears in Human Brain Mapping, 40, 2377-2389. Mash, L. E., Linke, A. C., Olson, L. A., Fishman, I., Liu, T. T., & Müller, R.-A. Wiley, 2019. The dissertation author was the primary investigator and author of this paper.

Table 1.1 Sample Characteristics

A. Complete Sample Characteristics

	ASD (*n* = 62)	TD (*n* = 57)	Statistic	p
Sex	52 male	46 male	$X^2(1) = 0.21$	.651
Handedness	52 right	49 right	$X^2(1) = 0.10$	.750
Age	13.7 (2.5) [9.2 – 18.0]	13.1 (2.9) [6.9 – 17.6]	t(117) = 1.16	.250
RMSD	0.07 (0.03) [0.02 – 0.15]	0.06 (0.03) [0.02 – 0.17]	t(117) = 0.41	.687
VIQ	101 (18) [59 – 147]	108 (10) [78 – 133]	t(117) = -2.72	.007
NVIQ	104 (19) [53 – 140]	106 (14) [62 – 137]	t(117) = -0.70	.479
FSIQ	103 (17) [61 – 141]	108 (12) [79 – 132]	t(117) = -1.77	.074
SRS Total	81 (9) [58 – 96]	42 (5) [35 – 58]	t(115) = 28.0	<.001

B. Consecutive Data Sample Characteristics

	ASD (n = 55)	TD (n = 54)	Statistic	p
Sex	45 male	43 male	$X^2(1) = 0.08$	.772
Handedness	46 right	46 right	$X^2(1) = 0.05$	.824
Age	13.8 (2.5) [9.2 – 18]	13.1 (2.9) [6.9 – 17.6]	t(107) = 1.35	.180
RMSD	0.06 (0.03) [0.02 – 0.11]	0.06 (0.03) [0.02 – 0.17]	t(107) = -0.09	.926
VIQ	100 (18) [59 – 147]	108 (11) [78 – 133]	t(107) = -2.82	.006
NVIQ	105 (20) [53 – 140]	106 (14) [62 – 137]	t(107) = -0.59	.559
FSIQ	103 (18) [61 – 141]	108 (12) [79 – 132]	t(107) = -1.75	.084
SRS Total	82 (9) [58 – 96]	42 (5) [35 – 58]	t(105) = 27.48	<.001

Values are presented as Mean (SD), [min – max]. ASD = Autism Spectrum Disorder; TD = Typically Developing; RMSD = Root Mean Squared Displacement; VIQ = Verbal IQ; NVIQ = Nonverbal IQ; FSIQ = Full Scale IQ; SRS = Social Responsiveness Scale

Table 1.2 Significant Network-Level State Group Differences

ROIs			Direction	df	t	*p*	Hedges' g
State 1							
SM	-	SM	UC	79	-3.56	.006	-.81
SM	-	DMN	OC	79	5.65	<.001	1.29
Vis	-	Vis	OC	79	4.48	<.001	1.02
Vis	-	DMN	OC	79	9.48	<.001	2.16
Vis	-	SM	UC	79	-3.68	.01	-.84
State 2							
Aud	-	Aud	UC	104	-3.45	.005	-.67
DMN	-	Exec	OC	104	3.35	.03	.65
DMN	-	FP	OC	104	3.51	.02	.68
FP	-	Vis	UC	104	-3.34	.03	-.65

SM = sensorimotor; DMN = default mode network; Vis = visual; Aud = auditory; Exec = executive control; FP = frontoparietal; UC = underconnectivity; OC = overconnectivity

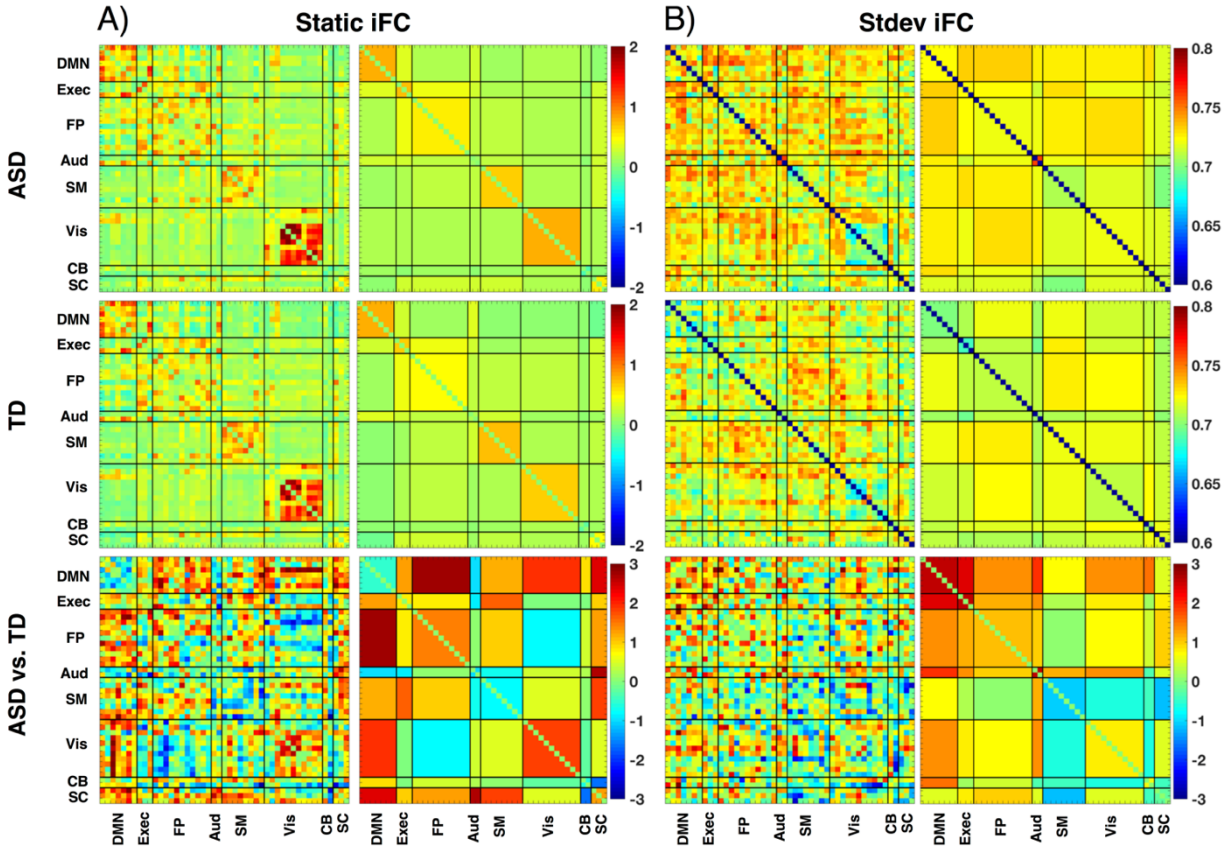

Figure 1.1 Static iFC and iFC Variability
Panel A: Static connectivity matrices at the ROI- and network-levels for each group, as well as relevant group comparisons. Colors represent Fisher's z values or t-scores for group comparisons (positive indicates ASD > TD). Panel B: stdev-iFC across windows at the ROI and network levels and relevant group comparisons. Colors represent standard deviations or t-scores for group comparisons. No group differences were significant after permutation testing. Abbreviated labels denote the following networks: Default Mode (DMN), Executive (Exec), Frontoparietal (FP), Auditory (Aud), Visual (Vis), Sensorimotor (SM), Cerebellar (CB), and Subcortical (SC).

Figure 1.2 Transient States and Group Differences
Panel A: State 1-4 connectivity matrices at the ROI-level for each group, as well as group comparisons with and without multiple comparison correction. Colors represent Fisher's z values, or t-scores for group comparisons (positive indicates ASD > TD). Panel B: Network-level correlation matrices for States 1 and 2 in each group and relevant group comparisons. Colors averaged Fisher's z values or t-scores for group comparisons. * indicates $p < .05$ after permutation testing. Note that significant underconnectivity was found within the auditory network, but this is not visible due to small network size (i.e., few contributing ROIs). Abbreviated labels denote the following networks: Default Mode (DMN), Executive (Exec), Frontoparietal (FP), Auditory (Aud), Visual (Vis), Sensorimotor (SM), Cerebellar (CB), and Subcortical (SC).

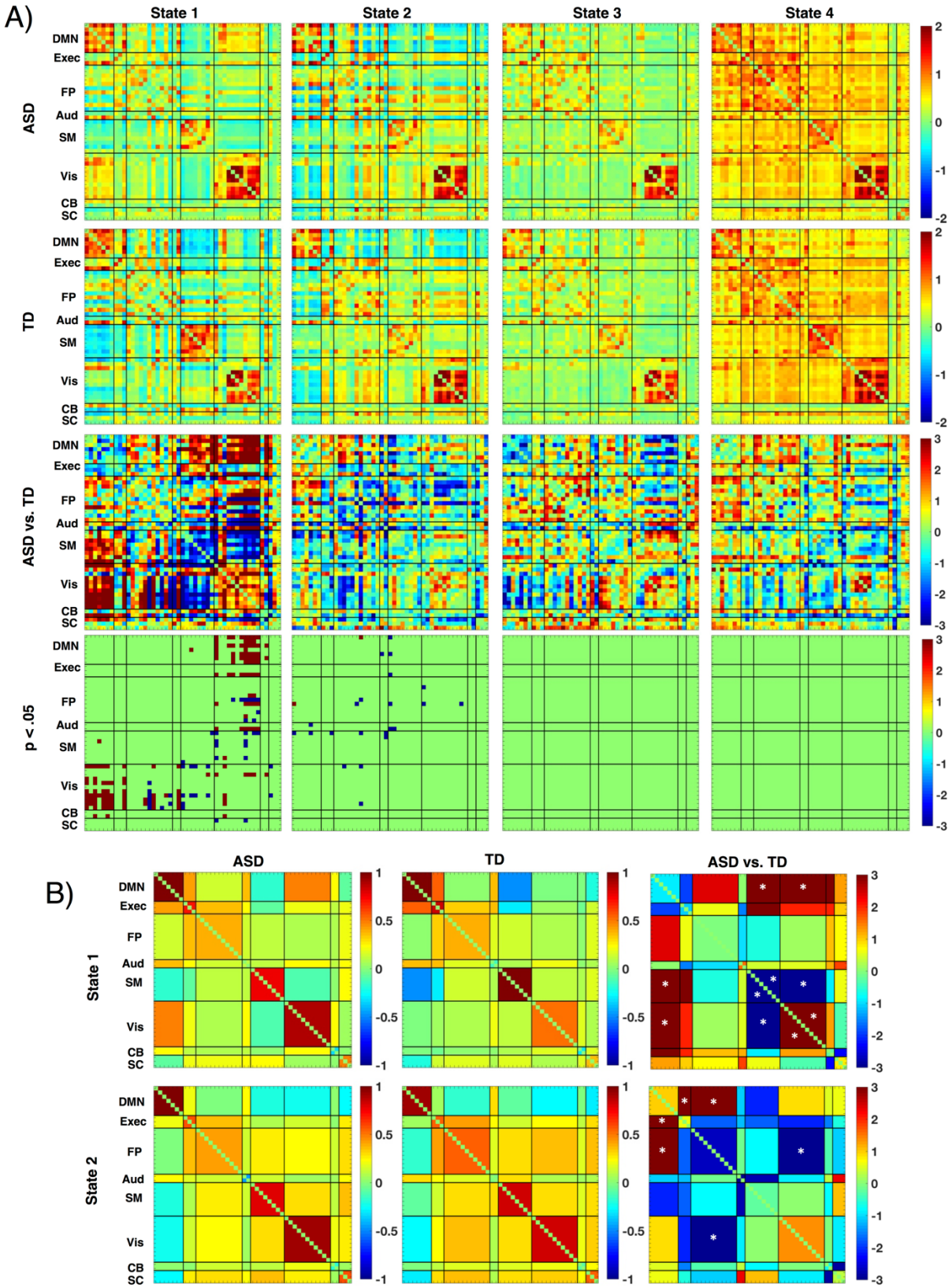
A)
State 1
State 2
State 3
State 4
ASD
TD
ASD vs. TD
p < .05
DMN
Exec
FP
Aud
SM
Vis
CB
SC
B)
ASD
TD
ASD vs. TD
State 1
State 2

References

Abbott, A. E., Nair, A., Keown, C. L., Datko, M., Jahedi, A., Fishman, I., & Müller, R. A. (2016). Patterns of Atypical Functional Connectivity and Behavioral Links in Autism Differ Between Default, Salience, and Executive Networks. *Cereb Cortex, 26*(10), 4034-4045. doi:10.1093/cercor/bhv191

Allen, E. A., Damaraju, E., Eichele, T., Wu, L., & Calhoun, V. D. (2017). EEG Signatures of Dynamic Functional Network Connectivity States. *Brain Topogr*. doi:10.1007/s10548-017-0546-2

Allen, E. A., Damaraju, E., Plis, S. M., Erhardt, E. B., Eichele, T., & Calhoun, V. D. (2014). Tracking whole-brain connectivity dynamics in the resting state. *Cereb Cortex, 24*(3), 663-676. doi:10.1093/cercor/bhs352

American Psychiatric Association. (2013). *Diagnostic and statistical manual of mental disorders : DSM-5* (pp. 947).

Belmonte, M. K., Allen, G., Beckel-Mitchener, A., Boulanger, L. M., Carper, R. A., & Webb, S. J. (2004). Autism and abnormal development of brain connectivity. *J Neurosci, 24*(42), 9228-9231. doi:10.1523/JNEUROSCI.3340-04.2004

Biswal, B., Yetkin, F. Z., Haughton, V. M., & Hyde, J. S. (1995). Functional connectivity in the motor cortex of resting human brain using echo-planar MRI. *Magn Reson Med, 34*(4), 537-541.

Britz, J., Van De Ville, D., & Michel, C. M. (2010). BOLD correlates of EEG topography reveal rapid resting-state network dynamics. *Neuroimage, 52*(4), 1162-1170. doi:10.1016/j.neuroimage.2010.02.052

Cerliani, L., Mennes, M., Thomas, R. M., Di Martino, A., Thioux, M., & Keysers, C. (2015). Increased Functional Connectivity Between Subcortical and Cortical Resting-State Networks in Autism Spectrum Disorder. *JAMA Psychiatry, 72*(8), 767-777. doi:10.1001/jamapsychiatry.2015.0101

Chen, C., Witte, M., Heemsbergen, W., & van Herk, M. (2013). Multiple comparisons permutation test for image based data mining in radiotherapy. *Radiat Oncol, 8*, 293, doi:10.1186/1748-717X-8-293.

Chen, H., Nomi, J. S., Uddin, L. Q., Duan, X., & Chen, H. (2017). Intrinsic functional connectivity variance and state-specific under-connectivity in autism. *Hum Brain Mapp*. doi:10.1002/hbm.23764

Chukoskie, L., Townsend, J., & Westerfield, M. (2013). Motor skill in autism spectrum disorders: a subcortical view. *Int Rev Neurobiol, 113*, 207-249. doi:10.1016/B978-0-12-418700-9.00007-1

Ciric, R., Nomi, J. S., Uddin, L. Q., & Satpute, A. B. (2017). Contextual connectivity: A framework for understanding the intrinsic dynamic architecture of large-scale functional brain networks. *Sci Rep, 7*(1), 6537. doi:10.1038/s41598-017-06866-w

Constantino, J. N., & Gruber, C. P. (2012). *Social Responsiveness Scale - Second Edition*. Torrance, CA: Western Psychological Services.

Cordes, D., Haughton, V. M., Arfanakis, K., Wendt, G. J., Turski, P. A., Moritz, C. H., . . . Meyerand, M. E. (2000). Mapping functionally related regions of brain with functional connectivity MR imaging. *AJNR Am J Neuroradiol, 21*(9), 1636-1644.

Cox, R. W. (1996). AFNI: software for analysis and visualization of functional magnetic resonance neuroimages. *Comput Biomed Res, 29*(3), 162-173.

Craig, F., Margari, F., Legrottaglie, A. R., Palumbi, R., de Giambattista, C., & Margari, L. (2016). A review of executive function deficits in autism spectrum disorder and attention-deficit/hyperactivity disorder. *Neuropsychiatr Dis Treat, 12*, 1191-1202. doi:10.2147/NDT.S104620

Dajani, D. R., & Uddin, L. Q. (2016). Local brain connectivity across development in autism spectrum disorder: A cross-sectional investigation. *Autism Res, 9*(1), 43-54. doi:10.1002/aur.1494

Damaraju, E., Allen, E. A., Belger, A., Ford, J. M., McEwen, S., Mathalon, D. H., . . . Calhoun, V. D. (2014). Dynamic functional connectivity analysis reveals transient states of dysconnectivity in schizophrenia. *Neuroimage Clin, 5*, 298-308. doi:10.1016/j.nicl.2014.07.003

de Lacy, N., Doherty, D., King, B. H., Rachakonda, S., & Calhoun, V. D. (2017). Disruption to control network function correlates with altered dynamic connectivity in the wider autism spectrum. *Neuroimage Clin, 15*, 513-524. doi:10.1016/j.nicl.2017.05.024

Delmonte, S., Gallagher, L., O'Hanlon, E., McGrath, J., & Balsters, J. H. (2013). Functional and structural connectivity of frontostriatal circuitry in Autism Spectrum Disorder. *Front Hum Neurosci, 7*, 430. doi:10.3389/fnhum.2013.00430

Di Martino, A., Kelly, C., Grzadzinski, R., Zuo, X. N., Mennes, M., Mairena, M. A., . . . Milham, M. P. (2011). Aberrant striatal functional connectivity in children with autism. *Biol Psychiatry, 69*(9), 847-856. doi:10.1016/j.biopsych.2010.10.029

Doyle-Thomas, K. A., Lee, W., Foster, N. E., Tryfon, A., Ouimet, T., Hyde, K. L., . . . NeuroDevNet, A. S. D. I. G. (2015). Atypical functional brain connectivity during rest in autism spectrum disorders. *Annals of Neurology, 77*(5), 866-876. doi:10.1002/ana.24391

Du, Y., Fryer, S. L., Fu, Z., Lin, D., Sui, J., Chen, J., . . . Calhoun, V. D. (2017). Dynamic functional connectivity impairments in early schizophrenia and clinical high-risk for psychosis. *Neuroimage*. doi:10.1016/j.neuroimage.2017.10.022

Easson, A. K., Fatima, Z., & McIntosh, A. R. (2018). Functional connectivity-based subtypes of individuals with and without autism spectrum disorder. *Network Neuroscience*, 1-19. doi:10.1162/netn_a_00067

Falahpour, M., Thompson, W. K., Abbott, A. E., Jahedi, A., Mulvey, M. E., Datko, M., . . . Müller, R. A. (2016). Underconnected, But Not Broken? Dynamic Functional Connectivity MRI Shows Underconnectivity in Autism Is Linked to Increased Intra-Individual Variability Across Time. *Brain Connect, 6*(5), 403-414. doi:10.1089/brain.2015.0389

Filippini, N., MacIntosh, B. J., Hough, M. G., Goodwin, G. M., Frisoni, G. B., Smith, S. M., . . . Mackay, C. E. (2009). Distinct patterns of brain activity in young carriers of the APOE-epsilon4 allele. *Proc Natl Acad Sci U S A, 106*(17), 7209-7214. doi:10.1073/pnas.0811879106

Fishman, I., Keown, C. L., Lincoln, A. J., Pineda, J. A., & Müller, R. A. (2014). Atypical cross talk between mentalizing and mirror neuron networks in autism spectrum disorder. *JAMA Psychiatry, 71*(7), 751-760. doi:10.1001/jamapsychiatry.2014.83

Fox, M. D., & Raichle, M. E. (2007). Spontaneous fluctuations in brain activity observed with functional magnetic resonance imaging. *Nat Rev Neurosci, 8*(9), 700-711. doi:10.1038/nrn2201

Fu, Z., Tu, Y., Di, X., Du, Y., Sui, J., Biswal, B. B., . . . Calhoun, V. D. (2018). Transient increased thalamic-sensory connectivity and decreased whole-brain dynamism in autism. *Neuroimage*. doi:10.1016/j.neuroimage.2018.06.003

Gotham, K., Risi, S., Pickles, A., & Lord, C. (2007). The Autism Diagnostic Observation Schedule: revised algorithms for improved diagnostic validity. *J Autism Dev Disord, 37*(4), 613-627. doi:10.1007/s10803-006-0280-1

Gonzalez-Castillo, J., & Bandettini, P. A. (2018). Task-based dynamic functional connectivity: Recent findings and open questions. *Neuroimage, 180*(Pt B), 526-533.

Hill, E. L. (2004). Executive dysfunction in autism. *Trends Cogn Sci, 8*(1), 26-32.

Hull, J. V., Jacokes, Z. J., Torgerson, C. M., Irimia, A., & Van Horn, J. D. (2016). Resting-State Functional Connectivity in Autism Spectrum Disorders: A Review. *Front Psychiatry, 7*, 205. doi:10.3389/fpsyt.2016.00205

Hutchison, R. M., Womelsdorf, T., Allen, E. A., Bandettini, P. A., Calhoun, V. D., Corbetta, M., . . . Chang, C. (2013). Dynamic functional connectivity: promise, issues, and interpretations. *Neuroimage, 80*, 360-378. doi:10.1016/j.neuroimage.2013.05.079

Itahashi, T., Yamada, T., Watanabe, H., Nakamura, M., Ohta, H., Kanai, C., . . . Hashimoto, R. (2015). Alterations of local spontaneous brain activity and connectivity in adults with high-functioning autism spectrum disorder. *Mol Autism, 6*, 30. doi:10.1186/s13229-015-0026-z

Jenkinson, M., & Smith, S. (2001). A global optimisation method for robust affine registration of brain images. *Med Image Anal, 5*(2), 143-156.

Just, M. A., Cherkassky, V. L., Keller, T. A., Kana, R. K., & Minshew, N. J. (2007). Functional and anatomical cortical underconnectivity in autism: evidence from an FMRI study of an executive function task and corpus callosum morphometry. *Cereb Cortex, 17*(4), 951-961. doi:10.1093/cercor/bhl006

Just, M. A., Cherkassky, V. L., Keller, T. A., & Minshew, N. J. (2004). Cortical activation and synchronization during sentence comprehension in high-functioning autism: evidence of underconnectivity. *Brain, 127*(Pt 8), 1811-1821. doi:10.1093/brain/awh199

Kana, R. K., Keller, T. A., Cherkassky, V. L., Minshew, N. J., & Just, M. A. (2006). Sentence comprehension in autism: thinking in pictures with decreased functional connectivity. *Brain, 129*(Pt 9), 2484-2493. doi:10.1093/brain/awl164

Keehn, B., Müller, R.-A., & Townsend, J. (2013). Atypical Attentional Networks and the Emergence of Autism. *Neuroscience and biobehavioral reviews, 37*(2), 164-183. doi:10.1016/j.neubiorev.2012.11.014

Keown, C. L., Shih, P., Nair, A., Peterson, N., Mulvey, M. E., & Müller, R. A. (2013). Local functional overconnectivity in posterior brain regions is associated with symptom severity in autism spectrum disorders. *Cell Rep, 5*(3), 567-572. doi:10.1016/j.celrep.2013.10.003

Khanna, A., Pascual-Leone, A., Michel, C. M., & Farzan, F. (2015). Microstates in resting-state EEG: current status and future directions. *Neurosci Biobehav Rev, 49*, 105-113. doi:10.1016/j.neubiorev.2014.12.010

Kleinhans, N. M., Richards, T., Sterling, L., Stegbauer, K. C., Mahurin, R., Johnson, L. C., . . . Aylward, E. (2008). Abnormal functional connectivity in autism spectrum disorders during face processing. *Brain, 131*(Pt 4), 1000-1012. doi:10.1093/brain/awm334

Koshino, H., Kana, R. K., Keller, T. A., Cherkassky, V. L., Minshew, N. J., & Just, M. A. (2008). fMRI investigation of working memory for faces in autism: visual coding and underconnectivity with frontal areas. *Cereb Cortex, 18*(2), 289-300. doi:10.1093/cercor/bhm054

Laird, A. R., Lancaster, J. L., & Fox, P. T. (2005). BrainMap: the social evolution of a human brain mapping database. *Neuroinformatics, 3*(1), 65-78.

Laumann, T. O., Snyder, A. Z., Mitra, A., Gordon, E. M., Gratton, C., Adeyemo, B., . . . Petersen, S. E. (2017). On the Stability of BOLD fMRI Correlations. *Cerebral Cortex, 27*(10), 4719-4732. doi:10.1093/cercor/bhw265

Lehmann, B. C. L., White, S. R., Henson, R. N., Cam, C., & Geerligs, L. (2017). Assessing dynamic functional connectivity in heterogeneous samples. *Neuroimage, 157*, 635-647, doi:10.1016/j.neuroimage.2017.05.065.

Linke, A. C., Olson, L., Gao, Y., Fishman, I., & Muller, R. A. (2017). Psychotropic medication use in autism spectrum disorders may affect functional brain connectivity. *Biol Psychiatry Cogn Neurosci Neuroimaging, 2*(6), 518-527. doi:10.1016/j.bpsc.2017.06.008

Lord, C., Rutter, M., & Le Couteur, A. (1994). Autism Diagnostic Interview-Revised: a revised version of a diagnostic interview for caregivers of individuals with possible pervasive developmental disorders. *J Autism Dev Disord, 24*(5), 659-685.

Marco, E. J., Hinkley, L. B., Hill, S. S., & Nagarajan, S. S. (2011). Sensory processing in autism: a review of neurophysiologic findings. *Pediatr Res, 69*(5 Pt 2), 48R-54R. doi:10.1203/PDR.0b013e3182130c54

Mash, L. E., Reiter, M. A., Linke, A. C., Townsend, J., & Müller, R. A. (2018). Multimodal approaches to functional connectivity in autism spectrum disorders: An integrative perspective. *Dev Neurobiol*. doi:10.1002/dneu.22570

Malaia, E., Bates, E., Seitzman, B., & Coppess, K. (2016). Altered brain network dynamics in youths with autism spectrum disorder. *Experimental Brain Research, 234*(12), 3425-3431. doi:10.1007/s00221-016-4737-y

Maximo, J. O., Keown, C. L., Nair, A., & Müller, R. A. (2013). Approaches to local connectivity in autism using resting state functional connectivity MRI. *Front Hum Neurosci, 7*, 605. doi:10.3389/fnhum.2013.00605

Mostofsky, S. H., Powell, S. K., Simmonds, D. J., Goldberg, M. C., Caffo, B., & Pekar, J. J. (2009). Decreased connectivity and cerebellar activity in autism during motor task performance. *Brain, 132*(Pt 9), 2413-2425. doi:10.1093/brain/awp088

Müller, R.-A. (2007). The study of autism as a distributed disorder. *Ment Retard Dev Disabil Res Rev, 13*, 85-95.

Müller, R. A., Shih, P., Keehn, B., Deyoe, J. R., Leyden, K. M., & Shukla, D. K. (2011). Underconnected, but how? A survey of functional connectivity MRI studies in autism spectrum disorders. *Cereb Cortex, 21*(10), 2233-2243, doi:10.1093/cercor/bhq296.

Murphy, K., Birn, R. M., Handwerker, D. A., Jones, T. B., & Bandettini, P. A. (2009). The impact of global signal regression on resting state correlations: are anti-correlated networks introduced? *Neuroimage, 44*(3), 893-905. doi:10.1016/j.neuroimage.2008.09.036

Musso, F., Brinkmeyer, J., Mobascher, A., Warbrick, T., & Winterer, G. (2010). Spontaneous brain activity and EEG microstates. A novel EEG/fMRI analysis approach to explore resting-state networks. *Neuroimage, 52*(4), 1149-1161. doi:10.1016/j.neuroimage.2010.01.093

Nair, S., Jao Keehn, R. J., Berkebile, M. M., Maximo, J. O., Witkowska, N., & Müller, R. A. (2017). Local resting state functional connectivity in autism: site and cohort variability and the effect of eye status. *Brain Imaging Behav*. doi:10.1007/s11682-017-9678-y

Nalci, A., Rao, B. D., & Liu, T. T. (2019). Nuisance effects and the limitations of nuisance regression in dynamic functional connectivity fMRI. *Neuroimage, 184*, 1005-1031. doi:10.1016/j.neuroimage.2018.09.024

Power, J. D., Mitra, A., Laumann, T. O., Snyder, A. Z., Schlaggar, B. L., & Petersen, S. E. (2014). Methods to detect, characterize, and remove motion artifact in resting state fMRI. *Neuroimage, 84*, 320-341. doi:10.1016/j.neuroimage.2013.08.048

Preti, M. G., Bolton, T. A., & Van De Ville, D. (2017). The dynamic functional connectome: State-of-the-art and perspectives. *Neuroimage, 160*, 41-54. doi:10.1016/j.neuroimage.2016.12.061

Rane, P., Cochran, D., Hodge, S. M., Haselgrove, C., Kennedy, D. N., & Frazier, J. A. (2015). Connectivity in Autism: A Review of MRI Connectivity Studies. *Harv Rev Psychiatry, 23*(4), 223-244. doi:10.1097/HRP.0000000000000072

Rashid, B., Blanken, L. M. E., Muetzel, R. L., Miller, R., Damaraju, E., Arbabshirani, M. R., . . . Calhoun, V. (2018). Connectivity dynamics in typical development and its relationship to autistic traits and autism spectrum disorder. *Hum Brain Mapp, 39*(8), 3127-3142. doi:10.1002/hbm.24064

Rashid, B., Damaraju, E., Pearlson, G. D., & Calhoun, V. D. (2014). Dynamic connectivity states estimated from resting fMRI Identify differences among Schizophrenia, bipolar disorder, and healthy control subjects. *Front Hum Neurosci, 8*, 897. doi:10.3389/fnhum.2014.00897

Rippon, G., Brock, J., Brown, C., & Boucher, J. (2007). Disordered connectivity in the autistic brain: challenges for the "new psychophysiology". *International Journal of Psychophysiology, 63*(2), 164-172.

Rudie, J. D., Brown, J. A., Beck-Pancer, D., Hernandez, L. M., Dennis, E. L., Thompson, P. M., . . . Dapretto, M. (2012). Altered functional and structural brain network organization in autism. *Neuroimage Clin, 2*, 79-94. doi:10.1016/j.nicl.2012.11.006

Rudie, J. D., Shehzad, Z., Hernandez, L. M., Colich, N. L., Bookheimer, S. Y., Iacoboni, M., & Dapretto, M. (2012). Reduced functional integration and segregation of distributed neural systems underlying social and emotional information processing in autism spectrum disorders. *Cereb Cortex, 22*(5), 1025-1037. doi:10.1093/cercor/bhr171

Schölvinck, M. L., Maier, A., Ye, F. Q., Duyn, J. H., & Leopold, D. A. (2010). Neural basis of global resting-state fMRI activity. *Proc Natl Acad Sci U S A, 107*(22), 10238-10243. doi:10.1073/pnas.0913110107

Shakil, S., Lee, C. H., & Keilholz, S. D. (2016). Evaluation of sliding window correlation performance for characterizing dynamic functional connectivity and brain states. *Neuroimage, 133*, 111-128. doi:10.1016/j.neuroimage.2016.02.074

Smith, S. M., Fox, P. T., Miller, K. L., Glahn, D. C., Fox, P. M., Mackay, C. E., . . . Beckmann, C. F. (2009). Correspondence of the brain's functional architecture during activation and rest. *Proc Natl Acad Sci U S A, 106*(31), 13040-13045. doi:10.1073/pnas.0905267106

Smith, S. M., Jenkinson, M., Woolrich, M. W., Beckmann, C. F., Behrens, T. E., Johansen-Berg, H., . . . Matthews, P. M. (2004). Advances in functional and structural MR image analysis and implementation as FSL. *Neuroimage, 23 Suppl 1*, S208-219. doi:10.1016/j.neuroimage.2004.07.051

Sohn, W. S., Yoo, K., Lee, Y. B., Seo, S. W., Na, D. L., & Jeong, Y. (2015). Influence of ROI selection on resting state functional connectivity: an individualized approach for resting state fMRI analysis. *Front Neurosci, 9*, 280. doi:10.3389/fnins.2015.00280

Supekar, K., Uddin, L. Q., Khouzam, A., Phillips, J., Gaillard, W. D., Kenworthy, L. E., . . . Menon, V. (2013). Brain hyperconnectivity in children with autism and its links to social deficits. *Cell Rep, 5*(3), 738-747. doi:10.1016/j.celrep.2013.10.001

Thompson, W. H., & Fransson, P. (2015). The mean-variance relationship reveals two possible strategies for dynamic brain connectivity analysis in fMRI. *Front Hum Neurosci, 9*, 398. doi:10.3389/fnhum.2015.00398

Van de Ville, D., Britz, J., & Michel, C. M. (2010). EEG microstate sequences in healthy humans at rest reveal scale-free dynamics. *Proc Natl Acad Sci U S A, 107*(42), 18179-18184, doi:10.1073/pnas.1007841107.

Vidaurre, D., Smith, S. M., & Woolrich, M. W. (2017). Brain network dynamics are hierarchically organized in time. *Proc Natl Acad Sci U S A*. doi:10.1073/pnas.1705120114

Watanabe, T., & Rees, G. (2017). Brain network dynamics in high-functioning individuals with autism. *Nat Commun, 8*, 16048. doi:10.1038/ncomms16048

Wechsler, D. (2011). *Wechsler Abbreviated Scale of Intelligence - Second Edition*. San Antonio, TX: NCS Pearson.

Wee, C. Y., Yap, P. T., & Shen, D. (2016). Diagnosis of Autism Spectrum Disorders Using Temporally Distinct Resting-State Functional Connectivity Networks. *CNS Neurosci Ther, 22*(3), 212-219. doi:10.1111/cns.12499

Wong, C. W., Olafsson, V., Tal, O., & Liu, T. T. (2012). Anti-correlated networks, global signal regression, and the effects of caffeine in resting-state functional MRI. *Neuroimage, 63*(1), 356-364. doi:10.1016/j.neuroimage.2012.06.035

Yerys, B. E., Gordon, E. M., Abrams, D. N., Satterthwaite, T. D., Weinblatt, R., Jankowski, K. F., . . . Vaidya, C. J. (2015). Default mode network segregation and social deficits in autism spectrum disorder: Evidence from non-medicated children. *Neuroimage Clin, 9*, 223-232. doi:10.1016/j.nicl.2015.07.018

Yuan, H., Zotev, V., Phillips, R., Drevets, W. C., & Bodurka, J. (2012). Spatiotemporal dynamics of the brain at rest--exploring EEG microstates as electrophysiological signatures of BOLD resting state networks. *Neuroimage, 60*(4), 2062-2072. doi:10.1016/j.neuroimage.2012.02.031

Zablotsky, B., Black, L. I., Maenner, M. J., Schieve, L. A., & Blumberg, S. J. (2015). Estimated Prevalence of Autism and Other Developmental Disabilities Following Questionnaire Changes in the 2014 National Health Interview Survey. *Natl Health Stat Report*(87), 1-20.

Zhu, Y., Zhu, X., Zhang, H., Gao, W., Shen, D., & Wu, G. (2016). Reveal Consistent Spatial-Temporal Patterns from Dynamic Functional Connectivity for Autism Spectrum Disorder Identification. *Med Image Comput Comput Assist Interv, 9900*, 106-114. doi:10.1007/978-3-319-46720-7_13

Chapter 3:

Study 2

The content within this section, titled "Chapter 3: Study 2," reflects material from a paper that has been submitted for publication. The citation is as follows:

Mash, L. E., Linke, A. C., Gao, Y., Wilkinson, M., Olson, M. A., Jao Keehn, R. J., & Müller, R.-A. (Under Review). BOLD lag patterns differ between rest and task conditions, but are largely typical in autism.

Abstract

Background/Introduction: Autism spectrum disorder (ASD) is characterized by atypical functional connectivity (FC) within and between distributed brain networks. However, FC findings have often been inconsistent, possibly due to focus on static FC rather than brain dynamics. Lagged connectivity analyses aim to evaluate temporal latency, and presumably neural propagation, between regions. This approach may therefore reveal a more detailed picture of network organization in ASD than traditional FC methods.

Methods: The current study evaluated whole-brain lag patterns in adolescents with ASD (n = 28) and their typically developing peers (n = 22). Functional MRI data were collected during rest and during a lexico-semantic decision task. Optimal lag was calculated for each pair of regions of interest using cross-covariance, and mean latency projections were calculated for each region.

Results: Latency projections did not regionally differ between groups, with the same regions emerging among the 'earliest' and 'latest.' Although many of the longest absolute latencies were preserved across resting-state and task conditions, lag patterns overall were affected by condition, as many regions shifted toward zero-lag during task performance. Lag structure was also strongly associated with literature-derived estimates of arterial transit time.

Discussion: Results suggest that lag patterns are broadly typical in ASD but undergo changes during task performance. Moreover, lag patterns appear to reflect a combination of neural and vascular sources, which should be carefully considered when interpreting lagged FC.

Keywords: Autism spectrum disorder; functional MRI; functional connectivity; BOLD dynamics

Introduction

Autism spectrum disorder (ASD) is a neurodevelopmental condition characterized by deficits in social communication and restricted interests, repetitive behaviors, or unusual sensory responses (American Psychiatric Association, 2013). Recent prevalence estimates approach 2% (Maenner et al., 2020). However, neurobiological underpinnings of ASD remain incompletely understood.

Neuroimaging research in recent decades has led to consensus that ASD is characterized by atypical communication among distributed brain networks (Di Martino et al., 2014), rather than focal abnormalities. However, ASD is highly heterogeneous (Geschwind & State, 2015; Lombardo, Lai, & Baron-Cohen, 2019; Olsson et al., 2015), and functional connectivity magnetic resonance imaging (fcMRI) studies have often reported discrepant or mixed findings of overconnectivity and underconnectivity involving various functional networks (Hull et al., 2016; Rane et al., 2015). Methodological variables likely explain some of these inconsistencies (Müller et al., 2011; Nair et al., 2014), but cannot fully account for the wide range of findings.

Most fcMRI research has focused exclusively on static functional connectivity (FC), based on correlations between regional timeseries across an entire scan. Blood oxygen level-dependent (BOLD) activity in regions belonging to common functional networks tend to be highly correlated (Biswal et al., 1995; Fox & Raichle, 2007). However, static FC is limited by its inability to capture continuous changes in BOLD correlations that occur over seconds or minutes. Alternative, dynamic FC approaches, such as sliding window and clustering analyses, have demonstrated that the configuration of BOLD networks and the 'strength' of individual connections vary on a timescale of seconds in typical development (Allen et al., 2014; Calhoun et al., 2014; Nomi et al., 2016). However, even the majority of dynamic FC studies assume that

BOLD activity between related regions is synchronous (i.e., at zero-lag). Recent findings suggest that neural propagation (i.e., temporal latency between activity in a source region and a destination region) may be observable at a timescale of seconds via BOLD activity. For example, resting-state lag analysis (RSLA), first described by Mitra et al. (2014), determines the optimal latencies between pairs of timeseries by calculating lagged cross-covariance at several points in either direction of zero-lag. Covariance estimates are then plotted at each lag, and parabolic interpolation is used to estimate timing of the peak covariance; this yields a pairwise lag estimate between each pair of brain regions examined. Finally, "latency projections" are calculated for each brain region as the mean lag with respect to all other regions. While pairwise lags describe the temporal relationship between any two regions, averaged latency projections are useful in identifying brain areas that are consistently 'early' or 'late' and may therefore serve as general sources or sinks of neural activity.

Using a large sample of typically developing (TD) individuals, Mitra et al. (2014) demonstrated highly reproducible patterns of "lag structure" across seven independent subsamples, with consistently 'early' and 'late' nodes emerging in several functional networks. In other words, latency projections were negative for 'early' regions and positive for 'late' regions, with respect to the rest of the brain. In a small group of extensively sampled participants, this method revealed stable lag structure within individuals, with a number of early regions serving multiple functional networks showing similar latency across all subjects (Raut, Mitra, Marek, et al., 2019). Mitra et al. (2014) found that RSLA estimates varied with eye status (open versus closed), after a button press task, and at different times of day (morning versus evening); this was interpreted as support for a neural basis of the observed latency structure. Furthermore, calcium/hemoglobin imaging and laminar recordings in a mouse model suggest

that spontaneous infra-slow activity, most often associated with BOLD fluctuations (He et al., 2008; Pan, Thompson, Magnuson et al., 2013), follows predictable propagation patterns that are distinct from those seen at higher frequencies (Mitra, Kraft, Wright et al., 2018). However, primarily vascular, non-neuronal explanations for BOLD lag have also been proposed (Aso, Jiang, Urayama et al., 2017).

A limited number of studies have explored resting-state BOLD latency in ASD using various approaches. Using RSLA, Mitra et al. (2017) reported atypical lag structure in a small ASD sample. Specifically, they found that frontopolar cortex and putamen were significantly 'earlier' in an ASD than a TD group, whereas occipital cortex was 'later.' Furthermore, in the ASD group earlier frontopolar activity was associated with increased attention problems, and earlier putamen activity was associated with increased restricted and repetitive behaviors. Another study compared resting-state FC between adults with and without ASD at different lags; broadly increased FC in ASD was discovered at greater lags (in both directions), despite an absence of group differences at zero-lag (King et al., 2018). This was accompanied by increased "sustained connectivity," or FC duration, in the ASD group. Finally, a recent resting-state study using ultrafast magnetic resonance encephalography (MREG; TR = 100 ms) reported atypical latency patterns in ASD across multiple networks, with the ASD group generally showing shorter lags than the TD group (Raatikainen, Korhonen, Borchardt et al., 2020). This study used dynamic lag analysis, which assesses lag by comparing the timing of resting-state BOLD peaks across high-resolution timeseries.

Although these first lag studies show promise, there are several limitations to consider. First, measurement of lagged cross-correlations is limited by the low temporal resolution of the BOLD signal. Second, latency analyses are particularly sensitive to data length (i.e., scan

duration), motion artefact, physiological artefact, and censored timepoints, all of which can affect sampling error and reliability of estimates (Chen, Lewis, Chang et al., 2020; Raut, Mitra, Snyder et al., 2019; Smith, Miller, Salimi-Khorshidi et al., 2011); similar concerns have been raised about the effects of motion and physiological artefact on dynamic FC (Laumann et al., 2016; Nalci et al., 2019). Third, hemodynamic and neural contributions to the BOLD signal cannot be entirely separated. In other words, it is unclear to what degree BOLD latency between two regions reflects directional neural communication, versus regional differences in vascular supply. Therefore, group differences in vascular measures, such as arterial supply and cerebral blood flow, may confound BOLD lag estimates (Tong, Yao, Chen et al., 2019). Mitra et al. (2014) reported a lateness bias for regions near large venous sinuses in TD participants but did not find any relationship between latency and perfusion. These concerns merit particular attention in ASD studies, as localized differences in the hemodynamic response (Yan et al., 2018), as well as altered cerebral blood flow (George, Costa, Kouris et al., 1992; Jann, Hernandez, Beck-Pancer et al., 2015; Starkstein, Vazquez, Vrancic et al., 2000; Yerys, Herrington, Bartley et al., 2018), have been documented in this population. To this end, the current study compared whole-brain lag maps to a publicly available map of vascular supply territories (including measures of cerebral perfusion and arterial transit time) to further examine associations between BOLD latency and blood supply.

The current study builds upon the few previous reports of atypical lag structure in ASD by examining regional latencies of multi-echo, simultaneous multi-slice (MESMS) BOLD data. These data offer higher temporal resolution than standard fMRI sequences (TR $\leq$ 1.25). Although one previous study has examined lag in ASD at even higher temporal resolution (Raatikainen et al., 2020), the MESMS protocol acquires data using three distinct echo times

(TE). This allows for multi-echo independent component analysis (ME-ICA) denoising, in which TE dependencies of ICA components are used to distinguish neural components from noise components. This method has shown superior artefact removal compared to standard denoising procedures (Kundu, Brenowitz, Voon et al., 2013; Kundu, Inati, Evans et al., 2012).

The previous literature has explored only resting-state lag structure in ASD, which relies on assumptions about the source and timing of neuronal events. In the absence of an explicit task, the degree to which synchronous BOLD activity reflects intrinsic connectivity versus state-specific processing remains ambiguous. Therefore, the current study assessed latency during rest as well as during a task, providing controlled data acquisition during which all participants are exposed to the same stimuli. A complex lexicosemantic decision task was selected, due to its recruitment of numerous brain regions and networks including primary visual cortex, motor regions, language networks, and executive regions involved in decision-making, inhibition, and initiation. Therefore, this task was considered suitable for comparing BOLD latency differences between a relatively uncontrolled state (with spontaneous signal fluctuations) and a relatively controlled state (with task-driven fluctuations). Comparisons between resting-state and task conditions may shed light on the degree to which BOLD latency structure reflects a history of directional co-activation versus task-specific cognitive demands. The current study aimed to clarify 1) differences in whole-brain lag structure in ASD compared to typical development, including between occipital, frontopolar, and subcortical areas previously implicated in ASD, 2) differences in lag structure in the presence versus absence of an explicit task, and 3) inter-individual variability of whole-brain lag structure. Secondarily, this study examined associations between latency projections and literature-derived measures of cerebral perfusion and arterial

blood supply, to assess the degree to which these variables may confound neural sources of lag in either group.

Methods

Participants

Seventy adolescents and young adults ages 12-21 years were enrolled and scanned as part of this study. Fourteen participants with ASD and six typically developing (TD) participants were excluded from analyses due to unacceptable data quality for one or more of the three functional scans. Criteria for exclusion were excessive motion (root mean squared displacement > .15 mm), < 60% accuracy on behavioral tasks, missing scans, preprocessing failure, or incidental MRI findings. This left a final sample of 50 participants (28 ASD, 22 TD) with high-quality data. All ASD diagnoses were confirmed using the Autism Diagnostic Observation Schedule, Second Edition (ADOS-2, Gotham, Risi, Pickles, & Lord, 2007), the Autism Diagnostic Interview–Revised (ADI-R, Lord, Rutter, & Le Couteur, 1994), and expert clinical judgment based on DSM-5 criteria (American Psychiatric Association, 2013). The Wechsler Abbreviated Scales of Intelligence-Second Edition (WASI-II, Wechsler, 2011) and Social Responsiveness Scale, Second Edition (SRS-2, Constantino & Gruber, 2012) parent report form were administered to individuals in both groups. Groups did not significantly differ with respect to age, handedness, gender, verbal IQ, nonverbal IQ, or in-scanner head motion (Table 1). Root mean squared displacement (RMSD) was used as an estimate of head motion across all time points for both conditions (task and resting state). All included participants had low estimates of motion in both conditions (RMSD ≤ .15 mm). A mixed analysis of variance (ANOVA) found no effect of condition, diagnosis, or the condition * diagnosis interaction on RMSD (all p values > .12). All TD participants were unmedicated. Eleven ASD participants reported taking

psychotropic medications, and co-occurring psychiatric diagnoses were documented in 10 ASD participants. Medication status and co-occurring conditions were not documented for one individual in the ASD group. Details regarding medication usage and co-occurring diagnoses are reported in Supplemental Table 1. Written informed consent was obtained from all participants and/or their caregivers, and written assent was obtained for participants under 18 years old. All procedures were approved by the San Diego State University and University of California, San Diego Institutional Review Boards.

Data Acquisition

Imaging data were acquired on a GE 3T MR750 scanner with a 32-channel head coil at the Center for Functional MRI (University of California, San Diego). High-resolution structural images were acquired with a standard FSPGR T1-weighted sequence (TR: 8.136ms, TE: 3.172 ms, flip angle: 8°; FOV 256 mm; matrix: 256 x 192 1mm^3 resolution; 172 slices). Functional T2*-weighted images were acquired using an accelerated multi-echo simultaneous multi-slice (MESMS) echo-planar (EPI) sequence (TR: 1250 ms; TE: 13.2, 30.3, and 47.4 ms; flip angle: 60°; 3 mm^3 resolution; FOV: 216mm; matrix: 72 x 72 with in-plane acceleration factor R: 2; in-plane resolution: 3 x 3; multiband acceleration factor R: 3; 54 slices). Two single-echo EPI sequences with the same parameters (TE: 30.3) and opposite phase-encoding directions were also acquired for later distortion correction (see section 2.3). The MESMS approach has been shown to improve detection of functional networks and substantially reduce motion and physiological artifact (see section 2.3 for preprocessing details; Kundu et al., 2013; Kundu et al., 2012). One 6-minute 26-second resting-state scan was obtained (309 volumes), followed by two task scans lasting seven minutes each (340 volumes). The functional scan protocol for 9 TD and 2 ASD participants differed slightly (TR = 1100 ms, 45 slices, 340 resting volumes, 6:14 resting

scan duration, 386 task volumes, 7:00 duration for each of two task scans). The mean temporal signal-to-noise ratio (tSNR) did not significantly differ between these participants and a sample of participants scanned with the standard protocol who were matched for motion and demographic variables (resting state: $t(20) = -.91$, $p = .37$, task run 1: $t(20) = -.61$, $p = .55$, task run 2: $t(20) = .32$, $p = .75$). The first nine volumes of each scan were discarded to account for T1-equilibration effects.

During resting-state scans, participants were instructed to fixate on a cross projected onto the middle of a screen, viewed through a mirror in the bore, and to "Let your mind wander, relax, but please stay as still as you can. Do not fall asleep." Compliance with instructions to remain still and awake was monitored via video recording. During task scans, participants performed a lexical decision task. In this task, participants were asked to distinguish between animal words (e.g., "cat"), standard (nonanimal) words (e.g., "chair"), and pseudowords (e.g., "blont"). Null trials consisting of a fixation string ("xxxxxx") were also included. Participants were asked to respond to standard words (90 trials) and animal words (30 trials) using their left index and middle fingers, respectively, and to withhold responses to pseudowords (30 trials). Stimuli were presented for 500 ms, followed by a 1500 ms fixation string to allow for response (total of 2s per trial). Conditions were matched for number of letters and syllables ($p > 0.1$). Animal and standard words were also matched for word frequency (Brysbaert & New, 2009; van Heuven, Mandera, Keuleers et al., 2014) and age of acquisition (Kuperman, Stadthagen-Gonzalez, & Brysbaert, 2012), using publicly available corpora ($p > 0.1$).

Data Processing

All structural and functional data were visually inspected for signal dropout, excessive motion artifact, and alignment errors at multiple preprocessing stages to ensure acceptable data

quality. Functional images were processed using Analysis of Functional NeuroImages software (AFNI v17.2.07; Cox, 1996) and FMRIB Software Library (FSL; v5.0; Smith et al., 2004). Two spin-echo EPI acquisitions with opposite phase encoding directions were used to minimize susceptibility-induced distortions via FSL's TOPUP (Smith, Jenkinson, Woolrich et al., 2004). Each functional volume was registered to the middle time point of the scan to adjust for motion via rigid-body realignment as implemented in AFNI. Functional images were co-registered to the anatomical scan via FSL's FLIRT (Jenkinson & Smith, 2001) and standardized to the atlas space of the Montreal Neurological Institute (MNI) template using FSL's nonlinear registration tool (FNIRT). AFNI's 3dBlurToFWHM was used to smooth functional images to a Gaussian full width at half-maximum (FWHM) of 6 mm. Functional MRI time series were either bandpass filtered ($.008 < f < .08$; resting-state scan) or highpass filtered ($.01 < f;$ task scans).

Denoising was conducted using multi-echo independent component analysis to remove artefactual components (ME-ICA; Kundu et al., 2013). Data from the three echoes were optimally combined to produce a single timeseries. Multi-echo weighted optimization and ME-ICA are described in detail by Olafsson, Kundu, Wong et al. (2015; see Appendix A), and implemented by meica.py, which is publicly available at http://afni.nimh.nih.gov/afni/. No censoring was applied to preserve the continuity of timeseries for lag analysis.

Analyses

Regions of Interest

An exploratory set of ROIs covering all cortical and subcortical regions was created by combining 100 regions from a widely used functional cortical parcellation (Schaefer, Kong, Gordon et al., 2018; https://github.com/ThomasYeoLab/CBIG/tree/master/stable_projects/brain_parcellation/Schaefe

r2018_LocalGlobal) with 14 regions from the Harvard-Oxford subcortical atlas (Bohland, Bokil, Allen et al., 2009). Cortical regions were assigned to one of seven functional networks, as described by (Yeo, Krienen, Sepulcre et al., 2011): visual, somatomotor, dorsal attention, ventral attention, limbic, frontoparietal control, and default-mode.

Functional Connectivity and Lag Analysis

For each participant, timeseries were extracted from all ROIs. Pearson correlations (transformed to Fisher's *z*) were calculated between timeseries for each ROI-ROI pairing, yielding a symmetrical FC matrix. FC at each ROI-ROI pair was compared between ASD and TD groups using independent samples *t*-tests. The distribution of group differences in FC was evaluated using a one-sample *t*-test of all group difference *t*-scores, to examine whether, on average, group differences across all ROI pairs differed significantly from zero in either direction. Significant findings were followed up with a supplemental analysis using censored data to examine potential effects of motion. Censoring was performed by removing volumes with greater than 0.5mm framewise displacement, as well as the three following volumes. If fewer than 18 usable timepoints fell between two censored timepoints, then all volumes in between were also censored.

Pairwise lag estimates and regional mean latency projections were calculated using the method developed and described in detail by (Mitra et al., 2014), using in-house MATLAB code. Cross-covariance between each pair of timeseries was calculated at zero-lag, as well as at -4 to 4 TR lag (using MATLAB's xcov function). Cross-covariance was plotted at each lag using piecewise cubic interpolation (MATLAB's pchip) and a local minimum or maximum was identified if possible. Parabolic interpolation was then used to estimate the optimal lag between two timeseries. If a local minimum or maximum could not be identified within three TRs of

zero-lag in either direction, the peak lag was considered unlikely to result from true neural signal (Raut, Mitra, Marek, et al., 2019) and was discarded. The number of discarded peak lags was considerably larger during resting state scans (ASD mean = 8.3%, TD mean = 8.8%) than task performance (ASD mean = 0.45%, TD mean = 0.39%), but did not significantly differ between groups in either rest or task conditions (p = .81 and p = .75, respectively).

The procedure above resulted in an anti-symmetric matrix of all pairwise lag values for each participant. "Latency projections" for each ROI, as defined by Mitra et al. (2014), were then calculated by averaging across all rows of the matrix, resulting in one mean lag value per column. In other words, latency projections represent the mean lag for a given ROI across all of its pairings with other ROIs. To compare lag structure across conditions, average resting-state and task-related latency projections (across 114 ROIs) were correlated separately for ASD and TD groups. To compare lag structure between groups, group-averaged latency projections were correlated separately for resting-state and task conditions. These correlational analyses were also conducted for pairwise lag estimates. Effects of diagnosis, condition, and their interaction on latency projections were evaluated using a mixed design ANOVA for each ROI (using simple_mixed_anova in MATLAB; Caplette, 2020), with diagnosis as a between-subjects variable and task condition as a within-subjects variable. Resulting p-values were adjusted to control for false discovery rate using the Benjamini-Hochberg linear step-up procedure (Benjamini & Hochberg, 1995).

Similarity Analysis

Recent research suggests that the organization of functional networks may be more idiosyncratic in ASD (i.e., characterized by increased within-group variability) than in typical development (Hahamy, Behrmann, & Malach, 2015; Nunes, Peatfield, Vakorin et al., 2019).

Therefore, similarity analyses were conducted to examine the inter-individual variability of FC and latency projections for both resting-state and task conditions. For each group, all participants' pairwise FC estimates were correlated with all other participants' FC estimates. The resulting correlation matrix was averaged across rows, yielding one similarity score per participant, which was then converted to a Fisher's *z*-score. These scores represent the average within-group similarity between each individual's whole-brain FC pattern and all other individuals' whole-brain FC patterns. A mixed ANOVA was conducted (as in lag analyses) to determine the effects of diagnosis, condition, and their interaction on within-group FC similarity. This similarity analysis procedure was repeated for latency projections.

All significant ANOVA effects were followed up with non-parametric permutation testing due to the non-independence of similarity scores. In this procedure, *p*-values were calculated by comparing *t*-scores to a null T_{max} distribution (Chen et al., 2013) consisting of *t*-scores derived from 1000 random permutations of the grouping variable of interest (i.e., ASD or TD; task or rest).

Hemodynamic Comparisons

To determine possible vascular contributions to lag structure, secondary analyses were conducted comparing whole-brain latency projections to 1) cerebral blood flow (CBF) maps obtained from the Pediatric Template of Brain Perfusion (Avants, Duda, Kilroy et al., 2015), and 2) arterial territory maps and associated median arterial transit times (ATT) reported by Mutsaerts, van Dalen, Heijtel et al. (2015). For the first analysis, CBF was extracted from all ROIs and correlated with latency projections for each group. For the second analysis, each cortical ROI was assigned to one of nine arterial flow territories from a publicly available map (Mutsaerts, 2015), based on descriptions by Tatu, Moulin, Bogousslavsky et al. (1998).

Assignments were made according to spatial overlap between each ROI and flow territory. For every ROI, each voxel was assigned a number (1-9) corresponding to the flow territory that encompassed that voxel. This resulted in a vector of voxel locations for each ROI. The modal value of each vector then determined the territory assignment for the corresponding ROI (Fig. S1). For 11 subcortical ROIs, the majority of voxels fell outside all nine flow territories. Therefore, these ROIs were excluded from hemodynamic analyses. Mean latency was calculated for each territory and correlated with median arterial transit time. Similarity of arterial flow patterns between groups was also examined by correlating ASD and TD mean latencies for all territories.

Results

Functional Connectivity Analyses

A one-sample *t*-test of all group comparison *t*-scores (all ROI pairings in the matrix), examining the overall distribution of group differences in FC, revealed a broad shift toward overconnectivity in the ASD relative to the TD group in both resting-state ($t(6440) = 101.42$, $p < .001$) and task conditions ($t(6440) = 158.64$, $p < .001$). On pairwise tests, resting-state overconnectivity (ASD > TD) between one pair of left visual ROIs (Vis 3-Vis 6, $t(48) = 4.97$, $p < .001$) survived correction for false-discovery rate (FDR). No other findings remained significant after FDR correction, given the large number of comparisons. A supplemental analysis revealed no substantial changes in either resting-state ($t(6440) = 95.34$, $p < .001$) or task-based ($t(6440) = 145.47$, $p < .001$) findings after censoring volumes with excessive motion. Finally, there were no significant differences in resting-state or task-based functional connectivity between medicated and unmedicated participants with ASD, nor were there

significant differences between participants with and without comorbid psychiatric diagnoses (all *p*-values > .05).

Lag Analyses

Latency projections revealed largely bilateral lag patterns across the brain in both groups (Fig. 1a-b), with estimates ranging from approximately -0.8 to +1.0 seconds. Similar lag patterns were observed between resting-state and task conditions with respect to both latency projections (Rest vs. Task, ASD: $r = .87$, $p < .001$; TD: $r = .78$, $p < .001$) and pairwise lag matrices (Rest vs. Task, ASD: $r = .78$, $p < .001$; TD: $r = .70$, $p < .001$). ASD and TD participants also showed highly similar patterns of group-averaged latency projections (ASD vs. TD, resting-state: $r = .90$, $p < .001$; task: $r = .95$, $p < .001$), as well as pairwise lag matrices (ASD vs. TD, resting-state: $r = .78$ $p < .001$; task: $r = .86$, $p < .001$).

Several regions consistently emerged among the earliest and latest in both groups. In the resting-state, 'early' regions included the putamen, inferior frontal gyrus, insula, lateral dorsal attention regions, and lateral somatomotor regions, while 'late' regions included visual areas, thalamus, caudate, cingulate, and medial parietal cortex. During task performance, a similar pattern emerged with 'early' activity in inferior frontal gyrus and insula, and 'late' activity in visual and medial parietal regions; mean latencies were close to zero for other structures (Fig. 1b). In general, anterior, lateral structures tended to be early relative to posterior, medial structures, and this pattern affected more ROIs in the resting-state condition than the task condition.

Mixed ANOVAs for each ROI found no main effects of diagnosis on latency, and no interactions between diagnosis and task condition (all corrected *p* values > .05). However, 37 ROIs spanning most networks showed main effects of condition (all corrected *p* values < .05;

Fig. 1c; Table S2), which consistently reflected reduced absolute latency in the task compared to the rest condition. In other words, many regions that were relatively early or late during the resting state showed latencies closer to zero during task performance. A post-hoc two-sample Kolmogorov-Smirnov test was conducted (using MATLAB's kstest2) to compare the distributions of mean pairwise lag values (6441 ROI pairs) in each condition. This test confirmed that group-averaged rest and task lag distributions differed from one another ($D^* = .19$, $p < .001$), such that the Gaussian distribution of resting latencies was flatter and more spread out than the task-related distribution, which showed a large number of ROI-ROI latencies clustered closer to zero (Fig. S2).

To ensure that lag differences between the task and resting-state conditions were not associated with acquisition length (i.e., one resting run versus two concatenated task runs), this analysis was repeated using individual task runs. Results were similar to those reported above when run 1 only ($D^* = .19$, $p < .001$) and run 2 only ($D^* = .17$, $p < .001$) were used (Fig. S2). Finally, to account for the greater number of pairwise lags that could not be calculated at rest, the analysis was repeated after eliminating ROI-ROI pairs that were unusable in resting-state data from the task data. This procedure produced similar results to those described above ($D^* = .19$, $p < .001$). Finally, independent-samples t-tests revealed no significant differences in resting-state or task-based latency between medicated and unmedicated participants with ASD, nor were there significant differences between participants with and without comorbid psychiatric diagnoses (all p-values > .05).

Similarity Analyses

A mixed ANOVA showed that within-group FC similarity was lower in the ASD relative to the TD group (ASD mean $z = .50$, TD mean $z = .59$, $F(1,48) = 65.28$, $p < .001$), and that FC

similarity was lower during the resting state than task performance (resting mean z = .46, task mean z = .62, $F(1,48) = 329.95$, $p < .001$). There was no interaction between diagnosis and condition. Post-hoc permutation tests corroborated both the main effects of diagnosis ($t(98) = -4.81$, $p < .001$) and condition ($t(49) = 18.51$, $p < .001$) on FC similarity.

Similarity analyses of latency projections revealed reduced within-group similarity during the resting state compared to task performance (rest mean z = .28, task mean z = .44, $F(1,48) = 80.02$, $p < .001$). There was no main effect of diagnosis, nor was there a diagnosis * condition interaction. Post-hoc permutation testing corroborated the main effect of condition ($t(49) = 8.64$, $p < .001$) on lag similarity. To account for differences in amount of data (two task runs vs. one resting state run), this analysis was repeated using individual task runs. A main effect of condition (resting < task) was similarly observed for both run 1 ($F(1,48) = 12.52$, $p < .001$) and run 2 ($F(1,48) = 12.27$, $p = .001$), and these effects were corroborated using permutation testing (Run 1: $t(49) = 5.31$, $p < .001$; Run 2 $t(49) = 5.32$, $p < .001$).

Hemodynamic Comparisons

Cerebral blood flow estimates from the Pediatric Template of Brain Perfusion (Avants et al., 2015) were not correlated with mean latency projections in either group in either the resting-state (ASD: r = -.12, p = .20; TD: r = -.06, p = .56) or task conditions (ASD: r = -.06, p = .53, TD: r = -.10, p = .27). However, mean latency of nine arterial flow territories was associated with median ATT reported by Mutsaerts et al. (2015), with stronger relationships emerging during task performance (ASD: r = .79, p = .01; TD: r = .73, p = .03) than resting-state scans (ASD: r = .60, p = .09; TD: r = .46, p = .21; Fig 2a). Furthermore, the ASD and TD groups showed extremely similar mean latency patterns across all flow territories in both resting-state (r = .94, $p < .001$) and task conditions (r = .99, $p < .001$; Fig. 2b). Overall, regions supplied by the

middle cerebral artery were earlier, on average, than regions supplied by the anterior and posterior cerebral arteries. Regions supplied by the distal branches of the anterior and posterior cerebral arteries were consistently latest (Fig. 2c).

Discussion

Using high-resolution multi-echo fMRI data, this study found broadly similar whole-brain lag patterns in adolescents with ASD compared to a typically developing cohort. Latency projections differed in both groups as a function of task condition, with many regions shifting toward zero-lag during task performance. In other words, the Gaussian distribution of lags observed at rest showed reduced variance during task performance as more lags clustered around zero (Fig. S2). While (zero-lag) FC was more variable in the ASD group than the TD group, there were no group differences in the variability of lag patterns. However, both FC and latency projections showed more inter-individual variability during task performance than at rest. Finally, latency projections in both groups were strongly related to arterial blood supply and transit time.

Similar lag structure observed in both groups

With respect to resting-state lag structure, similar regions emerged among the 'earliest' and 'latest' in both ASD and TD groups. A general pattern emerged of earlier activity in lateral, anterior regions, compared to posterior, medial regions. In line with previous studies, lag structure was largely bilateral. The earliest regions during the resting state included inferior frontal gyrus, insula, lateral somatomotor and dorsal attention areas, putamen, and pallidum. Among the latest regions were visual cortex, cingulate, thalamus, caudate, and medial parietal areas. Early cortical regions in the current study largely correspond to those identified by Raut, Mitra, Marek, et al. (2019) using resting-state fMRI from eleven extensively-sampled healthy

adults; specifically, they reported early activity in anterior insula (left earlier than right, as in the current study), lateral premotor regions, and inferior frontal gyrus. Raut et al. found that early regions were identified more consistently across individuals than late regions, and proposed that these presumed neural sources serve a wide range of tasks as part of a "multiple-demand" system (Duncan, 2010).

Lag patterns differ between resting-state and task performance

Average lag patterns for resting-state and task data were highly correlated, with similar patterns of 'early' and 'late' regions. However, absolute lag was reduced in many regions during task performance, resulting in differences in lag distributions between conditions. Compared to the resting-state, latency projections showed greater within-group similarity during task performance; this was also true of FC estimates. Finally, peak lag could not be calculated (presumably due to noise) in approximately 8% of resting-state ROI-ROI pairs, but this occurred in less than 1% of ROI-ROI pairs during task performance. Altogether, this suggests that compared to the resting-state condition, latency patterns during an explicit task are less susceptible to noise, show greater consistency between individuals, and show greater distinction between few 'early' (i.e., left anterior insula, inferior frontal) and 'late' regions (visual, medial parietal) as other regions shift toward zero-lag.

Changes in the pairwise lag distribution during task performance may suggest that neural activity contributes to observed lag patterns, despite high correlations between resting-state and task-related latencies. One possible interpretation of this finding is that resting-state BOLD latency patterns partially reflect temporal relationships sculpted by past experience (Dosenbach, Fair, Miezin et al., 2007), which are modified during task-related processing. However, the greater uncertainty of neural event timing for resting compared to task data may have contributed

to the higher rate of unidentifiable pairwise peak lags, and thus a wider distribution of lags around zero. Furthermore, shared input between regions during task performance has been shown to increase FC estimates (Cole, Ito, Schultz et al., 2019), which could result a lag distribution that is clustered around zero.

No regional lag differences between ASD and typical development

Across all cortical and subcortical ROIs, there was minimal evidence of regional group differences in latency during either rest or task performance. This contrasts with resting-state findings by Mitra et al. (2017), who reported group differences in frontopolar (late in TD, average in ASD), occipital (early in TD, late in ASD), and putamen latencies (average in TD, early in ASD). Interestingly, for these three regions, resting-state latencies found in both groups in the current study most closely resemble those reported for the ASD group by Mitra et al. (i.e., average latency in frontopolar cortex, early activity in the putamen, late activity in visual cortex).

Partly divergent findings may relate to methodological differences, including eye status (open versus closed), temporal resolution (TR = 1.25 versus 2.2 sec), and denoising approach (multi-echo ICA versus nuisance regressors), and differing ages of participants (adolescents vs. young adults). Multi-echo ICA denoising uses data-driven methods to identify and remove non-BOLD artefact from various sources, including motion, respiration, and pulse. Compared to standard denoising methods using nuisance and global signal regressors, this approach has demonstrated superior recovery of BOLD signal corresponding to known resting-state networks (Kundu et al., 2013; Kundu et al., 2012; Olafsson et al., 2015). Differences in findings compared to previous lag studies may therefore be related to different methods of artifact removal. In addition, eye status has been found to affect lag estimates in visual regions, with eyes-closed paradigms eliciting earlier activity in occipital cortex (Mitra et al., 2014). This may relate to

extensive effects of eye status on (zero-lag) BOLD correlations within visual cortices observed in a large multisite ASD sample (Nair et al., 2017). Furthermore, group differences in FC likely vary across development in ASD (Henry, Dichter, & Gates, 2018; Nomi & Uddin, 2015; Uddin, Supekar, & Menon, 2013). Compared to the current study, mean age was c. 3 and 9 years higher in the samples studied by Mitra et al. (2017) and Raatikainen et al. (2019), respectively. While it is currently unknown how lag patterns may differ through adolescence and young adulthood, maturational FC changes are another potential explanation for differences in results.

Finally, Raatikainen et al. (2020) found atypical lag between multiple resting state networks using dynamic lag analysis (DLA) in ultra-fast MREG in adults with ASD. However, aside from potential maturational changes mentioned above, this study differed in multiple crucial respects from the current one (e.g., peak-to-peak DLA, use of ICA-based distributed resting-state networks as ROIs, exceptionally short TR), making it difficult to attribute differences in findings to a specific variable.

While inter-individual variability for (zero-lag) FC patterns was greater in the ASD than the TD group, no group differences in variability were found for lag patterns. In typically developing individuals, FC similarity measures have sometimes been associated with motion artifact (Kopal, Pidnebesna, Tomeček et al., 2020; Raut, Mitra, Snyder, et al., 2019). However, in our sample, individual FC similarity scores across all participants were not significantly correlated with head motion (i.e., RMSD) in either the resting state ($r = -.21$, $p = .15$) or the task ($r = -.08$, $p = .56$) condition. Although our findings are therefore consistent with reports of 'idiosyncrasy' of static FC (Hahamy et al., 2015; Nunes et al., 2019), they do not suggest that variability in lag patterns play a major role in 'idiosyncratic' FC in ASD.

Latency projections correspond to arterial flow territories

Mitra et al. (2014) reported a minimal association between cerebral blood flow and latency projections. The current study corroborates this finding, with no evident relationship between latency projections and perfusion values from the Pediatric Template of Brain Perfusion (Avants et al., 2015). Mitra et al. (2014) also did not find a clear association between regional lag and standard vascular territories (Damasio, 1983). However, the current study determined that lateral regions supplied by the middle cerebral artery (MCA) tended to be earlier on average compared to medial regions supplied by the anterior and posterior cerebral arteries (ACA, PCA), with the highest latencies in regions supplied by the distal branches of the ACA and PCA. Furthermore, the current study is the first to use an independent measure of arterial blood flow (ATT) to assess potential vascular contributions to BOLD latencies, which may confound interpretation of lag patterns. Mean lag for each flow territory was positively related to literature-derived estimates of ATT (Mutsaerts et al., 2015), especially during task performance, with ATT accounting for >50% of the variance in lag patterns. However, ATT explained <30% of the variance in lag during the resting state condition. Mean latency for each territory was also highly correlated between ASD and TD participants, suggesting that any effect of arterial supply on BOLD latency was consistent across diagnostic groups. Therefore, ATT appears to heavily impact lag patterns, and positive latencies in visual and medial parietal regions (supplied by the distal branches of the ACA and PCA) should be interpreted with particular caution.

Open questions and limitations

Overall, our findings suggest that BOLD latency reflects both neural and vascular contributions, with a major role of the latter. On one hand, while the overall pattern of lag structure was similar in resting-state and task conditions, the distribution of latencies differed

between conditions. Task-based lag structure also showed more reliable peak latency detection and greater consistency between individuals compared to the resting state. Altogether, these changes associated with task performance suggest some neural contribution to lag structure.

However, relationships between latency and vascular supply (i.e., arterial flow territory, ATT) suggest that observed BOLD latencies are considerably influenced by hemodynamic factors. This is expected, as the BOLD signal is an indirect measure of neural activity that is based on neurovascular coupling and associated changes in magnetic resonance (Hillman, 2014). The current study is limited by its use of an approximate map of vascular territories, which were derived from arterial spin labeling (ASL) scans in a different sample of individuals (Mutsaerts et al., 2015). Additionally, this study used estimates of vascular territories, ATT, and CBF derived from samples that are not necessarily representative of our participants. Vascular territories and ATT estimates were calculated based on an elderly adult sample (Mutsaerts et al., 2015); although CBF estimates were drawn from a pediatric population (Avants et al., 2015), this sample did not include any individuals with ASD. Therefore, while the current study sheds light on a general relationship between vascular supply and BOLD latency, future research is necessary to more clearly separate the relative influences of neural and vascular contributions to the BOLD signal by combining fMRI with complementary imaging modalities, such as EEG or ASL, in a common sample of children with and without ASD. Additionally, the current study did not directly explore regional differences in the hemodynamic response function (cf. Yan et al., 2018) across groups or task conditions. This alternative approach to characterizing hemodynamic variables may allow for closer examination of both inter- and intra-individual differences. Future studies may also further explore associations between hemodynamic features and lag at the individual level, as opposed to the group level alone (as in the current study).

There are several other limitations to the current study. First, our sample was relatively small, which impacts sampling variability and therefore the precision of both FC and latency analyses. Although large samples can be obtained from publicly available datasets, such as the Autism Brain Imaging Database Exchange (Di Martino, O'Connor, Chen et al., 2017; Di Martino et al., 2014), our in-house data benefited from high temporal resolution multi-echo, simultaneous multi-slice acquisition, as well as combined availability of resting and task data in the same individuals. Additionally, our in-house sample provided data on psychotropic medication use and co-occurring conditions, both of which are common in the general ASD population (Hossain, Khan, Sultana et al., 2020; Jobski, Hofer, Hoffmann et al., 2017) and were therefore not considered exclusionary criteria. However, effects of medication (Linke et al., 2017), and multiple diagnoses (Mikita, Simonoff, Pine et al., 2016) on functional connectivity have been demonstrated, and may have affected the findings reported in this study. Moreover, inclusionary age ranged from early adolescence through young adulthood. This developmental period is associated with changes in FC (Klapwijk, Goddings, Burnett Heyes et al., 2013; Solé-Padullés, Castro-Fornieles, de la Serna et al., 2016; Teeuw, Brouwer, Guimarães et al., 2019) that may affect BOLD lag patterns. Finally, fMRI data are inherently limited by the slow nature of the BOLD signal. Coordinated brain dynamics take place across a range of frequencies, including high-frequency changes on a millisecond timescale that are not observable using fMRI. Multimodal imaging approaches, such as simultaneous EEG-fMRI, have shown great promise in early studies of lagged functional connectivity (Feige, Spiegelhalder, Kiemen et al., 2017) and dynamic brain activity (Allen et al., 2017; Bridwell et al., 2013; Musso, Brinkmeyer, Mobascher et al., 2010; Yuan, Zotev, Phillips et al., 2012). However, multimodal functional neuroimaging to date remains extremely limited in ASD (Mash et al., 2018).

Conclusions

Findings suggest that adolescents and young adults with ASD show typical patterns of BOLD latency across the brain during both resting-state and task performance. While the earliest and latest regions were preserved across resting-state and task conditions, many areas showed reduced absolute latency during task performance, which may indicate neural contributions to lag patterns. However, latency projections in both groups were strongly associated with arterial supply and transit time. Our findings, which suggest that BOLD lag patterns reflect a combination of vascular and neural factors, extend the previous literature and provide a foundation for future research exploring spatiotemporal BOLD dynamics in ASD.

Acknowledgements

We thank all participants and families who took part in this study. We also thank Kalekirstos Alemu for his role in participant recruitment and data management. All authors contributed substantially to this work. LEM conceived of the study, developed methods, conducted analyses, and wrote the original draft of the manuscript. ACL contributed to development of methods, implementation of analyses, and manuscript revision. YG, MW, and MAO contributed to data collection and manuscript revision. RJJK contributed to data collection, development of methods, project administration, and manuscript revision. RAM provided laboratory space and resources, acquired funding, supervised the design and implementation of the study, and revised the manuscript. This work was supported by the National Institute of Mental Health R01 MH101173 (RAM), National Science Foundation Graduate Research Fellowship 1321850 (LEM), and the San Diego State University Graduate Fellowship (MW).

Dissertation Author Note

Chapter 3, in full, is currently under review for publication. Mash, L. E., Linke, A. C., Gao, Y., Wilkinson, M., Olson, M. A., Jao Keehn, R. J., & Müller, R.-A. The dissertation author was the primary investigator and author of this paper.

Table 2.1 Sample Characteristics

	ASD (*n* = 28)	TD (*n* = 22)	Statistic	*p*
Sex	20 male	17 male	$X^2(1) = 0.22$	.640
Handedness	27 right	20 right	$X^2(1) = 0.67$	.415
Age	15.9 (2.2)	15.3 (1.9)	$t(48) = 1.01$	.319
	[12.9 – 20.1]	[12.4– 21.3]		
RMSD Rest	0.07 (0.03)	0.06 (0.02)	$t(48) = 1.07$	.290
	[0.01 – 0.13]	[0.02 – 0.11]		
RMSD Task	0.07 (0.02)	0.06 (0.03)	$t(48) = 1.67$	.102
	[0.03 – 0.13]	[0.03 – 0.15]		
VIQ	106 (17)	111 (13)	$t(48) = -1.27$	.210
	[68 – 134]	[85 – 135]		
NVIQ	108 (22)	110 (12)	$t(48) = -0.33$	.746
	[54 – 156]	[80 – 128]		
Task Accuracy (%)	88.0 (8.3)	94.7 (3.3)	$t(48) = -3.63$	< .001
	[70.7 – 99.0]	[85.0 – 98.7]		
ADOS-2 SA	8.8 (3.0)	---	---	---
	[3 – 14]	---	---	---
ADOS-2 RRB	2.4 (1.9)	---	---	---
	[0 – 9]	---	---	---
ADOS-2 Total	10.8 (3.4)	---	---	---
	[6 – 20]	---	---	---

Relevant characteristics are reported for both groups as: mean (sd), [min – max]. ASD and TD groups only differed with respect to task accuracy, which was lower in the ASD group. RMSD = Root Mean Squared Displacement; VIQ = Verbal IQ; NVIQ = Nonverbal IQ; ADOS = Autism Diagnostic Observation Schedule; SA = Social Affect; RRB = Restricted and Repetitive Behaviors

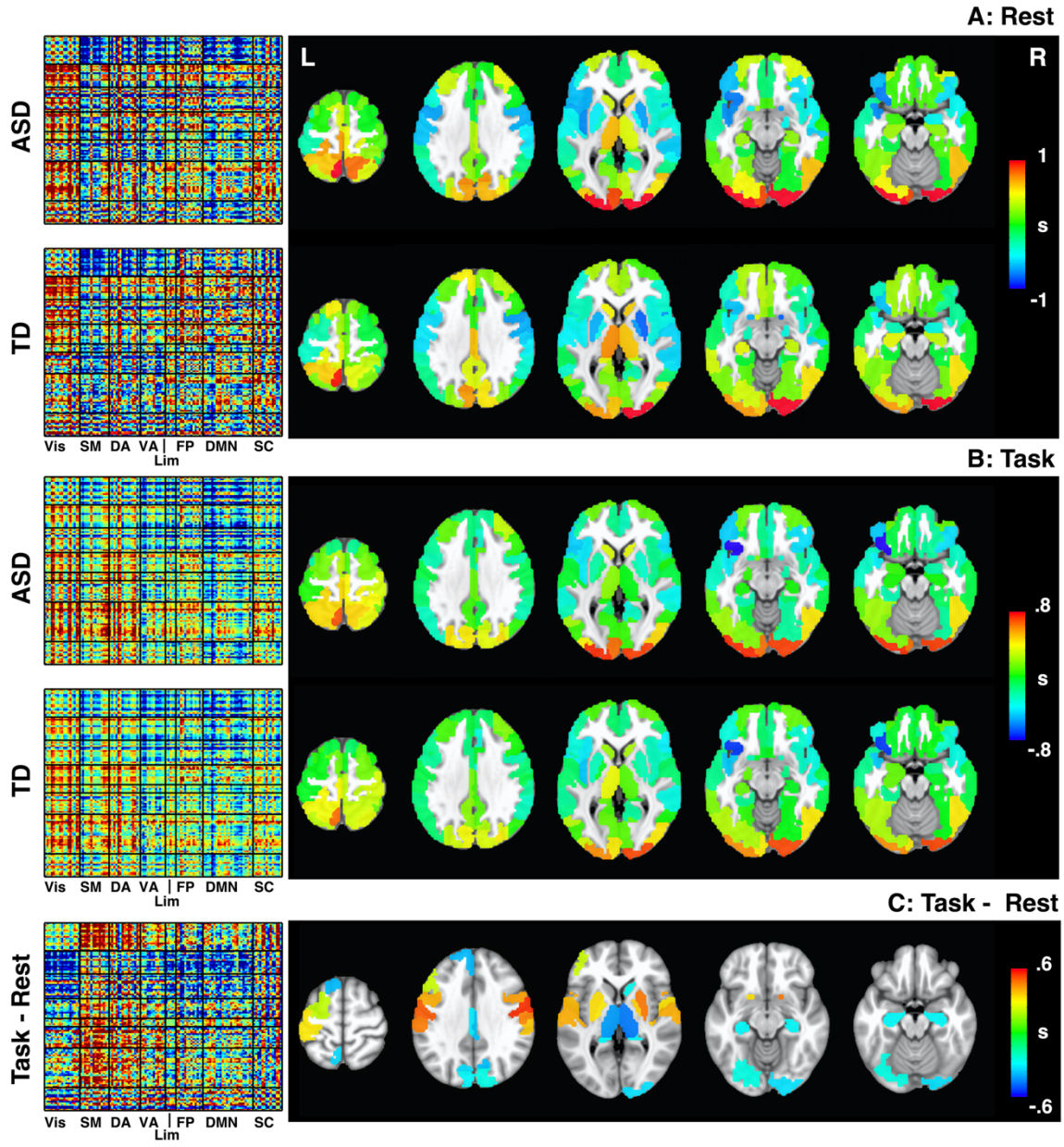

Figure 2.1 Pairwise Lag Matrices and Latency Projections
Pairwise lag matrices (left) and mean latency projections (right) are shown by group for the resting state (A) and task (B) conditions; colors represent lag in seconds. Differences between task and resting conditions for all participants combined are also presented (C). Only regions showing a significant main effect of condition on latency are shown on the right (FDR-corrected $p < .05$); colors represent mean difference in seconds. Pairwise lag matrices are organized by functional network (Vis = Visual; SM = somatomotor; DA = dorsal attention; VA = ventral attention; Lim = limbic; FP = frontoparietal; DMN = default mode; SC = subcortical). Each region's relationship to other regions is interpreted vertically, with 'earlier' networks appearing as blue columns and 'later' networks appearing as red columns.

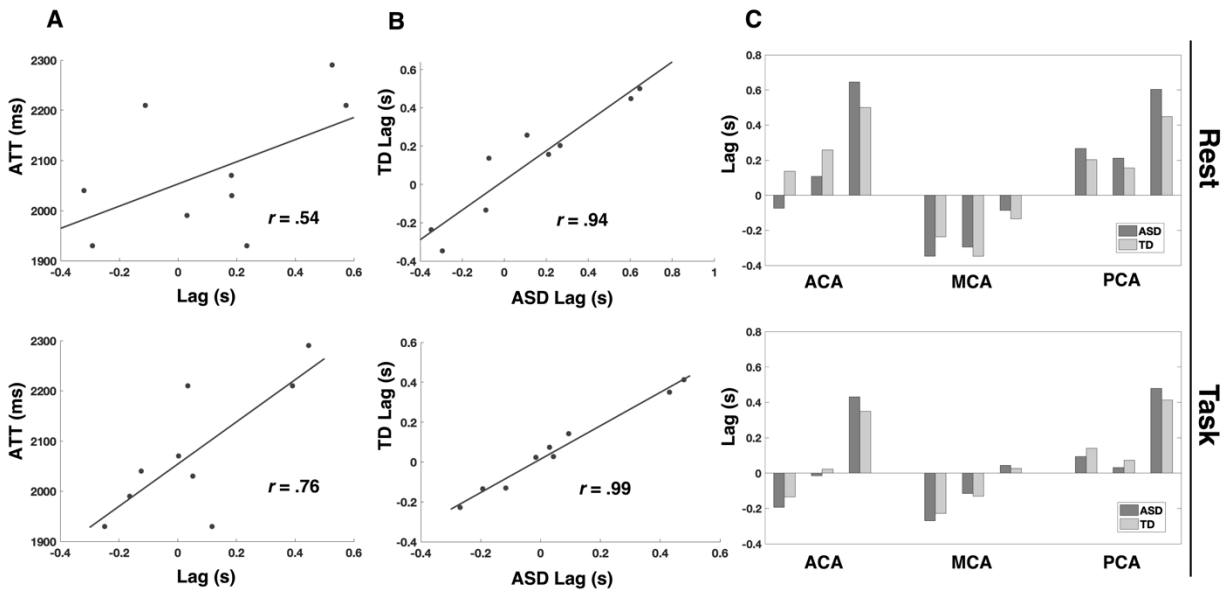

Figure 2.2 Associations Between Lag and Arterial Supply
A) Group-averaged correlations between mean latency and median arterial transit time (ATT; from Mutsaerts et al., 2015) for each of nine arterial flow territories are shown for the resting (top) and task (bottom) conditions. B) Correlations between ASD group and TD group mean latency for each arterial territory are shown for each condition. C) Mean latencies for the proximal, middle, and distal branches of the anterior cerebral artery (ACA), middle cerebral artery (MCA), and posterior cerebral artery (PCA) are shown for each group.

References

Allen, E. A., Damaraju, E., Eichele, T., et al. (2017). EEG Signatures of Dynamic Functional Network Connectivity States. *Brain Topogr*. doi:10.1007/s10548-017-0546-2

Allen, E. A., Damaraju, E., Plis, S. M., et al. (2014). Tracking whole-brain connectivity dynamics in the resting state. *Cereb Cortex, 24*(3), 663-676. doi:10.1093/cercor/bhs352

American Psychiatric Association. (2013). *Diagnostic and statistical manual of mental disorders : DSM-5* (Fifth edition. ed., pp. 947).

Aso, T., Jiang, G., Urayama, S. I., et al. (2017). A Resilient, Non-neuronal Source of the Spatiotemporal Lag Structure Detected by BOLD Signal-Based Blood Flow Tracking. *Front Neurosci, 11*, 256. doi:10.3389/fnins.2017.00256

Avants, B. B., Duda, J. T., Kilroy, E., et al. (2015). The pediatric template of brain perfusion. *Scientific Data, 2*(1), 150003. doi:10.1038/sdata.2015.3

Benjamini, Y., & Hochberg, Y. (1995). Controlling the False Discovery Rate - a Practical and Powerful Approach to Multiple Testing. *Journal of the Royal Statistical Society Series B-Statistical Methodology, 57*(1), 289-300. doi:DOI 10.1111/j.2517-6161.1995.tb02031.x

Biswal, B., Yetkin, F. Z., Haughton, V. M., et al. (1995). Functional connectivity in the motor cortex of resting human brain using echo-planar MRI. *Magn Reson Med, 34*(4), 537-541.

Bohland, J. W., Bokil, H., Allen, C. B., et al. (2009). The brain atlas concordance problem: quantitative comparison of anatomical parcellations. *PLoS One, 4*(9), e7200. doi:10.1371/journal.pone.0007200

Bridwell, D. A., Wu, L., Eichele, T., et al. (2013). The spatiospectral characterization of brain networks: fusing concurrent EEG spectra and fMRI maps. *Neuroimage, 69*, 101-111. doi:10.1016/j.neuroimage.2012.12.024

Brysbaert, M., & New, B. (2009). Moving beyond Kucera and Francis: a critical evaluation of current word frequency norms and the introduction of a new and improved word frequency measure for American English. *Behav Res Methods, 41*(4), 977-990. doi:10.3758/BRM.41.4.977

Calhoun, V. D., Miller, R., Pearlson, G., et al. (2014). The chronnectome: time-varying connectivity networks as the next frontier in fMRI data discovery. *Neuron, 84*(2), 262-274. doi:10.1016/j.neuron.2014.10.015

Caplette, L. (2020). Simple RM/Mixed ANOVA for any design: MATLAB Central File Exchange. Retrieved from https://www.mathworks.com/matlabcentral/fileexchange/64980-simple-rm-mixed-anova-for-any-design

Chen, C., Witte, M., Heemsbergen, W., et al. (2013). Multiple comparisons permutation test for image based data mining in radiotherapy. *Radiat Oncol, 8*, 293. doi:10.1186/1748-717X-8-293

Chen, J. E., Lewis, L. D., Chang, C., et al. (2020). Resting-state "physiological networks". *Neuroimage, 213*, 116707. doi:10.1016/j.neuroimage.2020.116707

Cole, M. W., Ito, T., Schultz, D., et al. (2019). Task activations produce spurious but systematic inflation of task functional connectivity estimates. *Neuroimage, 189*, 1-18. doi:10.1016/j.neuroimage.2018.12.054

Damasio, H. (1983). A computed tomographic guide to the identification of cerebral vascular territories. *Arch Neurol, 40*(3), 138-142. doi:10.1001/archneur.1983.04050030032005

Di Martino, A., O'Connor, D., Chen, B., et al. (2017). Enhancing studies of the connectome in autism using the autism brain imaging data exchange II. *Sci Data, 4*, 170010. doi:10.1038/sdata.2017.10

Di Martino, A., Yan, C. G., Li, Q., et al. (2014). The autism brain imaging data exchange: towards a large-scale evaluation of the intrinsic brain architecture in autism. *Mol Psychiatry, 19*(6), 659-667. doi:10.1038/mp.2013.78

Dosenbach, N. U., Fair, D. A., Miezin, F. M., et al. (2007). Distinct brain networks for adaptive and stable task control in humans. *Proc Natl Acad Sci U S A, 104*(26), 11073-11078. doi:10.1073/pnas.0704320104

Duncan, J. (2010). The multiple-demand (MD) system of the primate brain: mental programs for intelligent behaviour. *Trends Cogn Sci, 14*(4), 172-179. doi:10.1016/j.tics.2010.01.004

Feige, B., Spiegelhalder, K., Kiemen, A., et al. (2017). Distinctive time-lagged resting-state networks revealed by simultaneous EEG-fMRI. *Neuroimage, 145*(Pt A), 1-10. doi:10.1016/j.neuroimage.2016.09.027

Fox, M. D., & Raichle, M. E. (2007). Spontaneous fluctuations in brain activity observed with functional magnetic resonance imaging. *Nat Rev Neurosci, 8*(9), 700-711. doi:10.1038/nrn2201

George, M. S., Costa, D. C., Kouris, K., et al. (1992). Cerebral blood flow abnormalities in adults with infantile autism. *J Nerv Ment Dis, 180*(7), 413-417. doi:10.1097/00005053-199207000-00002

Geschwind, D. H., & State, M. W. (2015). Gene hunting in autism spectrum disorder: on the path to precision medicine. *Lancet Neurol, 14*(11), 1109-1120. doi:10.1016/S1474-4422(15)00044-7

Hahamy, A., Behrmann, M., & Malach, R. (2015). The idiosyncratic brain: distortion of spontaneous connectivity patterns in autism spectrum disorder. *Nat Neurosci, 18*(2), 302-309. doi:10.1038/nn.3919

He, B. J., Snyder, A. Z., Zempel, J. M., et al. (2008). Electrophysiological correlates of the brain's intrinsic large-scale functional architecture. *Proc Natl Acad Sci U S A, 105*(41), 16039-16044. doi:10.1073/pnas.0807010105

Henry, T. R., Dichter, G. S., & Gates, K. (2018). Age and Gender Effects on Intrinsic Connectivity in Autism Using Functional Integration and Segregation. *Biol Psychiatry Cogn Neurosci Neuroimaging, 3*(5), 414-422. doi:10.1016/j.bpsc.2017.10.006

Hillman, E. M. (2014). Coupling mechanism and significance of the BOLD signal: a status report. *Annu Rev Neurosci, 37*, 161-181. doi:10.1146/annurev-neuro-071013-014111

Hossain, M. M., Khan, N., Sultana, A., et al. (2020). Prevalence of comorbid psychiatric disorders among people with autism spectrum disorder: An umbrella review of systematic reviews and meta-analyses. *Psychiatry Res, 287*, 112922. doi:10.1016/j.psychres.2020.112922

Hull, J. V., Jacokes, Z. J., Torgerson, C. M., et al. (2016). Resting-State Functional Connectivity in Autism Spectrum Disorders: A Review. *Front Psychiatry, 7*, 205. doi:10.3389/fpsyt.2016.00205

Jann, K., Hernandez, L. M., Beck-Pancer, D., et al. (2015). Altered resting perfusion and functional connectivity of default mode network in youth with autism spectrum disorder. *Brain and Behavior, 5*(9), e00358. doi:10.1002/brb3.358

Jobski, K., Hofer, J., Hoffmann, F., et al. (2017). Use of psychotropic drugs in patients with autism spectrum disorders: a systematic review. *Acta Psychiatr Scand, 135*(1), 8-28. doi:10.1111/acps.12644

King, J. B., Prigge, M. B. D., King, C. K., et al. (2018). Evaluation of Differences in Temporal Synchrony Between Brain Regions in Individuals With Autism and Typical Development. *JAMA Netw Open, 1*(7), e184777. doi:10.1001/jamanetworkopen.2018.4777

Klapwijk, E. T., Goddings, A.-L., Burnett Heyes, S., et al. (2013). Increased functional connectivity with puberty in the mentalising network involved in social emotion processing. *Hormones and behavior, 64*(2), 314-322. doi:10.1016/j.yhbeh.2013.03.012

Kopal, J., Pidnebesna, A., Tomeček, D., et al. (2020). Typicality of Functional Connectivity robustly captures motion artifacts in rs-fMRI across datasets, atlases and preprocessing pipelines. *bioRxiv*, 2020.2003.2006.980193. doi:10.1101/2020.03.06.980193

Kundu, P., Brenowitz, N. D., Voon, V., et al. (2013). Integrated strategy for improving functional connectivity mapping using multiecho fMRI. *Proc Natl Acad Sci U S A, 110*(40), 16187-16192. doi:10.1073/pnas.1301725110

Kundu, P., Inati, S. J., Evans, J. W., et al. (2012). Differentiating BOLD and non-BOLD signals in fMRI time series using multi-echo EPI. *Neuroimage, 60*(3), 1759-1770. doi:10.1016/j.neuroimage.2011.12.028

Kuperman, V., Stadthagen-Gonzalez, H., & Brysbaert, M. (2012). Age-of-acquisition ratings for 30,000 English words. *Behav Res Methods, 44*(4), 978-990. doi:10.3758/s13428-012-0210-4

Laumann, T. O., Snyder, A. Z., Mitra, A., et al. (2016). On the Stability of BOLD fMRI Correlations. *Cereb Cortex*. doi:10.1093/cercor/bhw265

Linke, A. C., Olson, L., Gao, Y., et al. (2017). Psychotropic medication use in autism spectrum disorders may affect functional brain connectivity. *Biol Psychiatry Cogn Neurosci Neuroimaging, 2*(6), 518-527. doi:10.1016/j.bpsc.2017.06.008

Lombardo, M. V., Lai, M. C., & Baron-Cohen, S. (2019). Big data approaches to decomposing heterogeneity across the autism spectrum. *Mol Psychiatry, 24*(10), 1435-1450. doi:10.1038/s41380-018-0321-0

Maenner, M. J., Shaw, K. A., Baio, J., et al. (2020). Prevalence of Autism Spectrum Disorder Among Children Aged 8 Years - Autism and Developmental Disabilities Monitoring Network, 11 Sites, United States, 2016. *MMWR Surveill Summ, 69*(4), 1-12. doi:10.15585/mmwr.ss6904a1

Mash, L. E., Reiter, M. A., Linke, A. C., et al. (2018). Multimodal approaches to functional connectivity in autism spectrum disorders: An integrative perspective. *Dev Neurobiol, 78*(5), 456-473. doi:10.1002/dneu.22570

Mikita, N., Simonoff, E., Pine, D. S., et al. (2016). Disentangling the autism-anxiety overlap: fMRI of reward processing in a community-based longitudinal study. *Transl Psychiatry, 6*(6), e845. doi:10.1038/tp.2016.107

Mitra, A., Kraft, A., Wright, P., et al. (2018). Spontaneous Infra-slow Brain Activity Has Unique Spatiotemporal Dynamics and Laminar Structure. *Neuron, 98*(2), 297-305 e296. doi:10.1016/j.neuron.2018.03.015

Mitra, A., Snyder, A. Z., Constantino, J. N., et al. (2017). The Lag Structure of Intrinsic Activity is Focally Altered in High Functioning Adults with Autism. *Cereb Cortex, 27*(2), 1083-1093. doi:10.1093/cercor/bhv294

Mitra, A., Snyder, A. Z., Hacker, C. D., et al. (2014). Lag structure in resting-state fMRI. *J Neurophysiol, 111*(11), 2374-2391. doi:10.1152/jn.00804.2013

Müller, R. A., Shih, P., Keehn, B., et al. (2011). Underconnected, but how? A survey of functional connectivity MRI studies in autism spectrum disorders. *Cereb Cortex, 21*(10), 2233-2243. doi:10.1093/cercor/bhq296

Musso, F., Brinkmeyer, J., Mobascher, A., et al. (2010). Spontaneous brain activity and EEG microstates. A novel EEG/fMRI analysis approach to explore resting-state networks. *Neuroimage, 52*(4), 1149-1161. doi:10.1016/j.neuroimage.2010.01.093

Mutsaerts, H. J., van Dalen, J. W., Heijtel, D. F., et al. (2015). Cerebral Perfusion Measurements in Elderly with Hypertension Using Arterial Spin Labeling. *PLoS One, 10*(8), e0133717. doi:10.1371/journal.pone.0133717

Nair, A., Keown, C. L., Datko, M., et al. (2014). Impact of methodological variables on functional connectivity findings in autism spectrum disorders. *Hum Brain Mapp, 35*(8), 4035-4048. doi:10.1002/hbm.22456

Nair, S., Jao Keehn, R. J., Berkebile, M. M., et al. (2017). Local resting state functional connectivity in autism: site and cohort variability and the effect of eye status. *Brain Imaging Behav*. doi:10.1007/s11682-017-9678-y

Nalci, A., Rao, B. D., & Liu, T. T. (2019). Nuisance effects and the limitations of nuisance regression in dynamic functional connectivity fMRI. *Neuroimage, 184*, 1005-1031. doi:10.1016/j.neuroimage.2018.09.024

Nomi, J. S., Farrant, K., Damaraju, E., et al. (2016). Dynamic functional network connectivity reveals unique and overlapping profiles of insula subdivisions. *Hum Brain Mapp, 37*(5), 1770-1787. doi:10.1002/hbm.23135

Nomi, J. S., & Uddin, L. Q. (2015). Developmental changes in large-scale network connectivity in autism. *Neuroimage Clin, 7*, 732-741. doi:10.1016/j.nicl.2015.02.024

Nunes, A. S., Peatfield, N., Vakorin, V., et al. (2019). Idiosyncratic organization of cortical networks in autism spectrum disorder. *Neuroimage, 190*, 182-190. doi:10.1016/j.neuroimage.2018.01.022

Olafsson, V., Kundu, P., Wong, E. C., et al. (2015). Enhanced identification of BOLD-like components with multi-echo simultaneous multi-slice (MESMS) fMRI and multi-echo ICA. *Neuroimage, 112*, 43-51. doi:10.1016/j.neuroimage.2015.02.052

Olsson, M. B., Westerlund, J., Lundstrom, S., et al. (2015). "Recovery" from the diagnosis of autism - and then? *Neuropsychiatr Dis Treat, 11*, 999-1005. doi:10.2147/NDT.S78707

Pan, W. J., Thompson, G. J., Magnuson, M. E., et al. (2013). Infraslow LFP correlates to resting-state fMRI BOLD signals. *Neuroimage, 74*, 288-297. doi:10.1016/j.neuroimage.2013.02.035

Raatikainen, V., Korhonen, V., Borchardt, V., et al. (2020). Dynamic lag analysis reveals atypical brain information flow in autism spectrum disorder. *Autism Res, 13*(2), 244-258. doi:10.1002/aur.2218

Rane, P., Cochran, D., Hodge, S. M., et al. (2015). Connectivity in Autism: A Review of MRI Connectivity Studies. *Harv Rev Psychiatry, 23*(4), 223-244. doi:10.1097/HRP.0000000000000072

Raut, R. V., Mitra, A., Marek, S., et al. (2019). Organization of Propagated Intrinsic Brain Activity in Individual Humans. *Cerebral Cortex*. doi:10.1093/cercor/bhz198

Raut, R. V., Mitra, A., Snyder, A. Z., et al. (2019). On time delay estimation and sampling error in resting-state fMRI. *Neuroimage, 194*, 211-227. doi:10.1016/j.neuroimage.2019.03.020

Schaefer, A., Kong, R., Gordon, E. M., et al. (2018). Local-Global Parcellation of the Human Cerebral Cortex from Intrinsic Functional Connectivity MRI. *Cereb Cortex, 28*(9), 3095-3114. doi:10.1093/cercor/bhx179

Smith, S. M., Jenkinson, M., Woolrich, M. W., et al. (2004). Advances in functional and structural MR image analysis and implementation as FSL. *Neuroimage, 23 Suppl 1*, S208-219. doi:10.1016/j.neuroimage.2004.07.051

Smith, S. M., Miller, K. L., Salimi-Khorshidi, G., et al. (2011). Network modelling methods for FMRI. *Neuroimage, 54*(2), 875-891. doi:10.1016/j.neuroimage.2010.08.063

Solé-Padullés, C., Castro-Fornieles, J., de la Serna, E., et al. (2016). Intrinsic connectivity networks from childhood to late adolescence: Effects of age and sex. *Developmental Cognitive Neuroscience, 17*, 35-44. doi:10.1016/j.dcn.2015.11.004

Starkstein, S. E., Vazquez, S., Vrancic, D., et al. (2000). SPECT findings in mentally retarded autistic individuals. *J Neuropsychiatry Clin Neurosci, 12*(3), 370-375. doi:10.1176/jnp.12.3.370

Tatu, L., Moulin, T., Bogousslavsky, J., et al. (1998). Arterial territories of the human brain: cerebral hemispheres. *Neurology, 50*(6), 1699-1708. doi:10.1212/wnl.50.6.1699

Teeuw, J., Brouwer, R. M., Guimarães, J. P. O. F. T., et al. (2019). Genetic and environmental influences on functional connectivity within and between canonical cortical resting-state networks throughout adolescent development in boys and girls. *Neuroimage, 202*, 116073. doi:10.1016/j.neuroimage.2019.116073

Tong, Y., Yao, J. F., Chen, J. J., et al. (2019). The resting-state fMRI arterial signal predicts differential blood transit time through the brain. *J Cereb Blood Flow Metab, 39*(6), 1148-1160. doi:10.1177/0271678X17753329

Uddin, L. Q., Supekar, K., & Menon, V. (2013). Reconceptualizing functional brain connectivity in autism from a developmental perspective. *Front Hum Neurosci, 7*, 458. doi:10.3389/fnhum.2013.00458

van Heuven, W. J., Mandera, P., Keuleers, E., et al. (2014). SUBTLEX-UK: a new and improved word frequency database for British English. *Q J Exp Psychol (Hove), 67*(6), 1176-1190. doi:10.1080/17470218.2013.850521

Yan, W., Rangaprakash, D., & Deshpande, G. (2018). Aberrant hemodynamic responses in autism: Implications for resting state fMRI functional connectivity studies. *Neuroimage Clin, 19*, 320-330. doi:10.1016/j.nicl.2018.04.013

Yeo, B. T., Krienen, F. M., Sepulcre, J., et al. (2011). The organization of the human cerebral cortex estimated by intrinsic functional connectivity. *J Neurophysiol, 106*(3), 1125-1165. doi:10.1152/jn.00338.2011

Yerys, B. E., Herrington, J. D., Bartley, G. K., et al. (2018). Arterial spin labeling provides a reliable neurobiological marker of autism spectrum disorder. *J Neurodev Disord, 10*(1), 32. doi:10.1186/s11689-018-9250-0

Yuan, H., Zotev, V., Phillips, R., et al. (2012). Spatiotemporal dynamics of the brain at rest--exploring EEG microstates as electrophysiological signatures of BOLD resting state networks. *Neuroimage, 60*(4), 2062-2072. doi:10.1016/j.neuroimage.2012.02.031

Chapter 4:

Study 3

The content within this section, titled "Chapter 4: Study 3," reflects material from a paper that has been published in the journal *Brain Connectivity.* The full citation is as follows:

Mash, L. E., Keehn, B., Linke, A. C., Liu, T. T., Helm, J. L., Haist, F., Townsend, J., & Müller, R.-A. (2020). Atypical relationships between spontaneous EEG and fMRI activity in autism. *Brain Connectivity*, *10,* 18-28. https://doi.org/10.1089/brain.2019.0693

Abstract

Autism spectrum disorders (ASDs) have been linked to atypical communication among distributed brain networks. However, despite decades of research, the exact nature of these differences between typically developing (TD) individuals and those with ASDs remains unclear. ASDs have been widely studied using resting state neuroimaging methods, including both functional MRI (fMRI) and electroencephalography (EEG). However, little is known about how fMRI and EEG measures of spontaneous brain activity are related in ASDs. In the current study, two cohorts of children and adolescents underwent resting-state EEG (n = 38 per group) or fMRI (n = 66 ASD, 57 TD), with a subset of individuals in both the EEG and fMRI cohorts (n = 17 per group). In the EEG cohort, parieto-occipital EEG alpha power was found to be reduced in ASDs. In the fMRI cohort, blood oxygen level-dependent (BOLD) power was regionally increased in right temporal regions and there was widespread overconnectivity between thalamus and cortical regions in the ASD group relative to the TD group. Finally, multimodal analyses indicated that while TD children showed consistently positive relationships between EEG alpha power and regional BOLD power, these associations were weak or negative in ASDs. These findings suggest atypical links between alpha rhythms and regional BOLD activity in ASDs, possibly implicating neural substrates and processes that coordinate thalamocortical regulation of the alpha rhythm.

Keywords: Autism, Functional MRI, EEG, Alpha, Resting State

Introduction

Autism spectrum disorders (ASDs) are neurodevelopmental disorders defined behaviorally by social communication deficits and the presence of restricted/repetitive patterns of behavior or interest (American Psychiatric Association 2013). It is currently estimated that one in 59 eight-year-olds in the United States are on the autism spectrum (Baio et al. 2018). However, the neurobiological basis of these disorders remains poorly understood. Research clarifying the nature of brain differences in ASDs may improve treatment and diagnostic strategies and is therefore a high priority.

Over the past several decades, interest in brain functioning in ASDs has grown rapidly. Studies using functional MRI (fMRI) and electroencephalography (EEG) to examine neural activity in vivo comprise the majority of this literature. While fMRI research broadly supports atypical coordination (i.e., functional connectivity; FC) across distributed brain networks in ASDs, there have been mixed and sometimes conflicting reports of underconnectivity and overconnectivity involving numerous regions and functional networks (Di Martino et al. 2014, Hull et al. 2016). However, findings of atypical thalamocortical circuitry have been relatively consistent, with multiple studies reporting overconnectivity between thalamus and sensorimotor cortical regions (Cerliani et al. 2015, Nair et al. 2015, Woodward et al. 2017). These findings are further supported by evidence of structural thalamic differences in ASDs (Schuetze et al. 2016). Much like the fMRI literature, EEG studies have produced mixed results with respect to both power and coherence across a range of frequencies (Wang et al. 2013, O'Reilly et al. 2017). Despite these inconsistencies, one of the best replicated findings in ASDs is decreased power in the alpha frequency band (i.e., 8-12 Hz) at rest (Dawson et al. 1995, Chan et al. 2007, Murias et al. 2007, Sheikhani et al. 2012, Tierney et al. 2012, Keehn et al. 2017).

To date, there has been little progress relating findings across modalities in ASDs (Mash et al. 2018), and it is currently unknown how reports of reduced EEG alpha power and atypical thalamocortical activity may be associated. While EEG directly measures postsynaptic potentials (Niedermeyer et al. 2011, Heller & Volegov 2014), fMRI detects the blood oxygen level-dependent (BOLD) signal, an indirect measure of neural activity influenced by vascular and metabolic factors (Hillman 2014). Therefore, measures of magnitude (i.e., power) and synchronicity (i.e., FC) derived from different modalities may reflect neuronal communication in fundamentally different ways. Studies combining both modalities in the same individuals allow for joint analysis and direct comparison of EEG and fMRI results.

In typically developing (TD) adults, a large body of simultaneous EEG-fMRI work has consistently demonstrated that spontaneous EEG alpha power is positively associated with thalamic BOLD activity (Goldman et al. 2002, de Munck et al. 2007, Bridwell et al. 2013) and negatively related to cortical BOLD activity (Goldman et al. 2002, Laufs et al. 2003, Olbrich et al. 2009, Bridwell et al. 2013). The relationship between EEG alpha power and BOLD FC is less well established; however, there is some evidence that increased EEG alpha power is associated with reduced anticorrelation (i.e., less negative correlations) between thalamic and cortical regions (Scheeringa et al. 2012, Allen et al. 2018). Multimodal imaging research in ASDs remains very limited. To our knowledge, only two small EEG-fMRI studies in ASDs have been published, both of which explored neural processing during auditory and language processing tasks using concurrent EEG-fMRI (Jochaut et al. 2015, Hames et al. 2016). While these efforts provide first glimpses of potential links between electrophysiological and hemodynamic measures during task performance in ASDs, they cannot speak to unimodal resting state findings involving EEG alpha power and thalamocortical networks.

To our knowledge, there are currently no published resting state EEG-fMRI studies of ASDs. However, established relationships between thalamocortical networks and EEG alpha power in typical development described above provide a compelling direction for future ASD research combining EEG and fMRI. Although there are advantages to simultaneous data acquisition, this procedure is often lengthy and uncomfortable. This is especially problematic for children with developmental disorders. Separately acquired EEG-fMRI data cannot speak to concurrent fluctuations in regional BOLD activity/coordination and EEG alpha power within individuals. However, these data may still provide important insight into multimodal relationships between individuals.

In order to investigate links between separately acquired EEG and fMRI, suitable summary measures for EEG alpha power, BOLD activity, and BOLD FC must be selected. EEG alpha power can be averaged over an acquisition period to yield a specific value for each participant. Calculating a single representative BOLD value over an entire scan period for an individual, on the other hand, is challenging as BOLD units are arbitrary and only relative BOLD activity changes can be interpreted meaningfully. Therefore, spontaneous BOLD activity (i.e., power) is best summarized by the amplitude of low frequency fluctuations (ALFF; Zang et al. 2007), a measure that captures power in BOLD frequencies typically around .01-.1 Hz. ALFF is often reported together with fractional ALFF (fALFF), i.e., the ratio between low frequency power and total power of all frequencies (Zou et al. 2008); ALFF tends to have better test-retest reliability, whereas fALFF is considered more robust to non-neuronal artefact (Zuo et al. 2010). However, ALFF/fALFF has only played a minimal role in the ASD neuroimaging literature to date. A few relevant studies have reported varying findings, from broadly increased ALFF (Supekar et al. 2013) to regionally increased fALFF in right frontal and temporal regions (Di

Martino et al. 2014) and decreased fALFF in occipital regions (Di Martino et al. 2014, Itahashi et al. 2015)

The primary aims of this study were to 1) clarify previous unimodal EEG and fMRI findings in ASDs described above, and 2) to establish inter-individual relationships between EEG alpha power and thalamic activity, cortical activity, and thalamocortical FC in a sample of adolescents with and without ASDs.

Methods

Participants

Resting-state EEG was collected from 76 individuals (38 ASD, 38 TD) ages 7-18 years. Groups did not significantly differ with respect to age, handedness, sex, nonverbal IQ, or EEG length after preprocessing (Table 1a). None of the TD participants were taking psychotropic medications or had any documented history of psychiatric or developmental disorders. In the ASD group, medication status was documented for 23 of 38 individuals. Of these, six reported taking psychotropic medications.

Functional MRI data were separately acquired from 123 individuals (66 ASD, 57 TD) ages 6-18 years. ASD and TD groups did not significantly differ with respect to age, handedness, sex, nonverbal IQ, RMSD, a measure of in-scanner head motion (Table 1b). As in the EEG sample, none of the TD participants were taking psychotropic medications or had any documented history of psychiatric or developmental disorders. In the ASD group, 23 individuals reported taking psychotropic medications, 37 were unmedicated, and medication status was undocumented for six individuals.

A subset of participants underwent fMRI and EEG acquisition within three months of one another (22 ASD, 25 TD, ages 12-17 years; Table 1c). Four individuals with ASDs and six

typically developing individuals were excluded from multimodal analyses due to excessive fMRI artefact. One individual with ASD was excluded due to an incidental finding on MRI. Two additional typically developing individuals were excluded from the multimodal sample to improve matching and to maintain equal sample sizes. The final EEG-fMRI sample consisted of 17 individuals per group with high-quality data in both modalities. Of these participants, six ASD participants were prescribed medications and the remaining 11 were unmedicated. All available medication and comorbidity data are summarized in Table S1.

Across all samples, ASD diagnoses were confirmed based on the Autism Diagnostic Interview–Revised (ADI-R, Lord, Rutter, & Le Couteur, 1994), the Autism Diagnostic Observation Schedule- Generic (ADOS-G; Lord et al. 2000) or Autism Diagnostic Observation Schedule, Second Edition (ADOS-2; Gotham et al. 2007), and expert clinical judgment according to DSM-5 criteria. The Wechsler Abbreviated Scales of Intelligence (WASI, Wechsler, 1999) or Wechsler Abbreviated Scales of Intelligence, Second Edition (WASI-II, Wechsler, 2011) was administered to all participants. Informed assent and consent were obtained from all participants and caregivers in accordance with the University of California, San Diego and San Diego State University Institutional Review Boards.

Electroencephalography (EEG)

Acquisition

Continuous EEG was recorded using a Biosemi ActiveTwo system with 68 Ag/AgCl active electrodes. Sixty-four electrodes were mounted in an elastic cap according to locations in the modified International 10–20 system. Remaining electrodes were placed below the right eye, on the outer canthus of the left eye (to monitor blinks and saccades), and over the left and right mastoids (reference). EEG data were recorded at a sampling rate of 256 Hz and direct current (DC)

offsets were kept below 25 mV at all channels. Participants completed six minutes of eyes-open EEG, during which a black central fixation crosshair was presented on a grey background. Participants were instructed to relax, remain as still as possible, and look at the crosshair.

Data Processing

Data were processed in EEGLAB (Delorme and Makeig 2004) high-pass filtered at 1 Hz, and re-referenced to the grand average. Independent component analysis (ICA) was applied using the Fieldtrip toolbox (Oostenveld et al. 2011). Each participant's component activations were first visually inspected for motor artifact, and noisy segments were manually rejected. Component activations and their scalp maps were then examined to identify ocular artifacts, and artifact-contaminated components were removed (Jung et al. 2000, Jung et al. 2000). Finally, noisy channels were excluded and replaced as missing values. After preprocessing, all participants had at least two minutes of remaining data for subsequent analyses (Table 1a, Table 1c). For each channel, a fast Fourier transform (EEGLab's spectopo) was applied to continuous (unepoched) data to determine the magnitude of power at frequencies ranging from .25 to 128 Hz, at .25 Hz increments. The spectral power values were converted from decibels to microvolts squared (μV^2).

Alpha Power Analysis

Alpha power, expressed as microvolts squared (μV^2) was extracted from and averaged across parieto-occipital (Oz, POz, O1, O2, PO3, PO4) electrodes. There is strong evidence that peak alpha frequency varies substantially between individuals (Haegens et al. 2014), shifts throughout childhood and adolescence (Cragg et al. 2011, Miskovic et al. 2015), and may differ between ASDs and typical development (Edgar et al. 2015, Dickinson et al. 2018). Therefore, it has been recommended that alpha frequency windows be individually defined for each participant (Klimesch 1999). For this study, the alpha peak was defined as the local maximum of the average

parieto-occipital power spectrum between 7-13 Hz. Because the alpha rhythm is most prominent in posterior regions (Britton et al. 2016), only parieto-occipital electrodes were used to optimize signal-to-noise ratio and improve peak estimates. Parieto-occipital alpha power (referred to henceforth as "alpha power") was then extracted from the 4-Hz window surrounding this midpoint (e.g., an alpha window of 7-11 Hz for a participant with an alpha peak at 9 Hz). For participants with no clear alpha peak (n =7, all ASD), a standard window of 8-12 Hz was applied. Individual alpha peaks ranged from 7.5 Hz to 12.5 Hz and did not differ significantly between groups (ASD mean (sd) = 9.76 (.87) Hz, TD mean (sd) = 9.80 (.73) Hz, p = .82).

Absolute and relative parieto-occipital alpha power were compared between groups using two-sample t-tests with degrees of freedom adjusted for unequal variances (using Satterthwaite's approximation). These group analyses were repeated on an unmedicated subsample of ASD participants and a matched TD group. To ensure that our findings were not primarily due to differences in individual alpha windows, a standard alpha window of 8-12 Hz was compared to our method described above for calculating alpha windows. Absolute parieto-occipital alpha power calculated using a standard alpha window was highly correlated with the individualized window method (r = .99, p < .00001; Figure S1).

Functional MRI (fMRI)

Acquisition

Imaging data were acquired on a GE 3T MR750 scanner with an 8-channel head coil at the Center for Functional MRI (University of California, San Diego). High-resolution structural images were acquired with a standard FSPGR T1-weighted sequence (TR: 8.108ms, TE: 3.172 ms, flip angle: 8°; FOV 256 mm; 1mm^3 resolution; 172 slices). Functional T2*-weighted images were acquired using a single-shot gradient-recalled, echo-planar imaging pulse sequence (TR:

2000ms; TE: 30 ms; flip angle: 90°; 3.4mm isotropic resolution; FOV: 220mm; matrix: 64 x 64; 42 axial slices). One 6 minute 10 second resting-state scan was obtained consisting of 185 whole-brain volumes. The first five volumes were discarded to account for T1-equilibration effects. Subjects were instructed to fixate on a cross projected onto the middle of a screen, viewed through a mirror in the bore, and to "Let your mind wander, relax, but please stay as still as you can. Do not fall asleep." Compliance with instructions to remain still and awake was monitored via video recording.

Data Processing

Functional images were processed using Analysis of Functional NeuroImages software (AFNI v17.2.07; Cox, 1996) FMRIB Software Library (FSL; v5.0; Smith et al., 2004), and Freesurfer (Dale et al. 1999, Fischl et al. 1999, Fischl 2012). Images were slice-time corrected and each functional volume was registered to the middle time point of the scan to adjust for motion via rigid-body realignment as implemented in AFNI. Field map correction was applied to minimize distortions due to magnetic field inhomogeneity. The functional images were registered to the anatomical scan via FSL's FLIRT (Jenkinson & Smith, 2001). Anatomical and functional images were resampled to 3mm isotropic voxels and standardized to the atlas space of the Montreal Neurological Institute (MNI) template using FSL's nonlinear registration tool (FNIRT). AFNI's 3dBlurToFWHM was used to smooth functional images to a Gaussian full width at half-maximum (FWHM) of 6 mm. Functional MRI time series were highpass filtered at .008 Hz using a second-order Butterworth filter, which was also applied to the 10 nuisance regressors (see further down in this section).

Given the known impact of motion on BOLD correlations (Power et al., 2014), additional measures were taken to correct for motion. The mean signal from ventricles and white matter

masks (obtained from Freesurfer segmentation of T1-weighted structural image and eroded by 1 voxel) as well as six motion parameters (obtained from rigid-body realignment) and their first temporal derivatives were regressed from the signal. Residuals from nuisance regression were used for all subsequent functional connectivity analyses. Root mean squared displacement (RMSD), an estimate of head motion across all time points, was calculated for each participant. Framewise displacement (FD) was calculated as a volume-by-volume measure of motion. Time points with > 0.5 mm FD as well the two subsequent time points were censored. Time series fragments with < 10 consecutive time points remaining after censoring were also excluded. Minimal censoring was performed (ASD mean = 2.8% censored, TD mean = 2.2% censored), and groups did not differ with respect to the number of remaining timepoints (Table 1b). All structural and functional data were visually inspected at every preprocessing stage by at least two blinded reviewers to ensure acceptable data quality.

For ALFF and fractional ALFF (fALFF) analyses, data were processed as above with the exception of highpass filtering and censoring, in order to preserve the full timeseries and range of frequencies. In FC analyses, minimal censoring was necessary in both groups (averages of 2.8% for ASD and 2.2% for TD). Therefore, including these few outlier timepoints for ALFF/fALFF analyses is unlikely to affect findings, which summarize the entire timeseries. Bandpass filtering was applied for ALFF analyses in subsequent analysis steps (described below).

Performing GSR to remove global noise from resting state fMRI time series is controversial and a consensus has not been reached (Liu et al. 2017, Murphy and Fox 2017, Power et al. 2017a, b; Uddin 2017). While the global BOLD signal at least partially reflects physiological artefact (Power et al. 2017b) it also contains neural information (Fox et al. 2009, Schölvinck et al. 2010). We matched ASD and TD groups on motion, included only participants

with high-quality data, and used white matter and CSF regressors, which have been shown to contain physiological artefact as well, for denoising. GSR was therefore not performed to avoid potential removal of true neuronal signal.

Amplitude of Low Frequency Fluctuations (ALFF)

All ninety-six cortical regions (Table S2) and the thalamus from the Harvard-Oxford Atlas (Bohland et al. 2009) were used as regions of interest (ROIs). This relatively coarse parcellation minimized the computational burden of the current brain-wide analysis. Furthermore, an anatomical parcellation avoids potential confounds related to the greater inter- and intra-individual variability of functional atlases (Salehi et al. 2019), which may be especially problematic when studying clinical groups. ALFF and fractional ALFF (fALFF) were extracted from each ROI using AFNI's 3dRSFC (Taylor and Saad 2013), with a frequency range of .008-.08 Hz specified for ALFF.

Functional Connectivity

Functional connectivity was assessed between left and right thalamus and all ipsilateral cortical ROIs, given predominantly ipsilateral connectivity between thalamus and cerebral cortex (Jones 2007). Average timecourses were extracted from each ROI using AFNI's 3dmaskave. Pearson correlations were calculated between ipsilateral thalamus and cortical ROIs and then transformed to Fisher's z values.

Analysis Approach

Groups were compared on fMRI measures (i.e., ALFF, fALFF, and thalamocortical FC) at two levels of analysis. 1) In order to reduce the dimensionality of the data while preserving broad regional patterns of interest, multilevel modeling was conducted separately for six mutually exclusive ROI groups in the left and right hemispheres (frontal, limbic, somatomotor,

temporal, parietal, occipital; Table S2), which included all 96 cortical ROIs. For example, group differences in ALFF were examined for all left frontal ROIs nested within subjects, all left limbic ROIs nested within subjects, and so on for all six ROI groups in both hemispheres (Figure S2). In other words, for these models each participant had one observation for diagnosis (ASD or TD), and *n* observations (where *n* = number of ROIs) for ALFF. Degrees of freedom for each multilevel model were calculated as: (number of participants x number of nested ROIs) – number of model parameters. This approach both reduces the number of comparisons and accounts for non-independence of multiple ROIs within each participant. 2) Following MLM, post-hoc analyses were conducted at the single ROI-level to characterize group differences in finer detail. For ALFF, fALFF, and thalamocortical FC, two-sample t-tests were conducted for each individual cortical ROI and the thalamus, with degrees of freedom adjusted for unequal variances. ROI-level analyses were repeated for an unmedicated subsample of ASD participants and a matched TD group.

Multimodal Analyses

For the 34 individuals described above with both EEG and fMRI data (Table 1c), multimodal analyses were conducted. First, the relationship between absolute EEG alpha power and ALFF, which is considered more comparable to absolute EEG power than fALFF (Luchinger et al. 2012), was examined. Furthermore, ALFF demonstrates better test-retest reliability than fALFF, and is therefore a more appropriate measure for evaluating between-subjects relationships (Zuo et al. 2010). As in fMRI-only analyses, effects of interest were examined with both MLM and at the single ROI-level. MLM was conducted for each of six groups of ROIs (as above) to determine the effect of diagnostic status, alpha power, and their interaction on ALFF. Sex and nonverbal IQ were not well-matched between multimodal groups

and were therefore included as covariates. As described above for fMRI MLM, each participant had one observation for each predictor and covariate, and *n* observations (where *n* = number of ROIs) for ALFF. At the ROI-level, analogous general linear models were used to examine these effects for each individual cortical ROI and the thalamus.

Finally, the relationship between alpha power and thalamocortical connectivity was explored. As in the multimodal ALFF analysis, MLM was conducted for each ROI group with thalamocortical functional connectivity (Fisher's *z*) as the dependent variable. General linear models were also run at the ROI-level, as described above.

Multiple Comparison Approach

The analyses described above involve numerous comparisons among cortical ROIs. Traditional approaches to multiple comparison correction rely on conservative adjustments to significance values (i.e., *p*-values), with the goal of reducing Type 1 error or false discovery rate. However, *p*-values are influenced by data precision, which is closely tied to sample size. Therefore, particularly in smaller samples, inferences based on *p*-values alone may lead to erroneous conclusions (c.f. Schmidt and Rothman 2014). Alternatively, hierarchical models (i.e., MLM) have been proposed to account for multiple comparisons without the adjustment of *p*-values (Gelman, Hill, & Yajima, 2012), and have demonstrated specific utility in neuroimaging (Friston et al., 2002; Friston & Penny, 2003). In order to balance between more liberal (i.e., uncorrected *p*-values for ROI analyses) and conservative approaches (i.e., corrections using MLM), we present results from MLM, followed up with uncorrected ROI-level comparisons to describe patterns driving MLM findings. Therefore, individual comparisons are best interpreted with caution, and in the context of MLM results.

Results

EEG Analyses

In the full sample with resting-state EEG data, the ASD group showed reduced absolute ($t(60.41) = 2.74$, $p = .008$) and relative ($t(73.42) = 3.83$, $p < .001$) power in the alpha frequency band (Figure 1). Groups did not differ with respect to alpha peak frequency ($t(58.40) = -0.23$, $p = .82$). In a supplemental analysis of only unmedicated ASD participants and a matched TD subgroup ($n = 17$ per group), similar differences were found in both absolute ($t(27.17) = -2.22$, $p = .04$) and relative alpha power ($t(31.30) = -2.39$, $p = .02$; Figure S3), and there were no significant group differences for alpha peak frequency ($t(30.13) = 1.24$, $p = .23$).

Functional MRI Analyses

MLM indicated increased fALFF (ASD > TD) in right temporal regions ($t(1843) = 2.45$, $p = .01$; Table S3). In ROI-level analyses, ALFF was increased in ASDs in both the anterior ($t(108.50) = 2.58$, $p = .01$) and posterior ($t(116.52) = 2.00$, $p = .048$) segments of the right middle temporal gyrus, and fALFF was increased in ASDs in 12 temporal and occipital ROIs spanning both hemispheres (p range = [.002, .046]; Figure 2A, Table S4). Finally, at the ROI-level there were no group differences in ALFF or fALFF in the thalamus (both $p > .70$).

With respect to thalamocortical FC, MLM revealed ipsilateral overconnectivity (ASD > TD) involving bilateral frontal, somatomotor, and temporal, as well as left limbic regions (p range = [.002, .03], Table S3). ROI-level results were consistent and are presented in Figure 2A and Table S4. Supplemental analyses of unmedicated ASD participants and a matched TD subsample ($n = 37$ per group) yielded similar results for ALFF, fALFF, and FC to those reported in the full sample (Figure S4).

Multimodal Analyses

Alpha Power and ALFF

MLM showed multiple alpha by diagnosis interactions with respect to ALFF (i.e., the alpha-ALFF relationship differing between groups) in bilateral frontal, limbic, and somatomotor ROI groups, with consistently less positive relationships between ALFF and alpha power in the ASD compared to the TD group (p range = [.01, .04]; Table S5). Furthermore, MLM combining all 96 cortical ROIs in the ASD group alone found that across the whole brain, there was an interaction between ADOS total score and alpha power ($t(1628) = -2.44$, $p = .01$), such that greater ASD symptom severity predicted an overall less positive relationship between alpha power and ALFF. Finally, within the ASD group there was no effect of medication on the overall relationship between alpha power and ALFF in whole-brain MLM ($p = .90$).

At the ROI-level, thalamic ALFF was not predicted by absolute alpha power, diagnosis, or their interaction (all $p > .09$). Findings for cortical ROIs were consistent with MLM analysis, suggesting that alpha-ALFF relationships differed between groups in 15 frontal, limbic, somatomotor, and temporal ROIs (Figure 2B, Figure S5, Table 2). Follow-up Pearson correlations determined that across all cortical ROIs, alpha power and ALFF were more positively related in the TD group (mean $r = .40$, range = [.11, .70]) than in the ASD group (mean $r = -.18$, range = [-.61, .17]). One-sample t-tests of alpha-ALFF correlations (transformed to Fisher's z) for each ROI corroborated that this relationship was significantly greater than zero in the TD group ($t(95) = 22.15$, $p < .0001$), but significantly less than zero in the ASD group ($t(95) = -10.90$, $p < .0001$).

Alpha Power and Thalamocortical FC

There was no effect of alpha, diagnosis, or their interaction on thalamocortical connectivity in MLM (all $p > .11$; Table S5). One-sample t-tests indicated that overall, the

correlation between EEG alpha and thalamocortical FC was significantly less than zero in both the ASD ($t(95) = -8.95$, $p < .0001$) and TD groups ($t(95) = -3.62$, $p < .001$). At the ROI-level, the ASD group showed a more positive relationship between alpha power and thalamocortical FC than the TD group for the right angular and supramarginal gyri, whereas the opposite effect of group was observed in the occipital pole (p range = [.003, .03]; Table 2).

Discussion

Our study replicates two commonly reported findings from the unimodal EEG and fMRI literatures, showing reduced alpha power as well as predominantly increased thalamocortical connectivity in children and adolescents with ASDs. Although no robust group differences were detected for ALFF, findings suggest spontaneous BOLD fluctuations in right temporal lobe may be increased in ASDs. Multimodal analyses identified group differences in the relationship between EEG alpha power and ALFF, but not between alpha power and thalamocortical FC.

Unimodal Group Differences

Reduced EEG alpha in ASDs

In line with previous research (Murias et al. 2007, Keehn et al. 2017) our EEG sample showed atypically reduced posterior (i.e., occipital or parietal) resting state alpha power in children and adolescents with ASDs. Although the resting alpha rhythm is most prominent at posterior electrodes, reduced alpha power in ASDs has also been reported more broadly in frontal and temporal regions (for review, see Wang et al. 2013). The resting alpha rhythm is inversely associated with autonomic arousal (i.e., electrodermal activity) in typically developing children (Barry et al. 2004), which is thought to be coordinated largely by inhibitory GABAergic interneurons (Jensen and Mazaheri 2010). In ASDs, an imbalance between excitatory and inhibitory neural activity has been proposed (Rubenstein and Merzenich 2003, Nelson and

Valakh 2015), which may lead to such changes in autonomic activity. This is supported by evidence of tonic hyperarousal (Palkovitz and Wiesenfeld 1980) as well as histological (Oblak et al. 2010, Hashemi et al. 2017) and magnetic resonance spectroscopy reports (Gaetz et al. 2014, Puts et al. 2017) of reduced GABA in this population.

Increased thalamocortical connectivity in ASDs

Previous findings with respect to thalamocortical FC in ASDs have been only partially consistent. Nair et al. (2015), who included a smaller sample partly overlapping with that of the current study, reported primarily reduced thalamocortical FC with frontal, parietal, and occipital regions and increased FC with auditory, primary motor, and limbic areas. These distinct findings may be attributed to methodological differences. For example, the focus on functional differences *within* the thalamus through voxelwise analyses by Nair et al. (2015) contrasts with focus on overall thalamic connectivity with each cortical ROI in the present study.

Similarly to Nair and colleagues (2015), Cerliani and colleagues (2015) reported overconnectivity between thalamus and primary sensory and motor networks (including somatosensory, motor, visual, and auditory regions) identified through independent component analysis in a larger sample of children and adults (ages 7-50; 166 ASD, 193 TD) from the Autism Brain Imaging Data Exchange (ABIDE) database; however, they did not find any evidence of thalamocortical underconnectivity. Another study using a large ABIDE sample (ages 6-40; n=228 per group) described overconnectivity between thalamus and primary sensory cortices (including somatosensory, motor, and temporal regions) as well as prefrontal cortex (Woodward et al. 2017). Furthermore, this study reported greatest overconnectivity in older adolescents (ages 13-18) compared to other age groups. These findings are consistent with

results from the current study, which also found exclusive overconnectivity with frontal, temporal, somatomotor, and limbic ROIs in children and adolescents.

Regionally Increased BOLD activity in ASDs

The results of the current study support increased BOLD activity (i.e., ALFF, fALFF) in bilateral (right more than left) temporal and occipital regions; no evidence of decreased ALFF or fALFF was found. These findings are only partly consistent with extremely limited previous research examining ALFF and fALFF in ASDs. In a multi-site study, Supekar et al. (2013) reported broadly increased ALFF across the brain in ASDs in multiple independent cohorts of children. In a large ABIDE sample, increased fALFF was found in right temporal regions (as in the current study), as well as in right dorsal superior frontal cortex (Di Martino et al. 2014). However, this same study and another (Itahashi et al. 2015) reported reduced fALFF in left and right occipital regions in ASDs. This is contrary to the findings from the current study, which were exclusively positive (i.e., ASD > TD) for both temporal and occipital regions.

EEG-fMRI Associations Differ Between Groups

EEG Alpha and ALFF

Relationships between EEG alpha power and fMRI measures were surprising and seemingly counterintuitive, in light of the well-established inverse relationship between concurrent (i.e., simultaneously acquired) EEG alpha and cortical BOLD activity in TD adults. However, simultaneous alpha and BOLD timeseries are distinct from overall alpha power and ALFF, which were measured in the current study. The former describes moment-to-moment fluctuations, but the latter provide summary measures of alpha and BOLD magnitude across an entire recording session. In the current study, alpha power had an overall *positive* relationship with spontaneous BOLD activity (ALFF) in TD adolescents, but a weakly negative relationship

with ALFF in those with ASDs. This difference was driven mainly by frontal, limbic, and somatomotor regions. Furthermore, a more negative alpha-ALFF relationship across the entire brain was associated with greater ASD symptom severity. The underlying neural basis of this relationship remains unclear but may relate to differences in inhibitory GABAergic activity, as described earlier. Importantly, GABA is thought to mediate thalamocortical regulation of the alpha rhythm (Hughes and Crunelli 2005, Lorincz et al. 2009, Lozano-Soldevilla et al. 2014). Therefore, impaired GABAergic signaling in ASDs could conceivably disrupt modulation of alpha rhythms by thalamic and cortical activity, leading to an atypically weak relationship between alpha and cortical BOLD magnitudes in ASDs.

EEG Alpha and Thalamocortical FC

Thalamocortical FC and EEG alpha power showed overall weakly negative associations in both ASD and TD groups across the brain. This diverges from findings described above for ALFF; while the magnitude of BOLD activity appears to be dissociated from alpha power in ASDs, coordination between thalamus and cortex showed a comparatively normal relationship with alpha power in the ASD group. This negative alpha-FC relationship across groups in our multimodal sample may be considered in relation to unimodal results in our larger EEG and fMRI samples. Specifically, the ASD samples showed reduced alpha power in EEG analyses, but widespread overconnectivity between thalamus and frontal, limbic, somatomotor, and temporal ROIs in functional connectivity MRI analyses. The overall negative relation between alpha and thalamocortical FC detected in both ASD and TD subsamples with multimodal data suggests that the two findings in the larger unimodal samples may be related, implying that children with ASDs with most severely reduced alpha power will also tend to show heavier overconnectivity between thalamus and cerebral cortex.

Limitations and Future Directions

The current study included a limited subsample of participants with high-quality data in both EEG and fMRI modalities. Only high-functioning individuals with ASDs were included, who may not represent the full autism spectrum. Furthermore, groups were not well matched for verbal IQ in the fMRI-only and multimodal samples. However, as verbal abilities are related to core ASD symptomatology in the sociocommunicative domain, verbal IQ was not included as a covariate in group analyses. Therefore, reported group differences cannot be definitively dissociated from verbal ability in the current study. Future research with larger, matched samples representing a broader range of ASD symptom severity may help to clarify some of the patterns suggested by the current study.

Another important consideration is the distinction between multimodal relationships within versus between individuals. Past research using simultaneous recordings has examined concurrent fluctuations in EEG and fMRI within typically developing adults, or "state-level" associations. Separately acquired data cannot answer this question, but they can speak to how these signals are related between individuals, at the "trait-level." For example, it has been established that within individuals (state-level), moment-to-moment increases in EEG alpha power are associated with concurrent decreases in cortical (but not thalamic) BOLD (Goldman et al. 2002, Laufs et al. 2003, Olbrich et al. 2009, Bridwell et al. 2013). However, the present study suggests a seemingly opposite relationship *between* typical developing individuals (trait-level), such that in typical development, those showing higher overall alpha power also show greater magnitude of spontaneous BOLD fluctuations. These trait-level associations are an important bridge between fMRI and EEG research in ASDs. Group differences reported by unimodal studies suggest that there are meaningful, interindividual differences between ASD and TD

groups. Therefore, a clear understanding of normative interindividual relationships between multimodal measures will provide a common context for interpreting past EEG and fMRI findings. Future research may further explore these important questions with simultaneous EEG-fMRI when possible, and by conducting both within-subjects analysis of temporal dynamics as well as between-subjects analysis of multimodal relationships.

Conclusion

This is the first known study to characterize relationships between resting state EEG and fMRI measures in ASDs. Reduced alpha power and broadly increased thalamocortical connectivity were found in ASDs relative to TD individuals. Results also suggest a positive relationship between EEG alpha power and cortical BOLD activity in typical development, which was not observed in ASDs. These findings raise questions for future research about potential abnormalities in thalamocortical regulation of the alpha rhythm in this disorder.

Acknowledgments

The authors would like to acknowledge Marissa Westerfield and Wen-Hsuan Chan for their contributions to the preprocessing EEG data, and Christopher Fong for preprocessing of fMRI data. This work was funded by the National Institutes of Health R01 MH081023 (RAM), R21 MH102578 (RAM, TTL), R01 MH101173 (RAM), R21 MH096582 (JT), National Institute of Neurological Disorders and Stroke Center Grant 2P50NS22343 (JT), and National Science Foundation Graduate Research Fellowship 1321850 (LEM). No competing financial interests exist.

Dissertation Author Note

Chapter 4, in full, is a reprint of the material as it appears in Brain Connectivity, 10, 18-28. Mash, L. E., Keehn, B., Linke, A. C., Liu, T. T., Helm, J. L., Haist, F., Townsend, J., & Müller, R.-A. Mary Ann Liebert, 2020. The dissertation author was the primary investigator and author of this paper.

Table 3.1 Sample Characteristics

A. EEG Sample				
	ASD (*n* = 38)	**TD (*n* = 38)**	**Statistic**	***p***
Sex	32 male	29 male	$\chi^2(1) = 0.75$	.39
Handedness	35 right	32 right	$\chi^2(1) = 1.13$	.29
Age	12.6 (2.4)	13.0 (2.8)	$t(74) = -0.57$	.57
	[7.1 – 17.1]	[7.1 – 18.0]		
Usable EEG (min)	4.9 (1.0)	5.2 (0.7)	$t(74) = -1.83$	.07
	[2.2 – 6.0]	[2.9 – 6.0]		
VIQ	105 (18)	108 (11)	$t(74) = -0.86$	.39
	[72 – 147]	[83 – 126]		
NVIQ	104 (18)	107 (12)	$t(74) = -0.61$	.54
	[64 – 140]	[77 – 129]		
ADOS SC	10 (4)			
	[1 – 19]			
ADOS RRB	4 (4)			
	[0 – 19]			
ADOS Total	14 (4)			
	[8 – 23]			
B. fMRI Sample				
	ASD (*n* = 66)	**TD (*n* = 57)**	**Statistic**	***p***
Sex	54 male	45 male	$\chi^2(1) = 0.16$	.69
Handedness	58 right	49 right	$\chi^2(1) = 0.10$	.75
Age	13.4 (2.6)	13.1 (2.8)	$t(121) = 0.53$	.60
	[8.0-18.0]	[6.9-17.6]		
Usable fMRI (timepoints)	175 (7)	176 (7)	$t(121) = -0.48$	.63
	[144 – 180]	[145 – 180]		
RMSD	0.08 (0.04)	0.07 (0.04)	$t(121) = 0.36$	.72
	[0.02 – 0.19]	[0.02 – 0.17]		
VIQ	101 (17)	107 (11)	$t(121) = -2.19$	.03
	[67 - 147]	[73 - 127]		
NVIQ	105 (17)	106 (13)	$t(121) = -0.58$	.56
	[53 – 140]	[62 - 137]		
ADOS SC	12 (4)			
	[6 – 22]			
ADOS RRB	2 (2)			
	[0 – 7]			

ADOS Total	14 (4) [7 – 24]			

C. EEG-fMRI Sample

	ASD (*n* = 17)	**TD (*n* = 17)**	**Statistic**	***p***
Sex	16 male	13 male	$\chi^2(1) = 2.11$	.15
Handedness	15 right	13 right	$\chi^2(1) = 0.81$	.37
Age	14.3 (1.5) [12.7 – 17.1]	14.5 (1.4) [12.4 – 16.8]	$t(32) = -0.43$	.67
Usable EEG (min)	5.3 (0.59) [3.9– 6.0]	5.2 (0.72) [2.9 – 5.9]	$t(32) = 0.07$	.94
Usable fMRI (timepoints)	176 (7) [153 – 180]	177 (5) [165 – 180]	$t(32) = -0.53$	.60
RMSD	0.07 (0.04) [0.02 – 0.15]	0.07 (0.04) [0.03 – 0.16]	$t(32) = -0.17$	.87
VIQ	116 (13) [88– 147]	107 (10) [87– 126]	$t(32) = 2.32$	.03
NVIQ	116 (11) [100 – 140]	110 (12) [86 – 129]	$t(32) = 1.67$	.11
ADOS SC	10 (3) [7 – 19]			
ADOS RRB	2 (1) [0 – 4]			
ADOS Total	12 (4) [8 – 23]			

Values are presented as mean (SD), [range]. VIQ = Verbal IQ; NVIQ = Nonverbal IQ; FSIQ = Full Scale IQ; ADOS = Autism Diagnostic Observation Schedule; SC = Social Communication; RRB = Restricted/Repetitive Behavior; RMSD = Root Mean Squared Displacement

Table 3.2 ROI-level EEG-fMRI Findings

Outcome	Region	df	Alpha*Group (*t*)	*p*
ALFF	L Frontal Medial Cortex	28	-2.40	.02
	L Frontal Operculum Cortex	28	-3.17	.004
	L Cingulate Gyrus (anterior)	28	-2.16	.04
	L Supplementary Motor Cortex	28	-2.53	.02
	L Temporal Fusiform Cortex (anterior)	28	-2.94	.007
	L Temporal Pole	28	-2.28	.03
	R Frontal Medial Cortex	28	-2.26	.03
	R Superior Frontal Gyrus	28	-2.32	.03
	R Cingulate Gyrus (anterior)	28	-2.38	.02
	R Paracingulate Gyrus	28	-2.24	.03
	R Parahippocampal Gyrus (anterior)	28	-2.28	.03
	R Supplementary Motor Cortex	28	-3.49	.002
	R Middle Temporal Gyrus (anterior)	28	-2.50	.02
	R Temporal Fusiform Cortex (anterior)	28	-2.30	.03
	R Temporal Fusiform Cortex (posterior)	28	-2.09	.046
Thalamocortical FC	R Angular Gyrus	28	3.21	.003
	R Supramarginal Gyrus (posterior)	28	2.33	.03
	R Occipital Pole	28	-2.52	.02

ROIs with group differences ($p < .05$, uncorr) are shown.

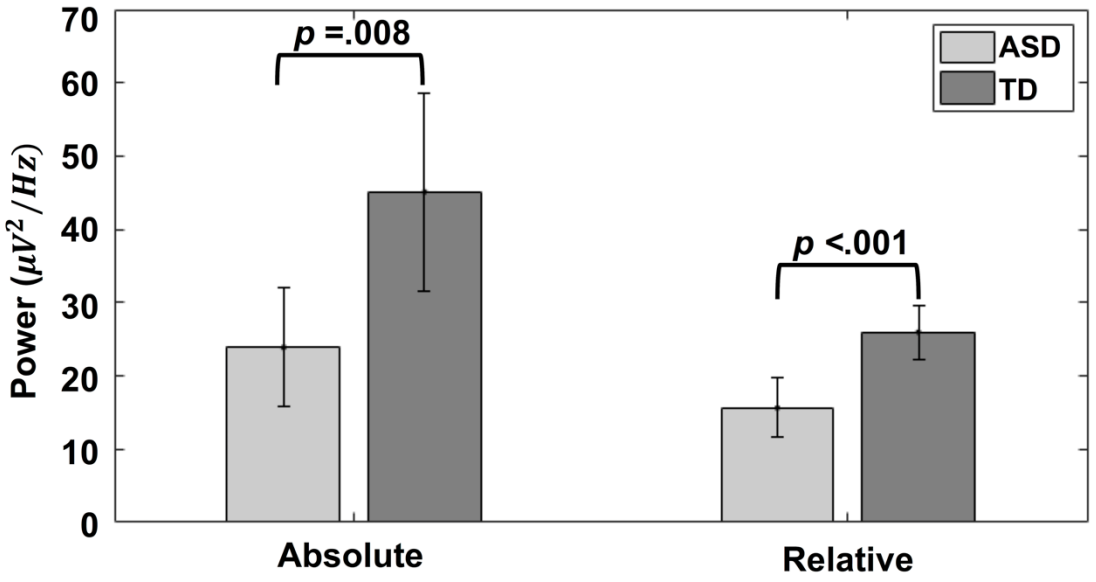

Figure 3.1 Group Differences in EEG Alpha Power
Bars show absolute and relative alpha power averaged across participants in each group. Both absolute and relative alpha power are smaller in the ASD group than the TD group.

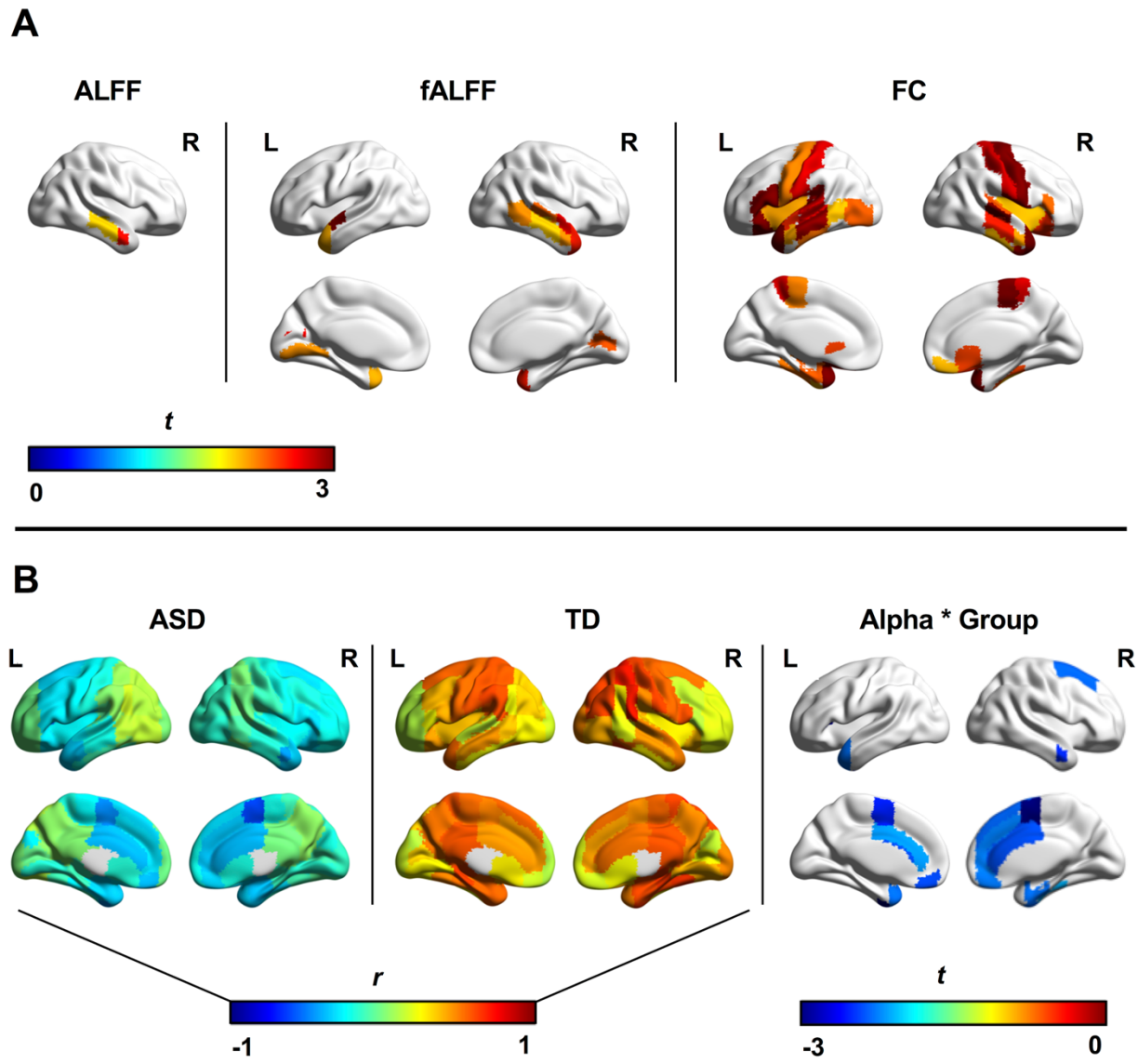

Figure 3.2 fMRI and Multimodal Group Differences
Panel A: ROIs showing group differences ($p < .05$, uncorr.) in ALFF (left), fALFF (middle), and thalamocortical FC (right) are depicted. Colors represent t-scores (positive indicates ASD > TD). Panel B: Pearson correlations (colors represent *r*) between EEG alpha power and ALFF are depicted for each cortical ROI in the ASD group (left) and the TD group (middle). Alpha-ALFF relationships are generally negative in the ASD group, but positive in the TD group. ROIs with group differences in the alpha-ALFF relationship (i.e., alpha by group interaction; $p < .05$, uncorr.) are shown (right). Colors represent t-scores (negative indicates a less positive alpha-ALFF association in ASD relative to TD). Figures were visualized with the BrainNet Viewer (Xia et al. 2013, http://www.nitrc.org/projects/bnv)

References

Allen, E. A., E. Damaraju, T. Eichele, L. Wu, V. D. Calhoun. 2018. EEG Signatures of Dynamic Functional Network Connectivity States. Brain Topogr 31(1): 101-116.

American Psychiatric Association (2013). Diagnostic and statistical manual of mental disorders : DSM-5 Arlington, VA, American Psychiatric Association**:** 947.

Baio, J., L. Wiggins, D. L. Christensen, M. J. Maenner, J. Daniels, Z. Warren, et al. 2018. Prevalence of Autism Spectrum Disorder Among Children Aged 8 Years - Autism and Developmental Disabilities Monitoring Network, 11 Sites, United States, 2014. MMWR Surveill Summ 67(6): 1-23.

Barry, R. J., A. R. Clarke, R. McCarthy, M. Selikowitz, J. A. Rushby, E. Ploskova. 2004. EEG differences in children as a function of resting-state arousal level. Clin Neurophysiol 115(2): 402-408.

Bohland, J. W., H. Bokil, C. B. Allen, P. P. Mitra. 2009. The brain atlas concordance problem: quantitative comparison of anatomical parcellations. PLoS One 4(9): e7200.

Bridwell, D. A., L. Wu, T. Eichele, V. D. Calhoun. 2013. The spatiospectral characterization of brain networks: fusing concurrent EEG spectra and fMRI maps. Neuroimage 69: 101-111.

Britton, J. W., L. C. Frey, J. L. Hopp, P. Korb, M. Z. Koubeissi, W. E. Lievens, et al. 2016. *Electroencephalography (EEG): An Introductory Text and Atlas of Normal and Abnormal Findings in Adults, Children, and Infants*. Chicago, IL: American Epilepsy Society.

Cerliani, L., M. Mennes, R. M. Thomas, A. Di Martino, M. Thioux, C. Keysers. 2015. Increased Functional Connectivity Between Subcortical and Cortical Resting-State Networks in Autism Spectrum Disorder. JAMA Psychiatry 72(8): 767-777.

Chan, A. S., S. L. Sze, M. C. Cheung. 2007. Quantitative electroencephalographic profiles for children with autistic spectrum disorder. Neuropsychology 21(1): 74-81.

Cox, R. W. (1996). AFNI: software for analysis and visualization of functional magnetic resonance neuroimages. *Comput Biomed Res, 29*(3), 162-173.

Cragg, L., N. Kovacevic, A. R. McIntosh, C. Poulsen, K. Martinu, G. Leonard, T. Paus. 2011. Maturation of EEG power spectra in early adolescence: a longitudinal study. Dev Sci 14(5): 935-943.

Dale, A. M., B. Fischl, M. I. Sereno. 1999. Cortical surface-based analysis. I. Segmentation and surface reconstruction. Neuroimage 9(2): 179-194.

Dawson, G., L. G. Klinger, H. Panagiotides, A. Lewy, P. Castelloe. 1995. Subgroups of autistic children based on social behavior display distinct patterns of brain activity. J Abnorm Child Psychol 23(5): 569-583.

de Munck, J. C., S. I. Goncalves, L. Huijboom, J. P. Kuijer, P. J. Pouwels, R. M. Heethaar, F. H. Lopes da Silva. 2007. The hemodynamic response of the alpha rhythm: an EEG/fMRI study. Neuroimage 35(3): 1142-1151.

Delorme, A., S. Makeig. 2004. EEGLAB: an open source toolbox for analysis of single-trial EEG dynamics including independent component analysis. J Neurosci Methods 134(1): 9-21.

Di Martino, A., C. G. Yan, Q. Li, E. Denio, F. X. Castellanos, K. Alaerts, et al. 2014. The autism brain imaging data exchange: towards a large-scale evaluation of the intrinsic brain architecture in autism. Mol Psychiatry 19(6): 659-667.

Dickinson, A., C. DiStefano, D. Senturk, S. S. Jeste. 2018. Peak alpha frequency is a neural marker of cognitive function across the autism spectrum. Eur J Neurosci 47(6): 643-651.

Edgar, J. C., K. Heiken, Y. H. Chen, J. D. Herrington, V. Chow, S. Liu, et al. 2015. Resting-state alpha in autism spectrum disorder and alpha associations with thalamic volume. J Autism Dev Disord 45(3): 795-804.

Fischl, B. 2012. FreeSurfer. Neuroimage 62(2): 774-781.

Fischl, B., M. I. Sereno, A. M. Dale. 1999. Cortical surface-based analysis. II: Inflation, flattening, and a surface-based coordinate system. Neuroimage 9(2): 195-207.

Fox, M. D., D. Zhang, A. Z. Snyder, M. E. Raichle. 2009. The global signal and observed anticorrelated resting state brain networks. J Neurophysiol 101(6): 3270-3283.

Friston, K. J., Glaser, D. E., Henson, R. N., Kiebel, S., Phillips, C., & Ashburner, J. (2002). Classical and Bayesian inference in neuroimaging: applications. *Neuroimage, 16*(2), 484-512. doi:10.1006/nimg.2002.1091

Friston, K. J., & Penny, W. (2003). Posterior probability maps and SPMs. *Neuroimage, 19*(3), 1240-1249.

Gaetz, W., L. Bloy, D. J. Wang, R. G. Port, L. Blaskey, S. E. Levy, T. P. Roberts. 2014. GABA estimation in the brains of children on the autism spectrum: measurement precision and regional cortical variation. Neuroimage 86: 1-9.

Gelman, A., Hill, J., & Yajima, M. (2012). Why We (Usually) Don't Have to Worry About Multiple Comparisons. *Journal of Research on Educational Effectiveness, 5*(2), 189-211. doi:10.1080/19345747.2011.618213

Goldman, R. I., J. M. Stern, J. Engel, Jr., M. S. Cohen. 2002. Simultaneous EEG and fMRI of the alpha rhythm. Neuroreport 13(18): 2487-2492.

Gotham, K., S. Risi, A. Pickles, C. Lord. 2007. The Autism Diagnostic Observation Schedule: revised algorithms for improved diagnostic validity. J Autism Dev Disord 37(4): 613-627.

Haegens, S., H. Cousijn, G. Wallis, P. J. Harrison, A. C. Nobre. 2014. Inter- and intra-individual variability in alpha peak frequency. Neuroimage 92: 46-55.

Hames, E. C., B. Murphy, R. Rajmohan, R. C. Anderson, M. Baker, S. Zupancic, et al. 2016. Visual, Auditory, and Cross Modal Sensory Processing in Adults with Autism: An EEG Power and BOLD fMRI Investigation. Front Hum Neurosci 10: 167.

Hashemi, E., J. Ariza, H. Rogers, S. C. Noctor, V. Martinez-Cerdeno. 2017. The Number of Parvalbumin-Expressing Interneurons Is Decreased in the Prefrontal Cortex in Autism. Cereb Cortex 27(3): 1931-1943.

Heller L., Volegov P. (2014) Electric and Magnetic Fields of the Brain. In: Supek S., Aine C. (eds) Magnetoencephalography. Springer, Berlin, Heidelberg

Hillman, E. M. 2014. Coupling mechanism and significance of the BOLD signal: a status report. Annu Rev Neurosci 37: 161-181.

Hughes, S. W., V. Crunelli. 2005. Thalamic mechanisms of EEG alpha rhythms and their pathological implications. Neuroscientist 11(4): 357-372.

Hull, J. V., Z. J. Jacokes, C. M. Torgerson, A. Irimia, J. D. Van Horn. 2016. Resting-State Functional Connectivity in Autism Spectrum Disorders: A Review. Front Psychiatry 7: 205.

Itahashi, T., T. Yamada, H. Watanabe, M. Nakamura, H. Ohta, C. Kanai, et al. 2015. Alterations of local spontaneous brain activity and connectivity in adults with high-functioning autism spectrum disorder. Mol Autism 6: 30.

Jensen, O., A. Mazaheri. 2010. Shaping functional architecture by oscillatory alpha activity: gating by inhibition. Front Hum Neurosci 4: 186.

Jochaut, D., K. Lehongre, A. Saitovitch, A. D. Devauchelle, I. Olasagasti, N. Chabane, et al. 2015. Atypical coordination of cortical oscillations in response to speech in autism. Front Hum Neurosci 9: 171.

Jones, E. G. 2007. *The Thalamus*: Cambridge University Press.p. 142-146

Jung, T. P., S. Makeig, C. Humphries, T. W. Lee, M. J. McKeown, V. Iragui, T. J. Sejnowski. 2000. Removing electroencephalographic artifacts by blind source separation. Psychophysiology 37(2): 163-178.

Jung, T. P., S. Makeig, M. Westerfield, J. Townsend, E. Courchesne, T. J. Sejnowski. 2000. Removal of eye activity artifacts from visual event-related potentials in normal and clinical subjects. Clin Neurophysiol 111(10): 1745-1758.

Keehn, B., M. Westerfield, R. A. Muller, J. Townsend. 2017. Autism, Attention, and Alpha Oscillations: An Electrophysiological Study of Attentional Capture. Biol Psychiatry Cogn Neurosci Neuroimaging 2(6): 528-536.

Klimesch, W. 1999. EEG alpha and theta oscillations reflect cognitive and memory performance: a review and analysis. Brain Res Brain Res Rev 29(2-3): 169-195.

Laufs, H., A. Kleinschmidt, A. Beyerle, E. Eger, A. Salek-Haddadi, C. Preibisch, K. Krakow. 2003. EEG-correlated fMRI of human alpha activity. Neuroimage 19(4): 1463-1476.

Liu, T. T., A. Nalci, M. Falahpour. 2017. The global signal in fMRI: Nuisance or Information? Neuroimage 150: 213-229.

Lord, C., S. Risi, L. Lambrecht, E. H. Cook, Jr., B. L. Leventhal, P. C. DiLavore, et al. 2000. The autism diagnostic observation schedule-generic: a standard measure of social and communication deficits associated with the spectrum of autism. J Autism Dev Disord 30(3): 205-223.

Lorincz, M. L., K. A. Kekesi, G. Juhasz, V. Crunelli, S. W. Hughes. 2009. Temporal framing of thalamic relay-mode firing by phasic inhibition during the alpha rhythm. Neuron 63(5): 683-696.

Lozano-Soldevilla, D., N. ter Huurne, R. Cools, O. Jensen. 2014. GABAergic modulation of visual gamma and alpha oscillations and its consequences for working memory performance. Curr Biol 24(24): 2878-2887.

Luchinger, R., L. Michels, E. Martin, D. Brandeis. 2012. Brain state regulation during normal development: Intrinsic activity fluctuations in simultaneous EEG-fMRI. Neuroimage 60(2): 1426-1439.

Mash, L. E., M. A. Reiter, A. C. Linke, J. Townsend, R. A. Müller. 2018. Multimodal approaches to functional connectivity in autism spectrum disorders: An integrative perspective. Dev Neurobiol 78(5): 456-473.

Miskovic, V., X. Ma, C. A. Chou, M. Fan, M. Owens, H. Sayama, B. E. Gibb. 2015. Developmental changes in spontaneous electrocortical activity and network organization from early to late childhood. Neuroimage 118: 237-247.

Murias, M., S. J. Webb, J. Greenson, G. Dawson. 2007. Resting state cortical connectivity reflected in EEG coherence in individuals with autism. Biol Psychiatry 62(3): 270-273.

Murphy, K., M. D. Fox. 2017. Towards a consensus regarding global signal regression for resting state functional connectivity MRI. Neuroimage 154: 169-173.

Nair, A., R. A. Carper, A. E. Abbott, C. P. Chen, S. Solders, S. Nakutin, et al. 2015. Regional specificity of aberrant thalamocortical connectivity in autism. Hum Brain Mapp 36(11): 4497-4511.

Nelson, S. B., V. Valakh. 2015. Excitatory/Inhibitory Balance and Circuit Homeostasis in Autism Spectrum Disorders. Neuron 87(4): 684-698.

Niedermeyer, E., D. L. Schomer, F. H. Lopes da Silva. 2011. *Niedermeyer's electroencephalography : basic principles, clinical applications, and related fields*. Philadelphia: Wolters Kluwer Health/Lippincott Williams & Wilkins.p.

O'Reilly, C., J. D. Lewis, M. Elsabbagh. 2017. Is functional brain connectivity atypical in autism? A systematic review of EEG and MEG studies. PLoS One 12(5): e0175870.

Oblak, A. L., T. T. Gibbs, G. J. Blatt. 2010. Decreased GABAB receptors in the cingulate cortex and fusiform gyrus in Autism. Journal of Neurochemistry 114(5): 1414-1423.

Olbrich, S., C. Mulert, S. Karch, M. Trenner, G. Leicht, O. Pogarell, U. Hegerl. 2009. EEG-vigilance and BOLD effect during simultaneous EEG/fMRI measurement. Neuroimage 45(2): 319-332.

Oostenveld, R., P. Fries, E. Maris, J. M. Schoffelen. 2011. FieldTrip: Open source software for advanced analysis of MEG, EEG, and invasive electrophysiological data. Comput Intell Neurosci 2011: 156869.

Palkovitz, R. J., A. R. Wiesenfeld. 1980. Differential autonomic responses of autistic and normal children. J Autism Dev Disord 10(3): 347-360.

Power, J. D., T. O. Laumann, M. Plitt, A. Martin, S. E. Petersen. 2017. On Global fMRI Signals and Simulations. Trends Cogn Sci 21(12): 911-913.

Power, J. D., Mitra, A., Laumann, T. O., Snyder, A. Z., Schlaggar, B. L., & Petersen, S. E. (2014). Methods to detect, characterize, and remove motion artifact in resting state fMRI. *Neuroimage, 84*, 320-341. doi:10.1016/j.neuroimage.2013.08.048

Power, J. D., M. Plitt, T. O. Laumann, A. Martin. 2017. Sources and implications of whole-brain fMRI signals in humans. Neuroimage 146: 609-625.

Puts, N. A. J., E. L. Wodka, A. D. Harris, D. Crocetti, M. Tommerdahl, S. H. Mostofsky, R. A. E. Edden. 2017. Reduced GABA and altered somatosensory function in children with autism spectrum disorder. Autism Res 10(4): 608-619.

Rubenstein, J. L., M. M. Merzenich. 2003. Model of autism: increased ratio of excitation/inhibition in key neural systems. Genes Brain Behav 2(5): 255-267.

Salehi, M., A. S. Greene, A. Karbasi, X. Shen, D. Scheinost, R. T. Constable. 2019. There is no single functional atlas even for a single individual: Parcellation of the human brain is state dependent. bioRxiv: 431833.

Scheeringa, R., K. M. Petersson, A. Kleinschmidt, O. Jensen, M. C. Bastiaansen. 2012. EEG alpha power modulation of fMRI resting-state connectivity. Brain Connect 2(5): 254-264.

Schmidt, M., K. J. Rothman. 2014. Mistaken inference caused by reliance on and misinterpretation of a significance test. International Journal of Cardiology 177(3): 1089-1090.

Schölvinck, M. L., A. Maier, F. Q. Ye, J. H. Duyn, D. A. Leopold. 2010. Neural basis of global resting-state fMRI activity. Proc Natl Acad Sci U S A 107(22): 10238-10243.

Schuetze, M., M. T. Park, I. Y. Cho, F. P. MacMaster, M. M. Chakravarty, S. L. Bray. 2016. Morphological Alterations in the Thalamus, Striatum, and Pallidum in Autism Spectrum Disorder. Neuropsychopharmacology 41(11): 2627-2637.

Sheikhani, A., H. Behnam, M. R. Mohammadi, M. Noroozian, M. Mohammadi. 2012. Detection of abnormalities for diagnosing of children with autism disorders using of quantitative electroencephalography analysis. J Med Syst 36(2): 957-963.

Supekar, K., L. Q. Uddin, A. Khouzam, J. Phillips, W. D. Gaillard, L. E. Kenworthy, et al. 2013. Brain hyperconnectivity in children with autism and its links to social deficits. Cell Rep 5(3): 738-747.

Taylor, P. A., Z. S. Saad. 2013. FATCAT: (an efficient) Functional and Tractographic Connectivity Analysis Toolbox. Brain Connect 3(5): 523-535.

Tierney, A. L., L. Gabard-Durnam, V. Vogel-Farley, H. Tager-Flusberg, C. A. Nelson. 2012. Developmental trajectories of resting EEG power: an endophenotype of autism spectrum disorder. PLoS One 7(6): e39127.

Uddin, L. Q. 2017. Mixed Signals: On Separating Brain Signal from Noise. Trends Cogn Sci 21(6): 405-406.

Wang, J., J. Barstein, L. E. Ethridge, M. W. Mosconi, Y. Takarae, J. A. Sweeney. 2013. Resting state EEG abnormalities in autism spectrum disorders. J Neurodev Disord 5(1): 24.

Woodward, N. D., M. Giraldo-Chica, B. Rogers, C. J. Cascio. 2017. Thalamocortical dysconnectivity in autism spectrum disorder: An analysis of the Autism Brain Imaging Data Exchange. Biol Psychiatry Cogn Neurosci Neuroimaging 2(1): 76-84.

Xia, M., J. Wang, Y. He. 2013. BrainNet Viewer: a network visualization tool for human brain connectomics. PLoS One 8(7): e68910.

Zang, Y. F., Y. He, C. Z. Zhu, Q. J. Cao, M. Q. Sui, M. Liang, et al. 2007. Altered baseline brain activity in children with ADHD revealed by resting-state functional MRI. Brain Dev 29(2): 83-91.

Zou, Q. H., C. Z. Zhu, Y. Yang, X. N. Zuo, X. Y. Long, Q. J. Cao, et al. 2008. An improved approach to detection of amplitude of low-frequency fluctuation (ALFF) for resting-state fMRI: fractional ALFF. J Neurosci Methods 172(1): 137-141.

Zuo, X. N., A. Di Martino, C. Kelly, Z. E. Shehzad, D. G. Gee, D. F. Klein, et al. 2010. The oscillating brain: complex and reliable. Neuroimage 49(2): 1432-1445.

Chapter 5:

General Discussion

The three studies described above each explore alternative approaches to static, unimodal FC analysis, which has largely dominated the ASD neuroimaging literature to date. Each study offers novel insights into features of brain activity that may be overlooked by standard analyses, and how these features may (or may not) be altered in ASDs. Specifically, this dissertation examined the nature of transient FC patterns, BOLD lag structure, and EEG-fMRI associations in children and adolescents with and without ASDs. Study 1 found group differences in the patterns of two transient FC states, despite the absence of static FC group differences. Study 2 reported that BOLD lag patterns changed in response to task demands and were associated with arterial blood supply, but found no clear group differences in BOLD lag in either resting or task conditions. Finally, Study 3 showed that separately acquired EEG alpha power and regional BOLD activity were positively associated in typical development, whereas this association was weakly negative in ASDs. Altogether, this work highlights the importance of integrating dynamic and multimodal data to clarify and refine existing models of atypical FC in ASDs.

Functional Connectivity Dynamics: Transient States and Lag Patterns

Studies 1 and 2 take distinct, yet complementary approaches to evaluating the temporal structure of BOLD correlations. Study 1 used sliding window analysis and k-means clustering to reveal transient connectivity states and explore the variability of individual connections over time; in other words, this study focused on changes in simultaneous BOLD correlations across contiguous time segments. Study 2, on the other hand, examined lag between regional BOLD timeseries over an entire scan period using cross-covariance, which does not assume simultaneous coactivation between regions. It is unknown how or whether BOLD lag is

associated with transient FC states, but any evidence of atypical lag structure in ASDs could suggest a potential mechanism for transient FC group differences, particularly if atypical latencies were state-dependent (i.e., rest vs. task performance). However, while Study 1 revealed robust group differences in transient FC patterns, BOLD lag patterns in Study 2 did not differ between groups during either rest or task performance.

One interpretation of these findings is that atypical transient FC in ASDs is independent of BOLD lag structure, which appears to be similar across groups. However, there is currently little consensus about BOLD lag in ASDs, with the few other known studies of adults reporting atypical latencies in specific regions (Mitra et al., 2017) and across multiple networks (King et al., 2018; Raatikainen et al., 2020). Furthermore, Study 2 found that BOLD latency patterns differed across traditional arterial flow territories, and that mean latencies in these territories were highly associated with literature-derived estimates of arterial transit time, suggesting a substantial vascular contribution to observed BOLD lags. This finding highlights a key limitation of the BOLD signal as a means of examining brain dynamics. The slowness of the BOLD signal and its inherent association with hemodynamic factors complicate the separation of neural dynamics from regional differences in vasculature and other variables affecting neurovascular coupling. This is particularly problematic for lag analysis, which is highly influenced by regional differences in blood supply. However, the temporal resolution of sliding-window analysis is also considerably limited by the delay between neural activation and the BOLD signal peak. Dynamic fcMRI methods have the potential to improve our understanding of the extensive and often contradictory fcMRI literature in ASDs, but they represent only one component of a broader movement toward an integrated understanding of spatiotemporal brain dynamics.

Moving Toward Multimodal Research

The BOLD signal is a slow, hemodynamic measure with insufficient temporal resolution to capture neural dynamics at a millisecond timescale. Therefore, multimodal research combining fMRI with direct measurements of neural activity with high temporal resolution (i.e., EEG or MEG) are needed to fill critical gaps in our understanding of dynamic brain networks in ASDs. Concurrent EEG-fMRI relationships (i.e., simultaneously measured) are relatively well-established in neurotypical adults, but very few studies have combined these modalities in ASDs. Study 3 sought to characterize relationships between separately acquired EEG and fMRI measures, which are not well understood in either ASDs or typical development. Although separately acquired data cannot speak to dynamic network functioning, they may help to clarify group differences in previous, unimodal EEG and fMRI studies.

Study 3 found unimodal group differences similar to those reported in previous studies, including reduced parieto-occipital EEG alpha power and broadly increased thalamocortical FC, as well as increased right temporal BOLD activity (amplitude of low frequency fluctuations; ALFF) in children and adolescents with ASDs. Multimodal analyses revealed that overall, alpha power and thalamocortical FC were negatively associated in both groups; this is generally consistent with reduced alpha power and increased thalamocortical FC in ASDs observed in unimodal studies. However, the alpha-ALFF relationship was reversed between groups (positive in typical development, negative in ASDs), and a more negative relationship predicted greater symptom severity in the ASD group. This complicates the interpretation of unimodal findings and may suggest a disruption in the processes that coordinate the alpha rhythm with cortical activity at rest.

In a study using simultaneous EEG-fMRI recordings, transient fcMRI states (derived using the same sliding window method as Study 1 showed unique EEG spectral signatures during the resting state in neurotypical adults (Allen et al., 2017). Interestingly, one state showing increased thalamocortical anticorrelation was associated with decreased EEG alpha power (as well as increased power in theta and delta bands). This relationship is opposite from the alpha-thalamocortical FC association described for separately collected data in Study 3, which may be explained by differences between within-subject, concurrent data, and between-subjects, separately acquired data (see Study 3 for in-depth discussion). Nonetheless, this raises questions for future research about potential state-dependent EEG-fMRI relationships in autism, and their association with transient BOLD correlations (as in Study 1). For example, using concurrent recordings, it would be possible to examine whether alpha-ALFF or alpha-FC associations vary over time, and how these temporal features may characterize ASDs more clearly than static or unimodal measures.

It is also worthwhile to consider how EEG measures may inform BOLD lag analyses. Study 2 highlighted inherent difficulties interpreting lag differences between two BOLD timeseries, due to regional differences in vascular and hemodynamic features that affect the timing of both signals. However, simultaneous EEG-fMRI has been used to establish lag patterns between modalities, where only one modality is affected by hemodynamics. For example, thalamic BOLD signal increases have been found to *precede* corresponding increases in EEG alpha power by several seconds (de Munck et al., 2007; Feige et al., 2005; Feige et al., 2017). One of these studies further reported that BOLD activity preceded EEG power increases across a broader range of regions and frequency bands, while negative BOLD-EEG power associations were more common at zero-lag (Feige et al., 2017). Multimodal lag analyses may

improve our understanding of BOLD lag structure and may help to clarify temporal features of EEG-fMRI relationships, such as those described in Study 3.

Conclusions

The increasing prevalence of ASDs in recent decades has fueled a proliferation of research examining the neural underpinnings of these disorders. Neuroimaging studies have repeatedly implicated distributed brain network abnormalities in ASDs, but these findings have not been clear or consistent enough to reliably distinguish children diagnosed with ASDs from their typically developing peers. These shortcomings are partly associated with methodological limitations of noninvasive neuroimaging modalities, such as EEG and fMRI. However, advanced analytical approaches, such as dynamic fcMRI and combined EEG-fMRI analysis, have been increasingly used to explore complex spatiotemporal dynamics of brain networks in typical adults. The studies that comprise this dissertation are among the first to apply these methods to children and adolescents with ASDs.

This dissertation demonstrates the unique potential of dynamic and multimodal neuroimaging methods to reveal a more detailed picture of atypical brain function in ASDs. These three studies generate evidence that transient FC patterns and EEG-fMRI relationships may provide important clues about the neurobiology of ASDs that cannot be gleaned from traditional fcMRI and EEG analyses. However, many important questions remain about the timing, structure, and flexibility of coordinated brain activity in these heterogeneous disorders. Future multimodal work aimed at clarifying the nature of dynamic network communication in ASDs will be essential in moving this promising avenue of research forward.

References

Abbas, A., Bassil, Y., & Keilholz, S. (2019). Quasi-periodic patterns of brain activity in individuals with attention-deficit/hyperactivity disorder. *Neuroimage Clin, 21*, 101653. doi:10.1016/j.nicl.2019.101653

Abbas, A., Belloy, M., Kashyap, A., Billings, J., Nezafati, M., Schumacher, E. H., & Keilholz, S. (2019). Quasi-periodic patterns contribute to functional connectivity in the brain. *Neuroimage, 191*, 193-204. doi:10.1016/j.neuroimage.2019.01.076

Abrol, A., Damaraju, E., Miller, R. L., Stephen, J. M., Claus, E. D., Mayer, A. R., & Calhoun, V. D. (2017). Replicability of time-varying connectivity patterns in large resting state fMRI samples. *Neuroimage, 163*, 160-176. doi:10.1016/j.neuroimage.2017.09.020

Allen, E. A., Damaraju, E., Eichele, T., Wu, L., & Calhoun, V. D. (2017). EEG Signatures of Dynamic Functional Network Connectivity States. *Brain Topogr*. doi:10.1007/s10548-017-0546-2

Allen, E. A., Damaraju, E., Plis, S. M., Erhardt, E. B., Eichele, T., & Calhoun, V. D. (2014). Tracking whole-brain connectivity dynamics in the resting state. *Cereb Cortex, 24*(3), 663-676. doi:10.1093/cercor/bhs352

American Psychiatric Association. (2013). *Diagnostic and statistical manual of mental disorders : DSM-5* (Fifth edition. ed., pp. 947).

Barttfeld, P., Wicker, B., Cukier, S., Navarta, S., Lew, S., & Sigman, M. (2011). A big-world network in ASD: dynamical connectivity analysis reflects a deficit in long-range connections and an excess of short-range connections. *Neuropsychologia, 49*(2), 254-263. doi:10.1016/j.neuropsychologia.2010.11.024

Belmonte, M. K., Allen, G., Beckel-Mitchener, A., Boulanger, L. M., Carper, R. A., & Webb, S. J. (2004). Autism and abnormal development of brain connectivity. *J Neurosci, 24*(42), 9228-9231. doi:10.1523/JNEUROSCI.3340-04.2004

Biswal, B., Yetkin, F. Z., Haughton, V. M., & Hyde, J. S. (1995). Functional connectivity in the motor cortex of resting human brain using echo-planar MRI. *Magn Reson Med, 34*(4), 537-541.

Bowyer, S. M. (2016). Coherence a measure of the brain networks: past and present. *Neuropsychiatric Electrophysiology, 2*(1), 1. doi:10.1186/s40810-015-0015-7

Bridwell, D. A., Wu, L., Eichele, T., & Calhoun, V. D. (2013). The spatiospectral characterization of brain networks: fusing concurrent EEG spectra and fMRI maps. *Neuroimage, 69*, 101-111. doi:10.1016/j.neuroimage.2012.12.024

Buzsaki, G. (2006). *Rhythms of the Brain*: Oxford University Press.

Calhoun, V. D., Miller, R., Pearlson, G., & Adali, T. (2014). The chronnectome: time-varying connectivity networks as the next frontier in fMRI data discovery. *Neuron, 84*(2), 262-274. doi:10.1016/j.neuron.2014.10.015

Chang, C., Liu, Z., Chen, M. C., Liu, X., & Duyn, J. H. (2013). EEG correlates of time-varying BOLD functional connectivity. *Neuroimage, 72*, 227-236. doi:10.1016/j.neuroimage.2013.01.049

Chen, H., Nomi, J. S., Uddin, L. Q., Duan, X., & Chen, H. (2017). Intrinsic functional connectivity variance and state-specific under-connectivity in autism. *Hum Brain Mapp*. doi:10.1002/hbm.23764

Ciric, R., Nomi, J. S., Uddin, L. Q., & Satpute, A. B. (2017). Contextual connectivity: A framework for understanding the intrinsic dynamic architecture of large-scale functional brain networks. *Sci Rep, 7*(1), 6537. doi:10.1038/s41598-017-06866-w

Conner, C. R., Ellmore, T. M., Pieters, T. A., DiSano, M. A., & Tandon, N. (2011). Variability of the relationship between electrophysiology and BOLD-fMRI across cortical regions in humans. *J Neurosci, 31*(36), 12855-12865. doi:10.1523/JNEUROSCI.1457-11.2011

Cordes, D., Haughton, V. M., Arfanakis, K., Wendt, G. J., Turski, P. A., Moritz, C. H., . . . Meyerand, M. E. (2000). Mapping functionally related regions of brain with functional connectivity MR imaging. *AJNR Am J Neuroradiol, 21*(9), 1636-1644.

Dajani, D. R., & Uddin, L. Q. (2016). Local brain connectivity across development in autism spectrum disorder: A cross-sectional investigation. *Autism Res, 9*(1), 43-54. doi:10.1002/aur.1494

de Lacy, N., Doherty, D., King, B. H., Rachakonda, S., & Calhoun, V. D. (2017). Disruption to control network function correlates with altered dynamic connectivity in the wider autism spectrum. *Neuroimage Clin, 15*, 513-524. doi:10.1016/j.nicl.2017.05.024

de Munck, J. C., Goncalves, S. I., Huijboom, L., Kuijer, J. P., Pouwels, P. J., Heethaar, R. M., & Lopes da Silva, F. H. (2007). The hemodynamic response of the alpha rhythm: an EEG/fMRI study. *Neuroimage, 35*(3), 1142-1151. doi:10.1016/j.neuroimage.2007.01.022

Di Martino, A., Yan, C. G., Li, Q., Denio, E., Castellanos, F. X., Alaerts, K., . . . Milham, M. P. (2014). The autism brain imaging data exchange: towards a large-scale evaluation of the intrinsic brain architecture in autism. *Mol Psychiatry, 19*(6), 659-667. doi:10.1038/mp.2013.78

Easson, A. K., Fatima, Z., & McIntosh, A. R. (2018). Functional connectivity-based subtypes of individuals with and without autism spectrum disorder. *Network Neuroscience*, 1-19. doi:10.1162/netn_a_00067

Falahpour, M., Thompson, W. K., Abbott, A. E., Jahedi, A., Mulvey, M. E., Datko, M., . . . Müller, R. A. (2016). Underconnected, But Not Broken? Dynamic Functional Connectivity MRI Shows Underconnectivity in Autism Is Linked to Increased Intra-Individual Variability Across Time. *Brain Connect, 6*(5), 403-414. doi:10.1089/brain.2015.0389

Feige, B., Scheffler, K., Esposito, F., Di Salle, F., Hennig, J., & Seifritz, E. (2005). Cortical and subcortical correlates of electroencephalographic alpha rhythm modulation. *J Neurophysiol, 93*(5), 2864-2872. doi:10.1152/jn.00721.2004

Feige, B., Spiegelhalder, K., Kiemen, A., Bosch, O. G., Tebartz van Elst, L., Hennig, J., . . . Riemann, D. (2017). Distinctive time-lagged resting-state networks revealed by simultaneous EEG-fMRI. *Neuroimage, 145*(Pt A), 1-10. doi:10.1016/j.neuroimage.2016.09.027

Fishman, I., Keown, C. L., Lincoln, A. J., Pineda, J. A., & Müller, R. A. (2014). Atypical cross talk between mentalizing and mirror neuron networks in autism spectrum disorder. *JAMA Psychiatry, 71*(7), 751-760. doi:10.1001/jamapsychiatry.2014.83

Fox, M. D., & Raichle, M. E. (2007). Spontaneous fluctuations in brain activity observed with functional magnetic resonance imaging. *Nat Rev Neurosci, 8*(9), 700-711. doi:10.1038/nrn2201

Fu, Z., Tu, Y., Di, X., Du, Y., Sui, J., Biswal, B. B., . . . Calhoun, V. D. (2018). Transient increased thalamic-sensory connectivity and decreased whole-brain dynamism in autism. *Neuroimage*. doi:10.1016/j.neuroimage.2018.06.003

Gaglianese, A., Vansteensel, M. J., Harvey, B. M., Dumoulin, S. O., Petridou, N., & Ramsey, N. F. (2017). Correspondence between fMRI and electrophysiology during visual motion processing in human MT. *Neuroimage, 155*, 480-489. doi:10.1016/j.neuroimage.2017.04.007

Geschwind, D. H., & State, M. W. (2015). Gene hunting in autism spectrum disorder: on the path to precision medicine. *Lancet Neurol, 14*(11), 1109-1120. doi:10.1016/S1474-4422(15)00044-7

Gohel, S. R., & Biswal, B. B. (2015). Functional integration between brain regions at rest occurs in multiple-frequency bands. *Brain Connect, 5*(1), 23-34. doi:10.1089/brain.2013.0210

Goldman, R. I., Stern, J. M., Engel, J., Jr., & Cohen, M. S. (2002). Simultaneous EEG and fMRI of the alpha rhythm. *Neuroreport, 13*(18), 2487-2492. doi:10.1097/01.wnr.0000047685.08940.d0

Hames, E. C., Murphy, B., Rajmohan, R., Anderson, R. C., Baker, M., Zupancic, S., . . . Richman, D. (2016). Visual, Auditory, and Cross Modal Sensory Processing in Adults

with Autism: An EEG Power and BOLD fMRI Investigation. *Front Hum Neurosci, 10*, 167. doi:10.3389/fnhum.2016.00167

He, B. J., Snyder, A. Z., Zempel, J. M., Smyth, M. D., & Raichle, M. E. (2008). Electrophysiological correlates of the brain's intrinsic large-scale functional architecture. *Proc Natl Acad Sci U S A, 105*(41), 16039-16044. doi:10.1073/pnas.0807010105

Hillebrand, A., & Barnes, G. R. (2002). A quantitative assessment of the sensitivity of whole-head MEG to activity in the adult human cortex. *Neuroimage, 16*(3 Pt 1), 638-650.

Hillman, E. M. (2014). Coupling mechanism and significance of the BOLD signal: a status report. *Annu Rev Neurosci, 37*, 161-181. doi:10.1146/annurev-neuro-071013-014111

Hindriks, R., Adhikari, M. H., Murayama, Y., Ganzetti, M., Mantini, D., Logothetis, N. K., & Deco, G. (2016). Can sliding-window correlations reveal dynamic functional connectivity in resting-state fMRI? *Neuroimage, 127*, 242-256. doi:10.1016/j.neuroimage.2015.11.055

Hull, J. V., Jacokes, Z. J., Torgerson, C. M., Irimia, A., & Van Horn, J. D. (2016). Resting-State Functional Connectivity in Autism Spectrum Disorders: A Review. *Front Psychiatry, 7*, 205. doi:10.3389/fpsyt.2016.00205

Hutchison, R. M., Hashemi, N., Gati, J. S., Menon, R. S., & Everling, S. (2015). Electrophysiological signatures of spontaneous BOLD fluctuations in macaque prefrontal cortex. *Neuroimage, 113*, 257-267. doi:10.1016/j.neuroimage.2015.03.062

Hutchison, R. M., Womelsdorf, T., Allen, E. A., Bandettini, P. A., Calhoun, V. D., Corbetta, M., . . . Chang, C. (2013). Dynamic functional connectivity: promise, issues, and interpretations. *Neuroimage, 80*, 360-378. doi:10.1016/j.neuroimage.2013.05.079

Itahashi, T., Yamada, T., Watanabe, H., Nakamura, M., Ohta, H., Kanai, C., . . . Hashimoto, R. (2015). Alterations of local spontaneous brain activity and connectivity in adults with high-functioning autism spectrum disorder. *Mol Autism, 6*, 30. doi:10.1186/s13229-015-0026-z

Jiang, L., Hou, X. H., Yang, N., Yang, Z., & Zuo, X. N. (2015). Examination of Local Functional Homogeneity in Autism. *Biomed Res Int, 2015*, 174371. doi:10.1155/2015/174371

Jochaut, D., Lehongre, K., Saitovitch, A., Devauchelle, A. D., Olasagasti, I., Chabane, N., . . . Giraud, A. L. (2015). Atypical coordination of cortical oscillations in response to speech in autism. *Front Hum Neurosci, 9*, 171. doi:10.3389/fnhum.2015.00171

Jones, T. B., Bandettini, P. A., Kenworthy, L., Case, L. K., Milleville, S. C., Martin, A., & Birn, R. M. (2010). Sources of group differences in functional connectivity: an investigation applied to autism spectrum disorder. *Neuroimage, 49*(1), 401-414. doi:10.1016/j.neuroimage.2009.07.051

Just, M. A., Cherkassky, V. L., Keller, T. A., Kana, R. K., & Minshew, N. J. (2007). Functional and anatomical cortical underconnectivity in autism: evidence from an FMRI study of an executive function task and corpus callosum morphometry. *Cereb Cortex, 17*(4), 951-961. doi:10.1093/cercor/bhl006

Just, M. A., Cherkassky, V. L., Keller, T. A., & Minshew, N. J. (2004). Cortical activation and synchronization during sentence comprehension in high-functioning autism: evidence of underconnectivity. *Brain, 127*(Pt 8), 1811-1821. doi:10.1093/brain/awh199

Kana, R. K., Keller, T. A., Cherkassky, V. L., Minshew, N. J., & Just, M. A. (2006). Sentence comprehension in autism: thinking in pictures with decreased functional connectivity. *Brain, 129*(Pt 9), 2484-2493. doi:10.1093/brain/awl164

Keown, C. L., Datko, M. C., Chen, C. P., Maximo, J. O., Jahedi, A., & Müller, R. A. (2017). Network organization is globally atypical in autism: A graph theory study of intrinsic functional connectivity. *Biol Psychiatry Cogn Neurosci Neuroimaging, 2*(1), 66-75. doi:10.1016/j.bpsc.2016.07.008

Keown, C. L., Shih, P., Nair, A., Peterson, N., Mulvey, M. E., & Müller, R. A. (2013). Local functional overconnectivity in posterior brain regions is associated with symptom severity in autism spectrum disorders. *Cell Rep, 5*(3), 567-572. doi:10.1016/j.celrep.2013.10.003

King, J. B., Prigge, M. B. D., King, C. K., Morgan, J., Dean, D. C., 3rd, Freeman, A., . . . Anderson, J. S. (2018). Evaluation of Differences in Temporal Synchrony Between Brain Regions in Individuals With Autism and Typical Development. *JAMA Netw Open, 1*(7), e184777. doi:10.1001/jamanetworkopen.2018.4777

Kitzbichler, M. G., Khan, S., Ganesan, S., Vangel, M. G., Herbert, M. R., Hamalainen, M. S., & Kenet, T. (2015). Altered development and multifaceted band-specific abnormalities of resting state networks in autism. *Biol Psychiatry, 77*(9), 794-804. doi:10.1016/j.biopsych.2014.05.012

Kleinhans, N. M., Richards, T., Sterling, L., Stegbauer, K. C., Mahurin, R., Johnson, L. C., . . . Aylward, E. (2008). Abnormal functional connectivity in autism spectrum disorders during face processing. *Brain, 131*(Pt 4), 1000-1012. doi:10.1093/brain/awm334

Koshino, H., Carpenter, P. A., Minshew, N. J., Cherkassky, V. L., Keller, T. A., & Just, M. A. (2005). Functional connectivity in an fMRI working memory task in high-functioning autism. *Neuroimage, 24*(3), 810-821. doi:10.1016/j.neuroimage.2004.09.028

Koshino, H., Kana, R. K., Keller, T. A., Cherkassky, V. L., Minshew, N. J., & Just, M. A. (2008). fMRI investigation of working memory for faces in autism: visual coding and underconnectivity with frontal areas. *Cereb Cortex, 18*(2), 289-300. doi:10.1093/cercor/bhm054

Laufs, H., Kleinschmidt, A., Beyerle, A., Eger, E., Salek-Haddadi, A., Preibisch, C., & Krakow, K. (2003). EEG-correlated fMRI of human alpha activity. *Neuroimage, 19*(4), 1463-1476.

Laumann, T. O., Snyder, A. Z., Mitra, A., Gordon, E. M., Gratton, C., Adeyemo, B., . . . Petersen, S. E. (2016). On the Stability of BOLD fMRI Correlations. *Cereb Cortex*. doi:10.1093/cercor/bhw265

Logothetis, N. K., Pauls, J., Augath, M., Trinath, T., & Oeltermann, A. (2001). Neurophysiological investigation of the basis of the fMRI signal. *Nature, 412*(6843), 150-157. doi:10.1038/35084005

Maenner, M. J., Shaw, K. A., Baio, J., Washington, A., Patrick, M., DiRienzo, M., . . . Dietz, P. M. (2020). Prevalence of Autism Spectrum Disorder Among Children Aged 8 Years - Autism and Developmental Disabilities Monitoring Network, 11 Sites, United States, 2016. *MMWR Surveill Summ, 69*(4), 1-12. doi:10.15585/mmwr.ss6904a1

Magri, C., Schridde, U., Murayama, Y., Panzeri, S., & Logothetis, N. K. (2012). The amplitude and timing of the BOLD signal reflects the relationship between local field potential power at different frequencies. *J Neurosci, 32*(4), 1395-1407. doi:10.1523/JNEUROSCI.3985-11.2012

Mantini, D., Perrucci, M. G., Del Gratta, C., Romani, G. L., & Corbetta, M. (2007). Electrophysiological signatures of resting state networks in the human brain. *Proc Natl Acad Sci U S A, 104*(32), 13170-13175. doi:10.1073/pnas.0700668104

Mash, L. E., Linke, A. C., Olson, L. A., Fishman, I., Liu, T. T., & Muller, R. A. (2019). Transient states of network connectivity are atypical in autism: A dynamic functional connectivity study. *Hum Brain Mapp*. doi:10.1002/hbm.24529

Mash, L. E., Reiter, M. A., Linke, A. C., Townsend, J., & Müller, R. A. (2018). Multimodal approaches to functional connectivity in autism spectrum disorders: An integrative perspective. *Dev Neurobiol, 78*(5), 456-473. doi:10.1002/dneu.22570

Maximo, J. O., Keown, C. L., Nair, A., & Müller, R. A. (2013). Approaches to local connectivity in autism using resting state functional connectivity MRI. *Front Hum Neurosci, 7*, 605. doi:10.3389/fnhum.2013.00605

Mitra, A., Snyder, A. Z., Blazey, T., & Raichle, M. E. (2015). Lag threads organize the brain's intrinsic activity. *Proc Natl Acad Sci U S A, 112*(17), E2235-2244. doi:10.1073/pnas.1503960112

Mitra, A., Snyder, A. Z., Constantino, J. N., & Raichle, M. E. (2017). The Lag Structure of Intrinsic Activity is Focally Altered in High Functioning Adults with Autism. *Cereb Cortex, 27*(2), 1083-1093. doi:10.1093/cercor/bhv294

Mitra, A., Snyder, A. Z., Hacker, C. D., & Raichle, M. E. (2014). Lag structure in resting-state fMRI. *J Neurophysiol, 111*(11), 2374-2391. doi:10.1152/jn.00804.2013

Mostofsky, S. H., Powell, S. K., Simmonds, D. J., Goldberg, M. C., Caffo, B., & Pekar, J. J. (2009). Decreased connectivity and cerebellar activity in autism during motor task performance. *Brain, 132*(Pt 9), 2413-2425. doi:10.1093/brain/awp088

Mulert, C. (2013). Simultaneous EEG and fMRI: towards the characterization of structure and dynamics of brain networks. *Dialogues Clin Neurosci, 15*(3), 381-386.

Müller, R. A., Shih, P., Keehn, B., Deyoe, J. R., Leyden, K. M., & Shukla, D. K. (2011). Underconnected, but how? A survey of functional connectivity MRI studies in autism spectrum disorders. *Cereb Cortex, 21*(10), 2233-2243. doi:10.1093/cercor/bhq296

Murta, T., Chaudhary, U. J., Tierney, T. M., Dias, A., Leite, M., Carmichael, D. W., . . . Lemieux, L. (2017). Phase-amplitude coupling and the BOLD signal: A simultaneous intracranial EEG (icEEG) - fMRI study in humans performing a finger-tapping task. *Neuroimage, 146*, 438-451. doi:10.1016/j.neuroimage.2016.08.036

Murta, T., Leite, M., Carmichael, D. W., Figueiredo, P., & Lemieux, L. (2015). Electrophysiological correlates of the BOLD signal for EEG-informed fMRI. *Hum Brain Mapp, 36*(1), 391-414. doi:10.1002/hbm.22623

Muthukumaraswamy, S. D. (2013). High-frequency brain activity and muscle artifacts in MEG/EEG: a review and recommendations. *Front Hum Neurosci, 7*, 138. doi:10.3389/fnhum.2013.00138

Nair, A., Carper, R. A., Abbott, A. E., Chen, C. P., Solders, S., Nakutin, S., . . . Muller, R. A. (2015). Regional specificity of aberrant thalamocortical connectivity in autism. *Hum Brain Mapp, 36*(11), 4497-4511. doi:10.1002/hbm.22938

Nair, A., Keown, C. L., Datko, M., Shih, P., Keehn, B., & Müller, R. A. (2014). Impact of methodological variables on functional connectivity findings in autism spectrum disorders. *Hum Brain Mapp, 35*(8), 4035-4048. doi:10.1002/hbm.22456

Nair, A., Treiber, J. M., Shukla, D. K., Shih, P., & Muller, R. A. (2013). Impaired thalamocortical connectivity in autism spectrum disorder: a study of functional and anatomical connectivity. *Brain, 136*(Pt 6), 1942-1955. doi:10.1093/brain/awt079

Nair, S., Jao Keehn, R. J., Berkebile, M. M., Maximo, J. O., Witkowska, N., & Müller, R. A. (2017). Local resting state functional connectivity in autism: site and cohort variability and the effect of eye status. *Brain Imaging Behav*. doi:10.1007/s11682-017-9678-y

Nalci, A., Rao, B. D., & Liu, T. T. (2019). Nuisance effects and the limitations of nuisance regression in dynamic functional connectivity fMRI. *Neuroimage, 184*, 1005-1031. doi:10.1016/j.neuroimage.2018.09.024

Neuner, I., Arrubla, J., Werner, C. J., Hitz, K., Boers, F., Kawohl, W., & Shah, N. J. (2014). The default mode network and EEG regional spectral power: a simultaneous fMRI-EEG study. *PLoS One, 9*(2), e88214. doi:10.1371/journal.pone.0088214

Niedermeyer, E., Schomer, D. L., & Lopes da Silva, F. H. (2011). *Niedermeyer's electroencephalography : basic principles, clinical applications, and related fields* (6th ed.). Philadelphia: Wolters Kluwer Health/Lippincott Williams & Wilkins.

Nir, Y., Fisch, L., Mukamel, R., Gelbard-Sagiv, H., Arieli, A., Fried, I., & Malach, R. (2007). Coupling between neuronal firing rate, gamma LFP, and BOLD fMRI is related to interneuronal correlations. *Curr Biol, 17*(15), 1275-1285. doi:10.1016/j.cub.2007.06.066

Nir, Y., Mukamel, R., Dinstein, I., Privman, E., Harel, M., Fisch, L., . . . Malach, R. (2008). Interhemispheric correlations of slow spontaneous neuronal fluctuations revealed in human sensory cortex. *Nat Neurosci, 11*(9), 1100-1108.

Nomi, J. S., Farrant, K., Damaraju, E., Rachakonda, S., Calhoun, V. D., & Uddin, L. Q. (2016). Dynamic functional network connectivity reveals unique and overlapping profiles of insula subdivisions. *Hum Brain Mapp, 37*(5), 1770-1787. doi:10.1002/hbm.23135

Noonan, S. K., Haist, F., & Müller, R. A. (2009). Aberrant functional connectivity in autism: evidence from low-frequency BOLD signal fluctuations. *Brain Res, 1262*, 48-63. doi:10.1016/j.brainres.2008.12.076

O'Reilly, C., Lewis, J. D., & Elsabbagh, M. (2017). Is functional brain connectivity atypical in autism? A systematic review of EEG and MEG studies. *PLoS One, 12*(5), e0175870. doi:10.1371/journal.pone.0175870

Olbrich, S., Mulert, C., Karch, S., Trenner, M., Leicht, G., Pogarell, O., & Hegerl, U. (2009). EEG-vigilance and BOLD effect during simultaneous EEG/fMRI measurement. *Neuroimage, 45*(2), 319-332. doi:10.1016/j.neuroimage.2008.11.014

Olsson, M. B., Westerlund, J., Lundstrom, S., Giacobini, M., Fernell, E., & Gillberg, C. (2015). "Recovery" from the diagnosis of autism - and then? *Neuropsychiatr Dis Treat, 11*, 999-1005. doi:10.2147/NDT.S78707

Peters, J. M., Taquet, M., Vega, C., Jeste, S. S., Fernandez, I. S., Tan, J., . . . Warfield, S. K. (2013). Brain functional networks in syndromic and non-syndromic autism: a graph theoretical study of EEG connectivity. *BMC Med, 11*, 54. doi:10.1186/1741-7015-11-54

Pollonini, L., Patidar, U., Situ, N., Rezaie, R., Papanicolaou, A. C., & Zouridakis, G. (2010). Functional connectivity networks in the autistic and healthy brain assessed using Granger causality. *Conf Proc IEEE Eng Med Biol Soc, 2010*, 1730-1733. doi:10.1109/IEMBS.2010.5626702

Preti, M. G., Bolton, T. A., & Van De Ville, D. (2017). The dynamic functional connectome: State-of-the-art and perspectives. *Neuroimage, 160*, 41-54. doi:10.1016/j.neuroimage.2016.12.061

Raatikainen, V., Korhonen, V., Borchardt, V., Huotari, N., Helakari, H., Kananen, J., . . . Kiviniemi, V. (2020). Dynamic lag analysis reveals atypical brain information flow in autism spectrum disorder. *Autism Res, 13*(2), 244-258. doi:10.1002/aur.2218

Rane, P., Cochran, D., Hodge, S. M., Haselgrove, C., Kennedy, D. N., & Frazier, J. A. (2015). Connectivity in Autism: A Review of MRI Connectivity Studies. *Harv Rev Psychiatry, 23*(4), 223-244. doi:10.1097/HRP.0000000000000072

Raut, R. V., Mitra, A., Marek, S., Ortega, M., Snyder, A. Z., Tanenbaum, A., . . . Raichle, M. E. (2019). Organization of Propagated Intrinsic Brain Activity in Individual Humans. *Cerebral Cortex*. doi:10.1093/cercor/bhz198

Reynell, C., & Harris, J. J. (2013). The BOLD signal and neurovascular coupling in autism. *Dev Cogn Neurosci, 6*, 72-79. doi:10.1016/j.dcn.2013.07.003

Rudie, J. D., Brown, J. A., Beck-Pancer, D., Hernandez, L. M., Dennis, E. L., Thompson, P. M., . . . Dapretto, M. (2012). Altered functional and structural brain network organization in autism. *Neuroimage Clin, 2*, 79-94. doi:10.1016/j.nicl.2012.11.006

Rudie, J. D., Shehzad, Z., Hernandez, L. M., Colich, N. L., Bookheimer, S. Y., Iacoboni, M., & Dapretto, M. (2012). Reduced functional integration and segregation of distributed neural systems underlying social and emotional information processing in autism spectrum disorders. *Cereb Cortex, 22*(5), 1025-1037. doi:10.1093/cercor/bhr171

Scheeringa, R., Fries, P., Petersson, K. M., Oostenveld, R., Grothe, I., Norris, D. G., . . . Bastiaansen, M. C. (2011). Neuronal dynamics underlying high- and low-frequency EEG oscillations contribute independently to the human BOLD signal. *Neuron, 69*(3), 572-583. doi:10.1016/j.neuron.2010.11.044

Scheeringa, R., Petersson, K. M., Kleinschmidt, A., Jensen, O., & Bastiaansen, M. C. (2012). EEG alpha power modulation of fMRI resting-state connectivity. *Brain Connect, 2*(5), 254-264. doi:10.1089/brain.2012.0088

Shakil, S., Lee, C. H., & Keilholz, S. D. (2016). Evaluation of sliding window correlation performance for characterizing dynamic functional connectivity and brain states. *Neuroimage, 133*, 111-128. doi:10.1016/j.neuroimage.2016.02.074

Shih, P., Keehn, B., Oram, J. K., Leyden, K. M., Keown, C. L., & Müller, R. A. (2011). Functional differentiation of posterior superior temporal sulcus in autism: a functional connectivity magnetic resonance imaging study. *Biol Psychiatry, 70*(3), 270-277. doi:10.1016/j.biopsych.2011.03.040

Shmuel, A., & Leopold, D. A. (2008). Neuronal correlates of spontaneous fluctuations in fMRI signals in monkey visual cortex: Implications for functional connectivity at rest. *Hum Brain Mapp, 29*(7), 751-761. doi:10.1002/hbm.20580

Smith, D. M., Zhao, Y., Keilholz, S. D., & Schumacher, E. H. (2018). Investigating the Intersession Reliability of Dynamic Brain-State Properties. *Brain Connect, 8*(5), 255-267. doi:10.1089/brain.2017.0571

Supek, S., & Aine, C. J. (2014). *Magnetoencephalography : from signals to dynamic cortical networks*(pp. 1 online resource.). doi:10.1007/978-3-642-33045-2

Supekar, K., Uddin, L. Q., Khouzam, A., Phillips, J., Gaillard, W. D., Kenworthy, L. E., . . . Menon, V. (2013). Brain hyperconnectivity in children with autism and its links to social deficits. *Cell Rep, 5*(3), 738-747. doi:10.1016/j.celrep.2013.10.001

Tagliazucchi, E., von Wegner, F., Morzelewski, A., Brodbeck, V., & Laufs, H. (2012). Dynamic BOLD functional connectivity in humans and its electrophysiological correlates. *Front Hum Neurosci, 6*, 339. doi:10.3389/fnhum.2012.00339

Tsiaras, V., Simos, P. G., Rezaie, R., Sheth, B. R., Garyfallidis, E., Castillo, E. M., & Papanicolaou, A. C. (2011). Extracting biomarkers of autism from MEG resting-state functional connectivity networks. *Comput Biol Med, 41*(12), 1166-1177. doi:10.1016/j.compbiomed.2011.04.004

van den Broek, S. P., Reinders, F., Donderwinkel, M., & Peters, M. J. (1998). Volume conduction effects in EEG and MEG. *Electroencephalogr Clin Neurophysiol, 106*(6), 522-534.

Van Dijk, K. R., Hedden, T., Venkataraman, A., Evans, K. C., Lazar, S. W., & Buckner, R. L. (2010). Intrinsic functional connectivity as a tool for human connectomics: theory, properties, and optimization. *J Neurophysiol, 103*(1), 297-321. doi:10.1152/jn.00783.2009

Vidaurre, D., Smith, S. M., & Woolrich, M. W. (2017). Brain network dynamics are hierarchically organized in time. *Proc Natl Acad Sci U S A*. doi:10.1073/pnas.1705120114

Vissers, M. E., Cohen, M. X., & Geurts, H. M. (2012). Brain connectivity and high functioning autism: a promising path of research that needs refined models, methodological convergence, and stronger behavioral links. *Neurosci Biobehav Rev, 36*(1), 604-625. doi:10.1016/j.neubiorev.2011.09.003

Wang, J., Barstein, J., Ethridge, L. E., Mosconi, M. W., Takarae, Y., & Sweeney, J. A. (2013). Resting state EEG abnormalities in autism spectrum disorders. *J Neurodev Disord, 5*(1), 24. doi:10.1186/1866-1955-5-24

Watanabe, T., & Rees, G. (2017). Brain network dynamics in high-functioning individuals with autism. *Nat Commun, 8*, 16048. doi:10.1038/ncomms16048

Wee, C. Y., Yap, P. T., & Shen, D. (2016). Diagnosis of Autism Spectrum Disorders Using Temporally Distinct Resting-State Functional Connectivity Networks. *CNS Neurosci Ther, 22*(3), 212-219. doi:10.1111/cns.12499

Winter, W. R., Nunez, P. L., Ding, J., & Srinivasan, R. (2007). Comparison of the effect of volume conduction on EEG coherence with the effect of field spread on MEG coherence. *Stat Med, 26*(21), 3946-3957. doi:10.1002/sim.2978

Woodward, N. D., Giraldo-Chica, M., Rogers, B., & Cascio, C. J. (2017). Thalamocortical dysconnectivity in autism spectrum disorder: An analysis of the Autism Brain Imaging Data Exchange. *Biol Psychiatry Cogn Neurosci Neuroimaging, 2*(1), 76-84. doi:10.1016/j.bpsc.2016.09.002

Yan, W., Rangaprakash, D., & Deshpande, G. (2018). Aberrant hemodynamic responses in autism: Implications for resting state fMRI functional connectivity studies. *Neuroimage Clin, 19*, 320-330. doi:10.1016/j.nicl.2018.04.013

Ye, A. X., Leung, R. C., Schafer, C. B., Taylor, M. J., & Doesburg, S. M. (2014). Atypical resting synchrony in autism spectrum disorder. *Hum Brain Mapp, 35*(12), 6049-6066. doi:10.1002/hbm.22604

Yerys, B. E., Herrington, J. D., Satterthwaite, T. D., Guy, L., Schultz, R. T., & Bassett, D. S. (2017). Globally weaker and topologically different: resting-state connectivity in youth with autism. *Mol Autism, 8*, 39. doi:10.1186/s13229-017-0156-6

Zhu, Y., Zhu, X., Zhang, H., Gao, W., Shen, D., & Wu, G. (2016). Reveal Consistent Spatial-Temporal Patterns from Dynamic Functional Connectivity for Autism Spectrum Disorder Identification. *Med Image Comput Comput Assist Interv, 9900*, 106-114. doi:10.1007/978-3-319-46720-7_13